CORRELATION OF COMPRESSION-PERMEABILITY TESTING WITH FILTRATION

by

Max Steven Willis

A Dissertation Submitted to the
Graduate Faculty in Partial Fulfillment of
The Requirements for the Degree of
DOCTOR OF PHILOSOPHY

Major Subject: Chemical Engineering

Approved:

Signature was redacted for privacy.

In Charge of Major Work

Signature was redacted for privacy.

Head of Major Department

Signature was redacted for privacy.

Dean of Graduate College

Iowa State University
Of Science and Technology
Ames, Iowa

1962

TABLE OF CONTENTS

NOMENCLATURE

A = septum area, ft.

A_c = compression-permeability test cell septum area, ft.

C = volume of filtrate attributed to the septum when the septum is considered as a fictitious weight of cake, ft^3.

d = diameter, ft.

F_x = force in the x-direction of the flowing fluid on the wetted surface, lb_f.

g_c = proportionality constant relating force and mass, 32.2 $lb_m ft/lb_f\ sec^2$.

H = height of a fluid column causing flow through a porous mass, ft or cm.

h = hydraulic radius, for porous media ε/S, ft.

K = Ruth's parameter for the parabolic equation $(V+C)^2 = K(\theta + \theta_c)$.

K_o = D'Arcy's permeability constant defined by Equation 1.

k = Kozeny equation constant, usually taken as 5 ± 10 per cent.

L = bed height, for filtration, cake height, ft.

lb_m = pounds mass.

lb_f = pounds force.

m = mass ratio of wet cake to dry cake.

m' = initial slope from porosity-time data, (1/sec).

P = pressure, for constant pressure filtration it is the applied pressure, lb_f/ft^2.

P_x = liquid pressure at a distance x from the cake-septum interface, lb_f/ft^2.

P_1 = liquid pressure at cake-septum interface (x=0), lb_f/ft^2.

P_{sx} = solids compressive pressure at a distance x from the cake-septum interface, lb_f/ft^2.

P_s = solids compressive pressure on septum (x=0), lb_f/ft^2.

q = flow rate per unit of filter area or superficial velocity, for compressible filter cakes, superficial velocity at cake-septum interface, $(1/A)(dV/d\theta)$, ft^3/ft^2 sec.

q_x = superficial velocity at a distance x from the cake-septum interface, ft^3/ft^2 sec.

R_m = septum resistance, $R_m = P_1 A g_c/\mu(dV/d\theta)$, (1/ft).

r = radius, ft.

S = surface area of particles to total volume of porous mass, ft^2/ft^3.

S_o = specific surface of solids, area of particles to volume particles, ft^2/ft^3.

s = ratio of the mass of solids to mass of slurry.

v_x = fluid velocity in x-direction, ft/sec.

V = filtrate volume, ft^3.

W = mass of solids in a filter cake, lb_m.

dW_x = mass of solids in a differential element of a filter cake at a distance x from the cake-septum interface, lb_m.

W_c = mass of solids in compression-permeability test cell, lb_m.

Greek

α = specific filtration resistance; specific filtration resistance of an incompressible filter cake, ft/lb_m.

α_x = point specific resistance at a distance x from the cake-septum interface; specific resistance obtained from compression-permeability testing, ft/lb_m.

α_{av} = average specific filtration resistance for a compressible filter cake, ft/lb_m.

ϵ = porosity, ratio of void volume to cake volume.

ϵ_x = point porosity at a distance x from the cake-septum interface; porosity obtained from compression-permeability testing.

ϵ_{av} = average porosity of a compressible filter cake.

θ = time, seconds.

θ_c = time necessary to collect filtrate volume, C, seconds.

μ = viscosity, lb_m/ft sec.

ρ = liquid density, lb_m/ft^3

ρ_s = solid density, lb_m/ft^3

τ_{rx} = shear stress, force per unit area in the x-direction acting on a surface whose normal is in the r-direction.

ABSTRACT

Fundamental to the study of filtration is a knowledge of flow rates, pressure drop, nature of the deposited cake, porosity distribution and compressibility. One way to determine the nature of the filter cake and thus predict filtration results is through the use of a compression-permeability test cell. Use of compression-permeability data to predict filtration results involves certain assumptions.

The direct comparison of compression-permeability specific resistance data and filtration resistance data is considered to be inconclusive in determining the validity of the compression-permeability technique. In this thesis, instead of a direct comparison, each assumption necessary for the validity of compression-permeability testing is investigated by experiment.

The first experiment was designed to test the compression-permeability assumption that as solids pressure varies with time at a point in a filter cake, the porosity at any instant is the equilibrium porosity. Compression-permeability test cell porosity-time data taken at different step changes in solids pressure and extrapolated to zero indicate that the assumption is not valid and that some finite increment of solids pressure is necessary before there is any change in porosity.

The second experiment was designed to test the relation between liquid pressure, P_X, and solids pressure, P_{SX}, at a

point in a filter cake. Two expressions were considered, $dP_{sx}=-dP_x$ and $dP_{sx}=-\epsilon_x dP_x$. The second expression was arrived at by analogy with flow through an annulus. A specially designed filter chamber with a floating septum seems to confirm the validity of the second expression. The expression for average specific resistance and the differential equation describing filtrations when flow rate and specific resistance are functions of position and time were changed to agree with the relationship $dP_{sx}=-\epsilon_x dP_x$. The usual manner of plotting filtration data as $d\theta/dV$ versus V was found to be a curved rather than a straight line.

The third experiment was designed to test the assumption that P_{sx} fixes both porosity, ϵ_x, and specific resistance, α_x. A statistical analysis of 250 specific resistance determinations and 125 porosity determinations at P_{sx}=24.99 psi was made using a Latin square design. The conclusion is that α_x is affected by sources of variation in addition to those of sample, cell geometry and operator. These other sources of variation are not easily defined or practically controllable. Thus α_x is not determined solely by ϵ_x and P_{sx}. The assumption concerning the determination of ϵ_x by P_{sx} is considered to be valid, however the statistical analysis showed a significant variance component attributable to cell geometry. Cakes with a larger height to diameter ratio have higher porosities.

INTRODUCTION

In comparison to the fields of heat and mass transfer, single and multiple phase flow through porous media have received relatively little attention. This is so in spite of their importance in such fields as filtration, sedimentation, purification, absorption and drying. Two obstacles which have impeded progress in this area are (1) the complexity of even the most simple models describing the flow and (2) the difficulty in obtaining reproducible results.

Fundamental to the study of filtration is a knowledge of the flow rates, pressure drop, nature of the deposited cake, porosity distribution and compressibility. Compressibility of a filter cake is affected by the frictional drag forces, migration of fines, and the orientation and shape of the particles. Permeability or specific filtration resistance, which governs the flow rate and pressure drop, is intimately related to compressibility.

The development of the compression-permeability test cell by Ruth (66) has contributed significantly in the past few years to the theoretical and experimental studies of compressibility. Ruth's purpose in developing this cell was to provide industry with a simple tool by which the day to day changes in prefilt properties could be determined, thereby allowing the use of filtration theory to aid in the most economical design, selection and operation of filters.

Use of the compression-permeability test cell to predict filtration results involves certain assumptions. Assumptions given by Tiller (88) are:

1. Ultimate values of porosity are attained instantaneously. This assumption is probably valid for filtrations in which pressure increases slowly.

2. There is a point contact between particles. The basic equation, $P_x + P_{sx} = P$, where P_x is the hydraulic pressure, P_{sx} the solid compressive pressure, and P the applied filtration pressure, depends upon the postulate of point contact.

3. The point filtration resistance of a given solid is determined by the porosity, which in turn depends upon the compressive solid pressure P_{sx}.

4. The porosity or specific filtration resistance determined under a given mechanical loading P_{sx} in a compression permeability cell is the same as the porosity or resistance at a point in a filter cake where the solid pressure (computed by $P_{sx} = P - P_x$) is the same as the mechanical loading in the compression-permeability cell.

The results of Grace (30, 31, 32), Kottwitz (45) and Shirato and Okamura (77, 78) lend validity to the assumptions but the assumptions have not been completely verified. The experimental method for determining the validity of the assumptions has been to compare the specific filtration resistances obtained by compression-permeability testing and from actual filtrations. This method is inconclusive when the specific filtration resistances do not agree. The purpose of this thesis was to study each assumption individually by experiment. In this way, disagreement between permeability tests and filtrations can be attributed to the failure of one or more of the assumptions for the specific solid under examination.

REVIEW OF THE LITERATURE

The major variables of interest in the study of flow through porous media are the pressure drop and the flow rate. Probably the first attempt to relate these two variables for a porous media was by D'Arcy (24). His empirical equation provides that the ratio of the superficial velocity, q, to the pressure drop per height of medium, L, is a constant. An excellent review of D'Arcy's experiment is given by Hubbert (38), who gives D'Arcy's law as

$$q = - \frac{K_o}{\mu} \frac{dH}{dL} \tag{1}$$

where H is fluid head.

The similarity between D'Arcy's law and Poiseuille's law

$$q = \frac{d^2 g_c}{32 \mu} \frac{dH}{dL} \tag{2}$$

led early investigators to regard a sand bed as equivalent to a bundle of capillary channels. It follows that D'Arcy's permeability constant K_o should be proportional to the square of an equivalent diameter. Since this equivalent diameter cannot be measured directly, there have been various attempts to describe it in some equivalent. Seelheim (73) modified D'Arcy's law to include a term for effective particle size. In attempts to assign an effective diameter to particles, however, it was recognized that Equation 1 does not account for changes in porosity. Dupuit (25) assumed the fractional free area of a sand bed cross-section to be constant and equal to the porosity. With this assumption the rate of flow becomes q/ϵ, the interstitial velocity.

Other attempts to define a suitable "effective diameter" have been tried, but eventually a tendency to regard particle size not as a measure of diameter, but as a measure of specific surface, S_o, appeared. Such reasoning appears sound since a fluid in steady laminar flow encounters resistance which depends on exposed surface. Following this reasoning, an effective particle size can be defined as $d_m = 6/S_o$. This diameter is that of a sphere with the same specific surface as one of the non-uniform particles. Kruger (47) applied this d_m to sands with porosities from 0.30 to 0.40.

Blake (8) plotted dimensionless groups and assumed that a granular bed is equivalent to a group of parallel similar channels, such that the total internal surface is equal to the particle surface and total internal volume is equal to the pore-volume. He also defined a mean hydraulic radius, h, as the ratio of the volume of fluid in the bed to the surface presented to the fluid. Thus $h = \epsilon/S$ where ϵ is the porosity and $S = (1-\epsilon)S_o$. Blake further stated that since the path is tortuous, the length traversed by the fluid, L_e, is greater than the bed depth, L. Hence L_e is used in Blake's equation, which is still essentially D'Arcy's law, to obtain the interstitial velocity, q/ϵ.

Kozeny (46), in the study of flow of irrigation water, further modified Dupuit's assumption of interstitial velocity, q/ϵ. He postulated that in a direction normal to the direction of flow, the fractional free area is ϵ and the average velocity parallel to the direction of flow must be q/ϵ. Since the actual path followed by the fluid is sinuous, q/ϵ represents only the component of the velocity parallel to the direction of flow. Thus, the time taken for an actual element of fluid to pass over a sinuous path of length L_e at a velocity equal to $(q/\epsilon)(L_e/L)$, corresponds to that time for an element of fluid to traverse a path L, at a velocity equal to q/ϵ. Kozeny also assumed that the pore-space in a granular bed can be regarded as a single channel of very complicated shape but of constant cross-sectional area. The result is

$$q = \frac{\epsilon^3}{(1-\epsilon)^2} \frac{1}{k \mu S_0^2} \frac{\Delta P g_c}{L} \qquad (3)$$

which is the well-known Kozeny equation. The value of k is usually taken as 5.0 ± 10%. Carman and Malherbe (18) considered Kozeny's equation accurate enough to be used in determining specific surface of paint pigments by permeability measurements. A similar equation was proposed by Fair and Hatch (27).

The early work in filtration theory disregarded the available theory described above. In addition, the correct description of the filtration was hampered by the use of large-scale equipment under conditions which could not be defined or reproduced (15). Almy and Lewis (2), Webber and Herschey (98), and Baker (4) used commercial size equipment in their studies. Almy and Lewis proposed a fundamental filtration equation as $q = P^b/V^c$ where the exponents were to be determined by logrithmic plots of the filtration data.

Sperry (81, 82, 84) possibly was the first to use small scale equipment and a filtrate volume recorder to accurately and rapidly measure filtrate volume. He was strongly criticized for his work by Baker (4). Van Gilse et al. (92, 93, 94, 95) were the first to recognize that solids weight in the cake is important in determining filtration resistance. They concluded that the volume of fluid from which the cake is formed has no influence either on the structure or on the consequent resistance of the cake and that it is only the quantity of solid matter which determines the resistance. They used the concept of constant and equal resistance in all layers of a filter cake. This was later shown to be erroneous (69, 70, 71).

Ruth (67, 68) was the first to define specific cake resistance and recognize its variation with position in a compressible filter cake. He also presumed the existance of a mechanical or solids pressure exerted on the cake solids which is complimentary to the hydraulic pressure drop. Ruth, as well as Hinchley et al. (36), recognized the applicability of D'Arcy's law to filtration and he showed that the integrated form of D'Arcy's law for filtrations is a parabola of the form

$$(V + C)^2 = K(\theta + \theta_c) \tag{4}$$

Ruth believed that the agreement between filtration data and Equation 4 was excellent and that no essential difference existed in the behaviors of all classes of materials whether compressible or incompressible. The constant in Equation 4 can be determined from the linear equation

$$\frac{d\theta}{dV} = \frac{2}{K} V + \frac{2}{K} C \tag{5}$$

obtained by differentiation. From the slope, 2/K, the average specific cake resistance, α_{av}, which characterizes the filtered material, can be obtained from the relation

$$\alpha_{av} = \frac{2}{K} \frac{A^2 \ P(1-ms)g_c}{s \mu \rho} \tag{6}$$

In the differential form, the filtration equation is

$$\frac{dV}{d\theta} \frac{1}{A} = \frac{\Delta P g_c}{\frac{W\alpha}{A} + R_m} \tag{7}$$

where R_m is the septum resistance. This equation was used by Bonilla (9), Carman (16, 17), Grace (31), Ruth (66), Sperry (83), Foust et al. (28), Kottwitz (45), and Badger and Banchero (3).

Equation 7 can be compared with Equation 3 (Kozeny's equation) by neglecting septum resistance, R_m. Kozeny's equation in terms of cake weight is

$$\frac{dV}{d\theta}\frac{1}{A} = \frac{\epsilon^3 \quad \rho_s}{k(1-\epsilon)\ S_o^2}\frac{\Delta P\ g_c}{\mu\ \frac{W}{A}} \tag{8}$$

indicating that

$$\alpha_{av} = \frac{k(1-\epsilon)S_o^2}{\epsilon^3 \quad \rho_s} \tag{9}$$

According to Miller's reviews of published literature in the field of filtration (51, 52, 53, 54, 55, 56, 57, 58, 59), there were no significant advances in the mathematical treatment of filtration data between the work of Carman and Ruth and that of Grace and Tiller. Most of the literature in this period concerns, chiefly, equipment improvements and innovations.

Grace (30) investigated the Kozeny equation in its application to filtration of compressible cakes. He found that k and S_o vary with porosity and concluded that the Kozeny relationship is not satisfactory when applied to compressible filter cakes because of small particle agglomeration and the variation of fluid path with position in the cake. The use of Equation 9 with independently determined values of specific surface gives highly inaccurate values of specific cake resistance because of the unknown degree of flocculation existing before cake formation.

The compression-permeability test cell, devised by Ruth in 1946, has been used by Grace (30), Heertjes (33), Hutto (39), Igmanson et al. (43), Kottwitz (45), Michaels and Lin (49), Miller (50), Shirato and Okamura (76, 77, 78), Valeroy (91), Walas (97) and Willis (100). This cell, contingent upon the validity of certain assumptions, permits the independent variation of solids pressure and hydraulic pressure and enables the calculation of point specific resistance, α_x. Testing is done by placing a compressible cake under a controlled mechanical stress and noting the permeability. The porosity in the compressed cake is assumed uniform. The equation for determining average specific resistances from point specific resistances as defined by Ruth is

$$\alpha_{av} = \frac{P}{\int_0^P \frac{dP_{sx}}{\alpha_x}} \tag{10}$$

This equation was developed with the assumption that α_{av} is a function of only solids pressure, P_{sx}.

Tiller (86) proposed a method for calculating filtration times when septum resistance R_m and compression-permeability data are available. To do this, he rewrote Equation 7 as follows:

$$\frac{d\theta}{dV} = \frac{\mu s \rho}{A^2 g\ (1-ms)} \frac{\alpha_{av}}{P-P_1} V + \frac{\mu R_m}{A\ P_1\ g_c} \tag{11}$$

where P_1 is the hydraulic pressure at the cake septum interface, $P-P_1$ is the pressure drop across the cake and $W = Vs\rho/(1-ms)$. At zero filtrate volume $P_1 = P$ and the initial rate is given by

$$P_1 = P = \frac{\mu R_m}{Ag_c}\left(\frac{dV}{d\theta}\right)_{\theta=0} \tag{12}$$

He also revised the definition of α_{av}, as

$$\alpha_{av} = \frac{P-P_1}{\int_0^{P-P_1} \frac{dP_{sx}}{\alpha_x}} \tag{13}$$

where P_1 is obtained from Equation 12. Then for $\theta > 0$, Equation 11, rearranged, becomes

$$V = \frac{A^2 g_c (1-ms)}{\mu \rho s \frac{dV}{d\theta}} \int_0^{P-\mu R_m \frac{dV}{d\theta}/Ag_c} \frac{dP_{sx}}{\alpha_x} \tag{14}$$

By assuming values of $(dV/d\theta) < (dV/d\theta)_{\theta=0}$, the integral can be graphically integrated to give values of V. His calculations indicate that $d\theta/dV$ versus V is not a straight line. Sufficiently accurate filtration data have not been taken up to this time to verify these calculations.

Tiller also showed (88) that point specific resistances, α_x, can be obtained from data for average resistances, α_{av}, if $d\theta/dV$ versus V is not a straight line. If Equation 7 is written as

$$q = \frac{g_c P}{\mu(\alpha_{av} w + R_m)} \tag{15}$$

where $q = dV/Ad\theta$ and $w = W/A$, then

$$\alpha_{av} = \frac{(g_c P/\mu q) - R_m}{w} \tag{16}$$

which is equivalent to α_{av} being the tangent of the angle $[(g_c P/\mu q), (R_m), (g_c P/\mu q - R_m)]$. The intercept, R_m, of the plot of $g_c P/\mu q$ versus w is a curved line as indicated by Equation 14. An empirical relationship between α_{av} and the pressure $P-P_1=P_s$ is then obtained from analysis of the graph of $g_c P/\mu q$ versus w in accordance with Equation 16. Having the α_{av} versus $P-P_1=P_s$ data the point filtration resistance α_x can be obtained by differentiating Equation 13 with $P_s = P-P_1$ and solving for α_x, as

$$\alpha_x = \frac{\alpha_{av}}{1 - \dfrac{d \ln \alpha_{av}}{d \ln P_{sx}}} \tag{17}$$

Tiller and Cooper (89) suggested that due to the changes in m and ϵ_x with position in a compressible filter cake, the flow rate q_x through a filter cake increases from the cake surface to a maximum value at the cake-septum interface. A liquid material balance over a differential section of the cake on a unit area basis yields

$$\frac{\partial q_x}{\partial x} = -\frac{d\,\epsilon_x}{dP_{sx}}\,\frac{\partial P_{sx}}{\partial \theta} \tag{18}$$

where x is measured from the cake surface. The above equation and the modified D'Arcy equation

$$-g_c\,\frac{dP_x}{dx} = g_c\frac{dP_{sx}}{dx} = \alpha_x\,\mu\,\rho_s(1-\epsilon_x)q_x \tag{19}$$

represent simultaneous equations with $q_x = q_x(x, \theta)$ and $P_{sx} = P_{sx}(x, \theta)$. By eliminating q_x between Equations 18 and 19 the result is

$$g_c\frac{\partial^2 P_{sx}}{\partial x^2} = g_c\,\frac{d(\ln \alpha_x(1-\epsilon_x))}{dP_{sx}}\left(\frac{\partial P_{sx}}{\partial x}\right)^2 - \rho_s\,\mu\,\alpha_x(1-\epsilon_x)\frac{d\,\epsilon_x}{dP_{sx}}\left(\frac{\partial P_{sx}}{\partial \Theta}\right) \tag{20}$$

This equation is based on the assumptions that α_x and ϵ_x are functions of P_{sx} alone and that $-dP_x = dP_{sx}$. It is more general than Equation 11 which assumes $q_x = q_x(\theta)$ but is independent of position in the cake.

The average specific filtration resistance, α_{av}, as defined by Ruth in Equation 10 indicates that $\alpha_{av} = \alpha(P)$. As defined by Grace and Tiller in Equation 13, $\alpha_{av} = \alpha(P, \frac{dV}{d\theta})$. Tiller and Huang (90) showed that when the variable flow rate through a compressible cake is taken into account, $\alpha_{av} = \alpha(P, s, \frac{dV}{d\theta})$ where s is the slurry concentration. They define α_{av} as follows

$$\alpha_{av} = \frac{J(P-P_1)}{\int_0^{P-P_1} \frac{dP_{sx}}{\alpha x}} \tag{21}$$

where the factor J is defined by

$$J = \frac{1}{q_1 w} \int_0^w q_x dw_x = \int_0^1 \frac{q_x}{q_1} d\left(\frac{w_x}{w}\right) \tag{22}$$

The term $q_1 = \frac{dV}{d\theta}$ is the filtrate rate at the cake septum interface. J depends on the slurry concentration, s, and is less than unity.

Shirato and Okamura (77) have experimentally determined liquid pressure, P_x, distribution in constant pressure filtrations by means of vertical pressure probes placed at different heights in the filter chamber. They found that the liquid pressure distribution is independent of both position (x/L) and slurry concentration, s, for ignition-plug and diatom slurries. In comparing liquid pressure distributions (78) obtained from compression-permeability measurements with those obtained directly from constant-pressure filtrations they found the results did not agree for ignition-plug slurries. Experimental techniques in the operation of the compression-permeability test cell by Shirato and Okamura were different from those of previous workers. For their permeation experiments, distilled water was introduced into the hollow piston and brought under pressure by compressed air and a permeation measurement taken after the piston was fixed at a certain position. In addition, the permeation experiments were made at several different liquid pressures with the mechanical solids pressure, P_{sx}, held constant. These data were integrated graphically to obtain P_x at the position x using

$$\frac{x}{L} = \frac{\int_{P_x}^{P} y\,dP_x}{\int_{0}^{P} y\,dP_x} \tag{23}$$

where $y = \epsilon_x^3/k\,S_o^2(1-\epsilon_x)^2$. (The usual method for compression permeability testing is to allow the piston free movement and to increase the solids pressure, P_{sx}, while the liquid pressure, P_x, is held constant at some small value relative to P_{sx}.)

Shirato and Okamura also studied the behavior of Gairome-clay slurries in the compression-permeability test cell (76) and found that the specific resistance, α_x, at the same solids pressure, P_{sx}, decreased with increasing cake thickness, L. Willis (100) found this same behavior using calcium carbonate. Shirato and Okamura observed a curvature in the initial portion of the $d\theta/dV$ versus V plot and noted that α_{av} values depend upon slurry concentration, s.

In comparing compression-permeability estimates of α_{av}, m, ϵ and K with those obtained from constant pressure filtrations on ignition-plug slurries, Shirato and Okamura (75) determined that the m values had a deviation of $\pm$ 4%, the α_{av} values were within $\pm$ 2% and the ϵ and K values were within $\pm$ 3%. From these remarkable results they concluded that there always is equilibrium between cake compressive pressure, P_{sx} and ϵ_x at any position in both isobaric and constant rate filtrations. The constant rate filtrations performed with pressures predicted from compression-permeability data were within 3% of constant rate.

Shirato (74) gives a very complete review on filter media and blocking filtration as well as a criticism of the cake filtration theory and the pressure-filtration law. He arrives at the same conclusions as Tiller.

A different approach to the problem of flow through porous media which may be significant in filtration is a statistical approach advanced by Scheidegger (72). The idea of applying statistical methods to something which is difficult to understand at the microscopic level is not new. Scheidegger points out that the scheme was devised by Gibbs and developed by Einstein to describe Brownian motion. To apply the method to a porous media, a particle of fluid is considered as it passes through the media. As this particle moves through the porous media, its path is governed by the

Navier-Stokes equations and the boundary conditions. The difficulty is determining the boundary conditions. To circumvent this difficulty, the whole "ensemble" of systems (porous media) which are 'macroscopically identical' is considered. The idea then is to assume that a particle of fluid in a specific system (filter cake) will, in the long run, encounter all the conditions which are present in many systems (porous media) representing the "ensemble". The hypothesis that time-averages and ensemble averages are interchangeable among systems (ergodic hypothesis) allows the path of the particle through the system (filter cake) to be described by statistics*. The path of the particle of fluid is not random, but only the knowledge of the boundary conditions is random. The path of the particle is determined by the boundary conditions but the randomness of the boundary conditions can be manifested by representing the progress of the particle as a random path. Scheidegger applies the mathematics invented by Einstein for the theory of Brownian motion to the statistical ensemble and arrives at a diffusivity equation

$$\frac{\partial \Phi}{\partial t} = D \nabla \Phi \tag{24}$$

where D is a diffusivity constant and Φ is the probability function. Φ gives the probability of a specific fluid

---

*For a discussion of the method of taking averages, see Batchelor (5).

particle being at a position x at a given time, θ .

There are many references in the general area of flow through porous media which bear little relation to the filtration problems under consideration, however, a few are included here.

Adamson (1) carried out work on the electrokinetic properties of the interface between wool fibres and water and found that at porosities of the order 0.8, the Kozeny constant had values of 6.5. Baver (6) studied the retention of soil moisture. Cardwell and Parsons (13) considered methods for averaging permeabilities. When two permeabilities are in parallel, the average permeability is the simple-arithmetic average. Where the two permeabilities are in series, the average permeability is the harmonic mean. In the general case of a block of porous medium involving any number of different permeabilities and any type of directional variation, the equivalent permeability is between the harmonic and arithmetic averages. Comolet (22) showed experimentally that the critical Reynolds number at which water flowing in a tube becomes turbulent is changed greatly by a slight curvature of the tube. Eisenklam (26) discussed all types of porous mass from sintered metals to colloidal gels. Most of the workers in the flow of ground water such as Gardner et al. (29) and Richardson (64) use D'Arcy's law to eliminate velocity from the equation of continuity for incompressible fluids and arrive at Laplace's equation in pressure. This assumes the permeability is constant and hence is of limited interest in the case of compressible porous media.

THEORY

D'Arcy's law is the fundamental expression for laminar flow of fluids through porous media. This law relates the flow rate to the pressure gradient as

$$q_x = - \frac{K_o}{\mu} \left[g_c \frac{dP_x}{dx} + \rho g \sin\beta \right] \tag{25}$$

where β is the angle between the unidirectional flow through the porous body and the horizontal. Stated in words, D'Arcy's law relates the flow rate per unit area, q_x, at a given time and point along the path proportionally to the permeability, K_o, of the medium, the sum of the pressure gradient at the point and the hydrostatic head gradient along the direction of flow, and inversely proportional to the viscosity of the fluid.

The permeability K_o is a property of the medium alone. Thus K_o represents the fluid-flow conductivity through the cross-section at a point. The permeability applying to the point is the statistical average of the fluid flow conductivity of the group of pore spaces surrounding the point. This concept also applies to porosity or void space at a point.

The permeabilities could be different in each of the three coordinate directions of flow at a point and a more general set of D'Arcy equations is

$$q_x = - \frac{K_{ox}}{\mu} \frac{\partial P_x}{\partial x} g_c \tag{26}$$

$$q_y = - \frac{K_{oy}}{\mu} \frac{\partial P_y}{\partial y} g_c \tag{27}$$

$$q_z = - \frac{K_{oz}}{\mu} \left(g_c \frac{\partial P_z}{\partial z} + \rho g \right) \tag{28}$$

where K_{ox}, K_{oy}, K_{oz} are the directional permeabilities. For flow in one direction, the permeability of the medium could vary from point to point along the flow path. In this case, the dependence of permeability on position would have to be taken into account in integration of Equation 25.

The use of D'Arcy's law is restricted to cases in which the flow is laminar. This means low rates of flow where inertial effects are negligible at the turns and bends of the flow channels. Comolet (22) has shown that the start of turbulence is dependent upon the Reynolds number and the curvature of the flow channel. For this reason, it is generally accepted that for laminar flow through porous media, the Reynolds number should be less than unity (100).

D'Arcy's law for unidirectional flow is applied to filtration by considering the gradient of the hydrostatic head negligible when compared to the pressure gradient and by replacing bed height with cake weight such that

$$\frac{dW_x}{A} = \rho_s(1-\epsilon_x)\ dx \tag{29}$$

and

$$-g_c\ dP_x = \left[\frac{1}{K_{ox}\ \rho_s(1-\epsilon_x)}\right] \mu q \frac{dW_x}{A} \tag{30}$$

The term in brackets contains only properties of the medium and is defined as the specific filtration resistance, α_x. The fundamental filtration equation is therefore,

$$-g_c\ dP_x = \alpha_x\ q_x\ \mu\ \frac{dW_x}{A} \tag{31}$$

The usual method of solving Equation 31 for incompressible cake is to consider α_x, q and μ constant over a cake at some instant in time and integrating to obtain (3)

$$q = \frac{1}{A}\frac{dV}{d\theta} = \frac{g_c A\ (P-P_1)}{\alpha\ \mu\ W} \tag{32}$$

where P_1 is the pressure at the cake septum interface. In cases where P_1 is not known, Equation 32 is modified using a fictitious volume C which is that volume of filtrate attributed to the septum when the septum is considered as a fictitious weight of cake. Then V, for this particular case, is the actual volume of filtrate discharge. With these substitutions and a material balance

$$\frac{W}{s} = mW + \rho(V+C) \tag{33}$$

the filtration equation becomes

$$(V+C)\,d\,(V+C) = K\,d\theta \tag{34}$$

where $K = g_c A^2 P(1-ms)/\rho s \mu \alpha$. For P = constant, Equation 34 can be integrated with proper limits. If V is the actual volume of filtrate at time θ , then (V+C) is zero when $\theta = -\theta_c$, the time required to form the fictitious cake that accounts for the resistance of the filter medium. Thus

$$\int_0^{V+C} (V+C)\,d\,(V+C) = K \int_{-\theta_c}^{\theta} d\theta \tag{35}$$

and

$$(V+C)^2 = K(\theta + \theta_c) \tag{4}$$

The constants in Equation 4 are determined by differentiating to obtain Equation 5 and plotting $d\theta/dV$ versus V. The specific filtration resistance α is then obtained from Equation 6.

Frictional drag forces within a filter cake are manifested as mechanical compressive stress and the total of the drag force components perpendicular to the septum are transferred to the filter support. This mechanical compressive stress on the particles at any point in the cake is therefore the sum of the drag force components from the point to the cake surface. It is generally accepted (30, 33, 39, 43, 49, 50, 76, 91, 97, 100) that the build up of mechanical compressive stress, P_{sx}, is in accord with the relation

$$dP_{sx} = - dP_x \tag{36}$$

or upon integration

$$P_{sx} + P_x = P \tag{37}$$

Equation 36 is usually justified by means of a force balance around a single particle in the filter cake. To analyze the compressive solids stress, consider first flow through a horizontal, circular, straight tube of radius, R. A momentum balance and Newton's law of viscosity combine to give the velocity distribution as a function of radial position. The x-component of the force of the fluid on the wetted surface of the cylinder, F_x, is the momentum flux at the wall integrated over the wetted area:

$$F_x = (2\pi RL)\ \tau_{rx}\Big|_{r=R} = (2\pi RL)(-\mu \frac{dv_x}{dx})\Big|_{r=R} = \pi R^2(P-P_1) \tag{38}$$

In differential form then

$$dF_x = - \pi R^2\ dP_x \tag{39}$$

Defining solids compressive stress as $dP_{sx} = dF_x/\pi R^2$, then

$$dP_{sx} = - dP_x \tag{40}$$

Consider next (7) the flow through a horizontal annulus with an inner coaxial circular cylinder of radius κR and outer coaxial cylinder of radius R. Again the momentum balance and

Newton's law of viscosity lead to the velocity distribution as a function of $\kappa R \leq r \leq R$. The x-component of the force of the fluid on the wetted surface, F_x, is the sum of the momentum flux at the inner and outer cylinder, respectively

$$F_x = - \tau_{rx}\Big|_{r=\kappa R} \cdot 2\pi \kappa RL + \tau_{rx}\Big|_{r=R} \cdot 2\pi RL$$

$$F_x = \pi R^2(1-\kappa^2)(P-P_1) \tag{41}$$

In differential form

$$dF_x = - \pi R^2(1-\kappa^2)dP_x \tag{42}$$

Defining solids compressive stress based on the superficial area as $dP_{sx}=dF_x/\pi R^2$, then

$$dP_{sx} = - (1-\kappa^2)dP_x \tag{43}$$

The porosity ϵ is directly proportional to the quantity $(1-\kappa^2)$. By analogy, the equivalent relation for a differential element of porous media would be

$$dP_{sx} = - \epsilon_x dP_x \tag{44}$$

Defining the average porosity $(\epsilon_{av})_x$ for a portion of the cake from x to L as

$$(\epsilon_{av})_x = \frac{1}{P-P_x}\int_{P_x}^{P} \epsilon_x dP_x \tag{45}$$

This $(\epsilon_{av})_x$ on a length basis is

$$(\epsilon_{av})_x = \frac{1}{L-x}\int_0^L \epsilon_x \frac{dP_x}{dx}\,dx$$

Equation 44 can then be integrated. The integration constant is evaluated using the boundary conditions that P_x=P when P_{sx}=0. Thus

$$P_{sx} = (\epsilon_{av})_x\,(P-P_x) \tag{46}$$

If x is measured from the cake-septum interface to the cake surface then Equation 45 becomes

$$\epsilon_{av} = \frac{1}{P-P_1}\int_{P_1}^{P} \epsilon_x\, dP_x \tag{47}$$

and Equation 46 becomes

$$P_s = \epsilon_{av}(P-P_1) \tag{48}$$

where P_1 is the liquid pressure at the cake septum interface and P_s is then the compressive solids pressure on the septum.

A compressible cake is one in which the compressive solids pressure causes variation of α_x and ϵ_x throughout the cake. The higher the solids pressure (near the septum) the higher the specific resistance α_x and the lower the porosity ϵ_x. This means that compressible cakes should be relatively dry at the cake-septum interface and this is found to be so when cakes are visually examined.

Consider a point, x, in a compressible filter cake. At this point there will be a solids compressive pressure, P_{sx}, determined by Equation 44. The specific filtration resistance at this point is α_x, expressed mathematically by rearrangement of Equation 31

$$\alpha_x = \frac{-g_c \; A \; \frac{dP_x}{dW_x}}{q_x \, \mu} \tag{49}$$

This equation implies that if α_x is constant, any pressure gradient will have a unique flow rate. Now assume that α_x and ϵ_x are determined solely by the solids compressive pressure, P_{sx}. This assumption means that the specific resistance at point x in the filter cake can be reproduced outside the filter cake if the same solids compressive stress can be applied to the porous media. Suppose that a cake is confined and placed under a solids compressive stress of P_{sx} and a known liquid pressure gradient applied. By Equation 49, a unique flow rate q_x is obtained and α_x can be determined. This procedure is termed compression-permeability testing.

Compression-permeability test data are used in the following manner. Equation 31 is integrated over the cake at some instant of time with the assumption that α_x and ϵ_x are functions of only solids pressure, P_{sx}, and q_x=q is constant throughout the cake. The integration is performed by substituting $-dP_x = dP_{sx}/\epsilon_x$ and determining the limits of integration from Equation 46 when P_x=P and P_x=P_1. The result is

$$\int_{\epsilon_{av}(P-P_1)}^{0} \frac{dP_{sx}}{\alpha_x \epsilon_x} = \frac{q \mu W}{Ag_c} \tag{50}$$

For Equation 31, which was developed for an incompressible cake, to be applicable to a compressible cake, the substitution $\alpha = \alpha_{av}$ is made so that

$$\frac{P-P_1}{\alpha_{av}} = \frac{q \mu W}{Ag_c} \tag{51}$$

By comparing Equations 50 and 51, the average specific resistance, α_{av}, for a compressible filter cake can be defined as

$$\alpha_{av} = \frac{P-P_1}{\displaystyle\int_{\epsilon_{av}(P-P_1)}^{0} \frac{dP_{sx}}{\alpha_x \epsilon_x}} \tag{52}$$

This definition of α_{av} implies that it is a function of P, P_1 and ϵ_{av}. Since both P_1 and ϵ_{av} are functions of time, then α_{av} is a function of P and θ.

More explicit assumptions than those listed by Tiller (88) for proper use of compression-permeability testing are:

1. Since at a point, x, in a filter cake, the solids pressure, P_{sx}, and the porosity, ϵ_x are changing with time, then as P_{sx} increases by small increments, $P_{sx}(\theta_2)-P_{sx}(\theta_1) = \Delta P_{sx}(\theta)$, the porosity $\epsilon_x(\theta)$ has no time lag between $\epsilon_x(\theta_2)$, corresponding to $P_{sx}(\theta_2)$, and $\epsilon_x(\theta_1)$, correspond-

ing to $P_{sx}(\theta_1)$.

2. The relationship, $dP_{sx} = -\epsilon_x dP_x$, between solids compressive pressure and liquid pressure is valid.

3. The point specific resistance, α_x, of a given solid is determined by the porosity, ϵ_x, which in turn depends upon the solids compressive pressure, P_{sx}.

4. The porosity ϵ_x or specific filtration resistance α_x determined under a given mechanical loading P_{sx} in a compression-permeability test cell is the same as the porosity ϵ_x and α_x at a point in a filter cake where the solids compressive pressure is the same. (If assumption 3 is valid, so is assumption 4.)

Consider the following experiments to verify the assumptions necessary for the use of compression-permeability testing.

For assumption 1, a porous mass is confined in a compression-permeability test cell at a mechanical solids pressure of P_{sx}. At time $\theta = 0$ a step change of ΔP_{sx} is made and the initial slope, m', of the porosity versus time curve resulting from this step change is noted. This procedure is repeated using different step-change increments of solids pressure, ΔP_{sx}. The values of initial slope, m' versus the step-change, ΔP_{sx} are plotted and extrapolated to obtain m' as ΔP_{sx} approaches zero. If the value of m' also approaches zero, then assumption 1 is valid.

For assumption 2, Equation 48 and a filter chamber capable of measuring the solids compressive pressure on the septum P_s and the liquid pressure at the cake-septum interface, P_1, is necessary and the ratio $P_s/P-P_1$ can be examined.

For assumption 3, a statistical analysis of α_x and ϵ_x obtained from compression-permeability experiments at a given solids pressure, P_{sx}, must be made. The statistical experiment needs to be designed to analyze the components of variance which might affect the values of α_x and ϵ_x. The magnitude of the variances should indicate the validity of assumption 3, and hence assumption 4.

Equations 4, 32 and 51 have all been derived on the basis that q_x is a function of time but not of position in the cake. However, if the average porosity ϵ_{av} of the cake is decreasing, q_x varies from the cake surface through the solid reaching its maximum value at the cake-septum interface. The equation of continuity for a porous mass in which ϵ_x is a function of time is

$$\nabla \cdot \rho q = - \frac{\partial}{\partial \theta} (\rho \epsilon_x) \tag{53}$$

For an incompressible fluid and unidirectional flow, Equation 53 reduces to

$$\frac{\partial q_x}{\partial x} = - \frac{\partial \epsilon_x}{\partial \theta} \tag{54}$$

This equation can also be obtained by a liquid material balance over a differential section of the cake on a unit area basis (89). Assuming ϵ_x is a function of P_{sx} only, Equation 54 is

$$\frac{\partial q_x}{\partial x} = - \frac{d\epsilon_x}{dP_{sx}} \frac{\partial P_{sx}}{\partial \theta} \tag{55}$$

By using Equation 29, Equation 31 may be written as

$$-g_c \frac{\partial P_x}{\partial x} = \alpha_x \mu \ \rho_s (1-\epsilon_x) \ q_x \tag{56}$$

Equation 44 and Equation 56 then yield

$$g_c \frac{\partial P_{sx}}{\partial x} = \mu \rho_s \alpha_x \epsilon_x (1-\epsilon_x) \ q_x \tag{57}$$

Equations 55 and 57 represent simultaneous equations with q_x and P_{sx} as dependent variables and x and θ as independent variables. To eliminate q_x between Equations 55 and 57, Equation 57 can be differentiated with respect to x to give

$$g_c \frac{\partial^2 P_{sx}}{\partial x^2} = \mu \rho_s q_x \frac{d}{dP_{sx}} \left[\alpha_x(\epsilon_x - \epsilon_x^2)\right] \frac{\partial P_{sx}}{\partial x} + \mu \rho_s \alpha_x (\epsilon_x - \epsilon_x^2) \frac{\partial q_x}{\partial x} \tag{58}$$

If Equation 55 and 56 are substituted into Equation 58, then

$$g_c \frac{\partial^2 P_{sx}}{\partial x^2} = g_c \left(\frac{\partial P_{sx}}{\partial x}\right)^2 \frac{d}{dP_{sx}} \ln\left[\alpha_x(\epsilon_x - \epsilon_x^2)\right] - \mu \rho_s \alpha_x (\epsilon_x - \epsilon_x^2) \frac{d\epsilon_x}{dP_{sx}} \frac{\partial P_{sx}}{\partial \theta} \tag{59}$$

The preceding equation is based on the assumptions that α_x and ϵ_x are functions of only P_{sx} and that $dP_{sx} = - \epsilon_x dP_x$.

If ϵ_x is uniquely defined by P_{sx} but α_x is not, then it may be possible to calculate α_x values for a filter cake. If Equation 48 is substituted into Equation 52 and rearranged

$$- \int_0^{P_{sx}} \frac{dP_{sx}}{\alpha_x \epsilon_x} = \frac{P_s}{\alpha_{av} \epsilon_{av}} \tag{60}$$

When Equation 60 is differentiated with respect to P_s

$$- \frac{dP_{sx}}{\alpha_x \epsilon_x} = \frac{\alpha_{av} \epsilon_{av} \, dP_s - P_s \, d(\alpha_{av} \epsilon_{av})}{\alpha_{av}^2 \ \epsilon_{av}^2}$$

This equation is solved for α_x as

$$\alpha_x = \frac{1}{\epsilon_x} \left[\frac{\alpha_{av} \epsilon_{av} \frac{dP_{sx}}{d\theta}}{P_s \frac{d \ln (\alpha_{av} \epsilon_{av})}{d\theta} - \frac{dP_s}{d\theta}} \right] \tag{61}$$

where the total derivatives are used to indicate that the variables are measured at some fixed point in the filter cake and thus are functions of time only. If α_{av}, ϵ_{av}, P_{sx} and P_s data are known as a function of time from a filtration and if ϵ_x is known from compression-permeability measurements at each P_{sx}, then corresponding values of α_x for the filtration under consideration could be obtained.

The method usually used for determining the validity of the compression-permeability concept is the direct comparison of specific resistance data obtained from permeability testing and filtration. It is the objective of this thesis to test each of the assumptions individually by the experiments described in this section. Henceforth these experiments are referred to as experiment 1, 2, and 3 and thus are associated with assumptions 1, 2, and 3.

The equipment used in these experiments is described in the next section. The material studied in all the experiments is Baker and Adamson's reagent grade calcium carbonate. Thus the conclusions from these experiments must be restricted to this material.

EQUIPMENT AND PROCEDURE

Compression-Permeability Apparatus

Description of test cell

The compression-permeability test cell consists of a piston, cylinder and drainage-base. Figure 1 is a detailed drawing of the compression-permeability test cell used. With the exception of the piston, which was made of stainless steel, the cell was machined from a 4-inch diameter mild steel bar. The parts of the cell made from the mild steel were chrome-plated to prevent corrosion. Porous stainless steel obtained from the Micro-Metallics Corp., was used for the piston end and the top of the drainage-base. The porous plate used on the drainage-base was backed by 8-mesh stainless steel wire screen. The piston was provided with two O-rings to prevent filtrate leakage. A small brass ring held the filter paper over the piston end. The filter paper on the drainage-base was held in place by the cylinder. The Ames dial shown in Figure 1 was modified so that it read backwards and gave the height of the piston above the septum directly. The micrometer attached to the piston permitted the dial to be zeroed when the piston was resting on the drainage-base. An important feature of the test cell used was the addition of pressure-probes in the piston and cylinder which allowed the pressure drop over the cake to be measured and eliminated the

Figure 1. Detailed drawing of compression-permeability test cell

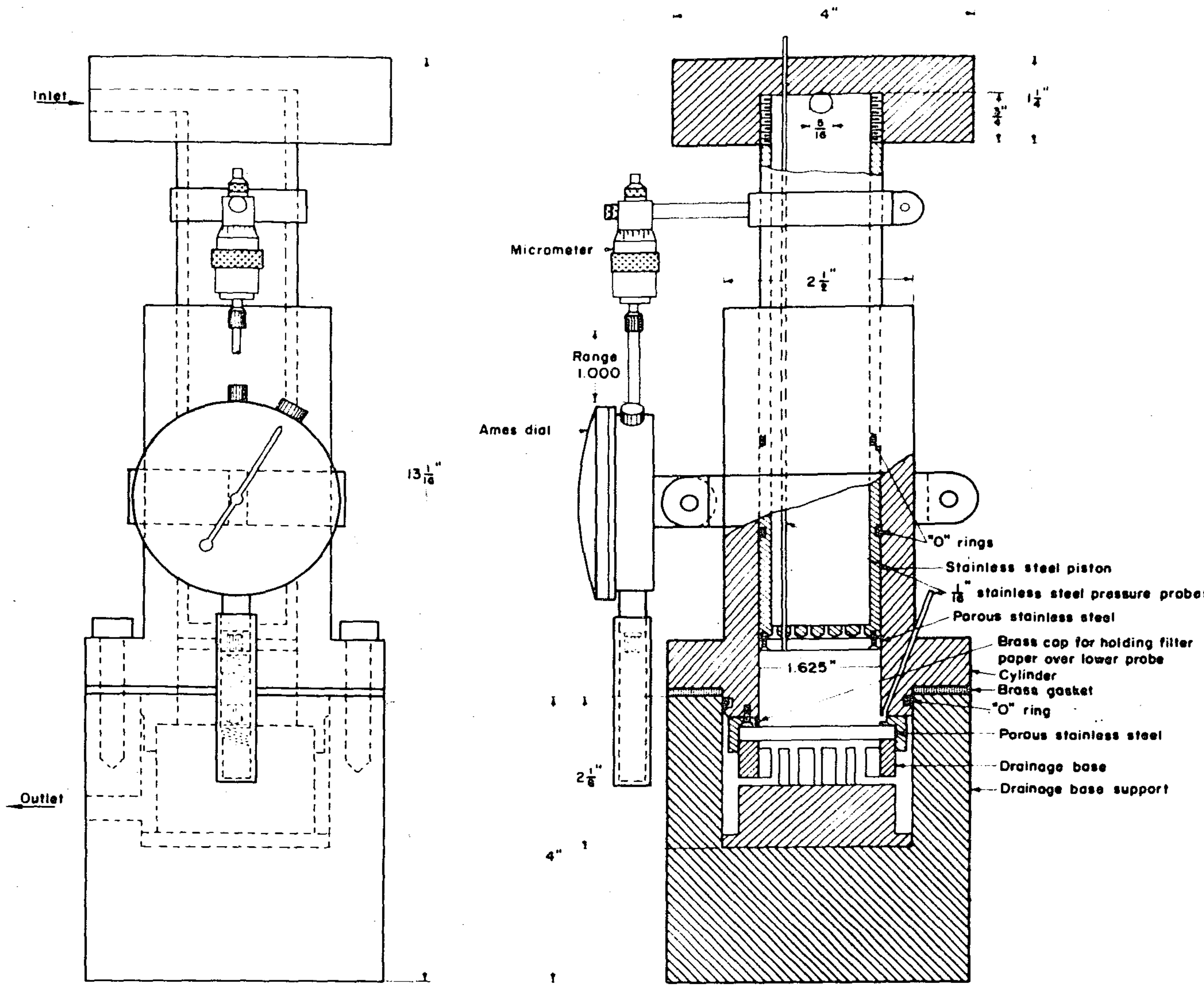
Inlet
Outlet
$13\frac{1}{16}$"
4"
$1\frac{1}{4}$"
$\frac{3}{4}$"
$\frac{5}{16}$
Micrometer
$2\frac{1}{2}$"
Range
1.000
Ames dial
"O" rings
Stainless steel piston
$\frac{1}{16}$" stainless steel pressure probes
Porous stainless steel
Brass cap for holding filter paper over lower probe
Cylinder
Brass gasket
"O" ring
1.625"
Porous stainless steel
Drainage base
Drainage base support
$2\frac{1}{8}$"
4"

effect of piston and drainage-base septum resistances. Mechanical loading was done by direct addition of weights to the piston. The solids compressive pressure was calculated from these weights and the piston area (2.0742 in^2).

The fluid feed and measuring accessories are shown in Figure 2. A 2-liter aspirator bottle was fitted with a stopper and glass tube to serve as a constant head tank. The total pressure drop was kept constant by using the 50-ml automatic buret in conjunction with the constant head tank. A 5-ml microburet was used to collect the filtrate flow when rate measurements were taken. The two manometers were connected to the pressure-probes in the compression-permeability test cell. The difference in height between the two manometers gave the pressure drop over the cake.

Procedure for using the compression-permeability cell

The testing procedure consisted of placing a thick slurry in the cell chamber, gently inserting the piston and loading it with weights, passing clear filtrate through the confined cake and measuring the rate in the 5-ml buret.

The most difficult part of the procedure was to assemble the cell without any trapped air bubbles. By immersing the cylinder, drainage-base and drainage-base support in water and then assembling, this problem was overcome. The Tygon tubing from the 50-ml buret was attached to the assembled cylinder

Figure 2. Schematic drawing of fluid feed and measuring accessories for the compression-permeability test cell

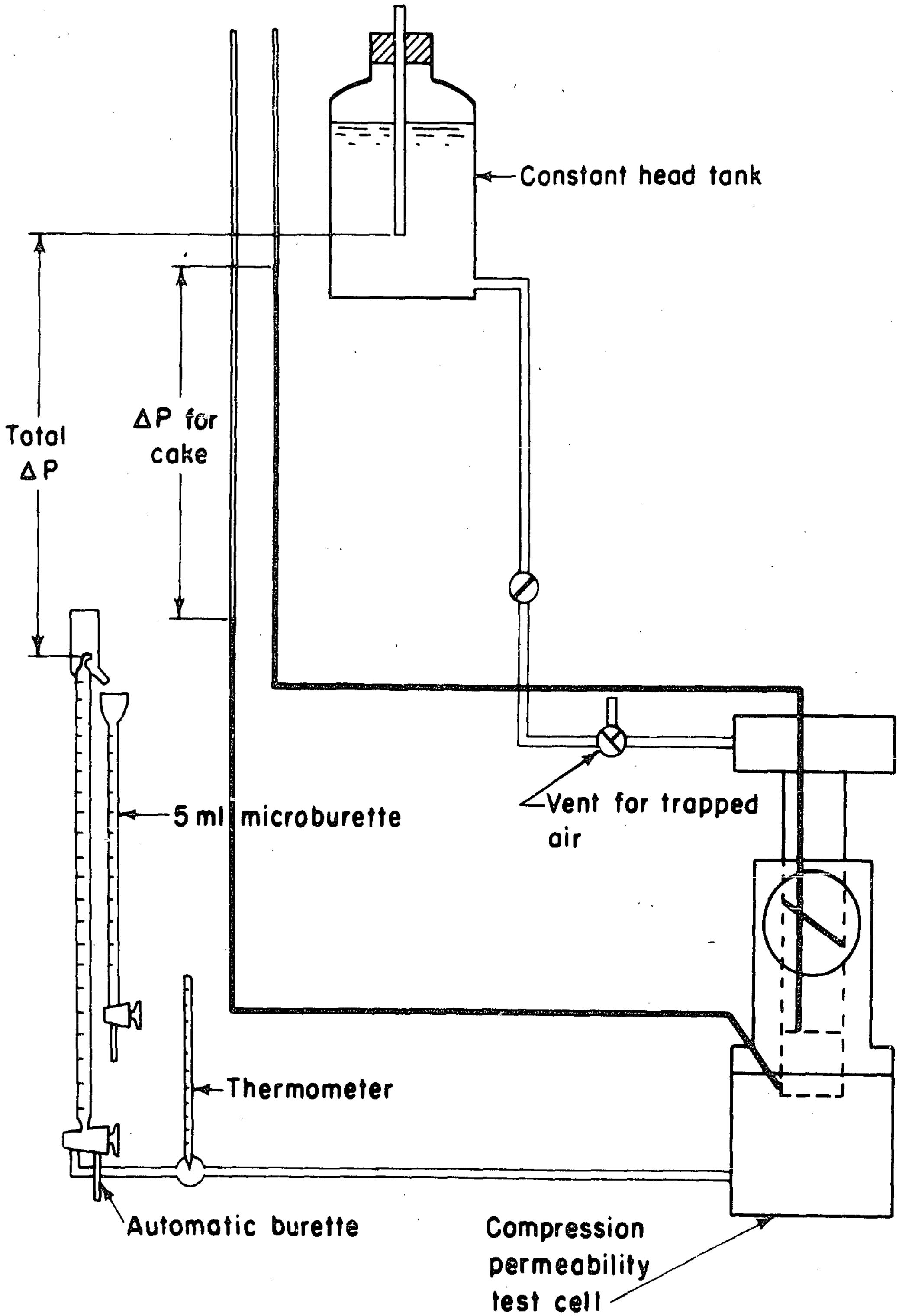
Constant head tank
Total
ΔP
ΔP for
cake
5 ml microburette
Vent for trapped
air
Thermometer
Automatic burette
Compression
permeability
test cell

and drainage-base support before it was removed from the water. After removing this portion of the cell from the water, some of the water was removed from the cylinder. The thick slurry was then poured into the cylinder.

The hollow piston was connected to the Tygon tubing from the constant-head tank and filled with water. A piece of filter paper was placed over the end of the piston and held there by the brass ring. The piston was then placed into the cylinder and the excess water along with any air was forced out and escaped by proper positioning of the 3-way stopcock. When the piston movement slowed, the 3-way stopcock was turned to allow flow from the constant-head tank. The weights were then added to the piston. About one-half hour was required for the manometers to stabilize. The dial gage reading was then taken for the porosity determinations. The pressure drop, rate and temperature were taken for the specific resistance determinations.

Constant Pressure Filtration Equipment

Description of apparatus

The essential items comprising this apparatus are the regulated nitrogen pressure cylinder, surge tank, stirred slurry tank, wash tank, filter chamber, and balance for determining filtration rates.

A schematic drawing of the filtration apparatus is shown in Figure 3. The nitrogen pressure was controlled by a Matheson gas regulator. The surge tank was an oxygen cylinder of the type and size used by skin divers.

The slurry tank and wash tank were made from two 12-inch lengths of 6-inch extra heavy seamless pipe with a wall thickness of 0.432-inches. The bottom closure was a 3/4-inch steel plate with a drain hole drilled and tapped for 3/8-inch pipe. The cover plate was 1 3/4-inches thick and held on with twelve 3/4-inch bolts. The lip to which the cover was attached was also 1 3/4-inches thick and was welded to the pipe. A 7-inch O-ring provided the seal for the cover plates. To prevent corrosion, the pressure tanks were cadmium plated. They were tested by Patzig Testing Laboratories, Ingersoll Avenue, Des Moines, Iowa. The following is quoted from a letter dated April 5, 1960 describing their test number 94694.

> "We assembled each of these pressure vessels with the bolts and O-rings furnished. Both vessels were pressurized to a water pressure of 1,000 pounds per square inch. The outside of the vessel was struck in various places with a 2 pound hammer. This pressure was held for a period of one hour or more. No leak was detected in either cylinder. After pressurizing at 1,000 pounds, the pressure was increased to the pressure of 1,500 psi and was maintained for a period of 10 to 15 minutes. Again, neither vessel showed leakage.
>
> The pressure was then increased to 2,000 pounds psi. Again, the pressure was maintained for 10 to 15 minutes and no leaking was detected at this pressure."

The slurry tank cover plate was fitted with a specially designed water-cooled high pressure packing gland and stirrer obtained from Autoclave Engineers. The pressure gages shown

Figure 3. Schematic drawing of constant pressure filtration apparatus and the external and internal wiring diagrams of the transducers

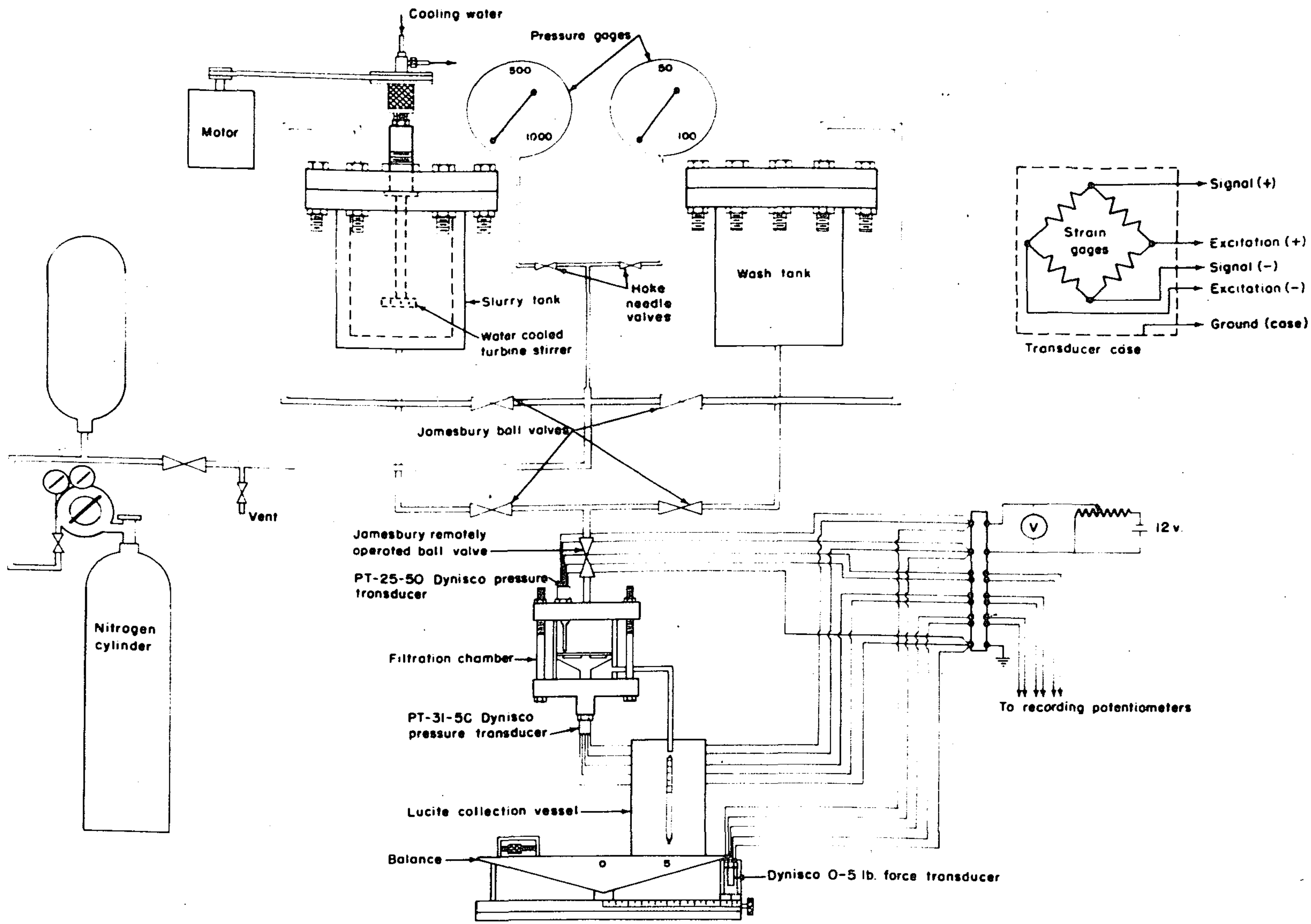

Cooling water
Pressure gages
500
1000
50
100
Motor
Slurry tank
Water cooled turbine stirrer
Hoke needle valves
Wash tank
Signal (+)
Strain gages
Excitation (+)
Signal (−)
Excitation (−)
Ground (case)
Transducer case
Jamesbury ball valves
Vent
Nitrogen cylinder
Jamesbury remotely operated ball valve
PT-25-50 Dynisco pressure transducer
Filtration chamber
PT-31-5C Dynisco pressure transducer
Lucite collection vessel
Balance
0
5
Dynisco 0-5 lb. force transducer
V
12 v.
To recording potentiometers

in Figure 3 were 0-1,000 psi and 0-100 psi Marshalltown gages.

A detailed drawing of the filter chamber, designed to measure the pressure at the cake-septum interface and the septum solids pressure is shown in Figure 4. The top and bottom plates and the movable septum support were machined from brass. The O-rings shown prevented leakage of filtrate and slurry. The cylinder forming the filter chamber was made of Lucite. The pressure at the cake-septum interface was measured by a PT-25-50 Dynisco transducer which converts pressure to a millivolt reading and is linear in the 0-50 psi range. The probe was 1/16-inch stainless steel tubing and extended to a point .065-inch above the septum. The septum solids pressure was measured by a PT-31-5C Dynisco transducer which converts the water pressure in the confined space above the transducer to a millivolt reading and is linear in the 0-500 psi range. A photograph of the component parts and assembled filter chamber is shown in Figure 5.

The clear filtrate was collected in a plexiglass cylinder which rests on a platform balance. An FT-5 Dynisco force transducer located beneath the movable platform converted force to millivolts. It is linear in the 1-5 lb_f range. A photograph of the balance is shown in Figure 6.

The output millivolt signals of the transducers were fed to two E. H. Sargent recorders and a Bristol's recorder. The range of the two Sargent recorders was 25 millivolts and the chart speed was 0.20 inch per second. The range of the

Figure 4. Detailed drawing of filter chamber which is designed to measure the pressure at the cake septum interface and septum solids pressure

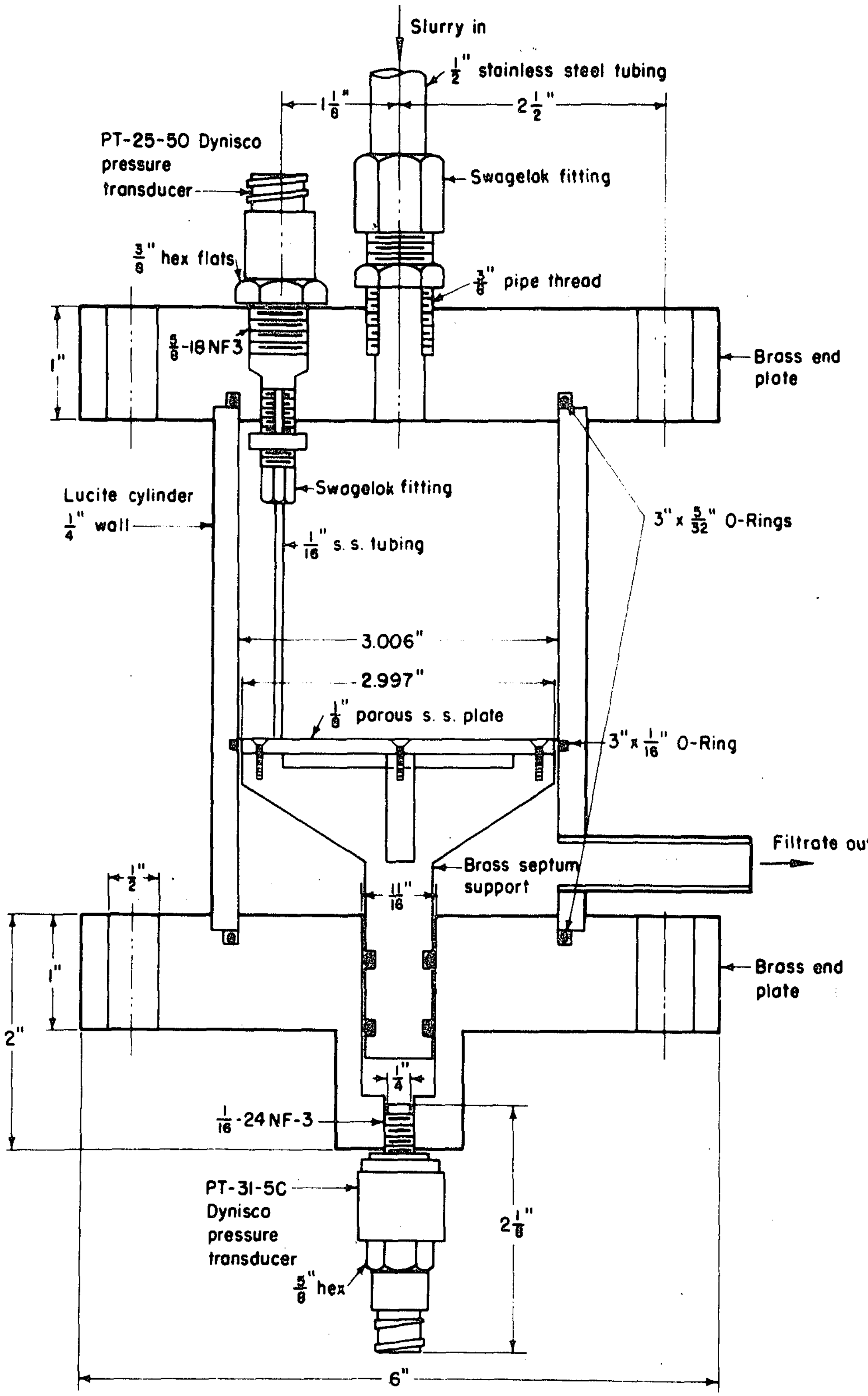
Slurry in
$\frac{1}{2}$" stainless steel tubing
$1\frac{1}{8}$"
$2\frac{1}{2}$"
PT-25-50 Dynisco pressure transducer
Swagelok fitting
$\frac{3}{8}$" hex flats
$\frac{3}{8}$" pipe thread
$\frac{5}{8}$-18 NF3
1"
Brass end plate
Lucite cylinder $\frac{1}{4}$" wall
Swagelok fitting
$\frac{1}{16}$" s. s. tubing
3" x $\frac{5}{32}$" O-Rings
3.006"
2.997"
$\frac{1}{8}$" porous s. s. plate
3" x $\frac{1}{16}$" O-Ring
Filtrate out
Brass septum support
$\frac{1}{2}$"
$\frac{11}{16}$"
1"
Brass end plate
2"
$\frac{1}{4}$"
$\frac{1}{16}$-24 NF-3
PT-31-5C Dynisco pressure transducer
$2\frac{1}{8}$"
$\frac{5}{8}$" hex
6"

Figure 5. Photographs of the component parts and assembled filter chamber

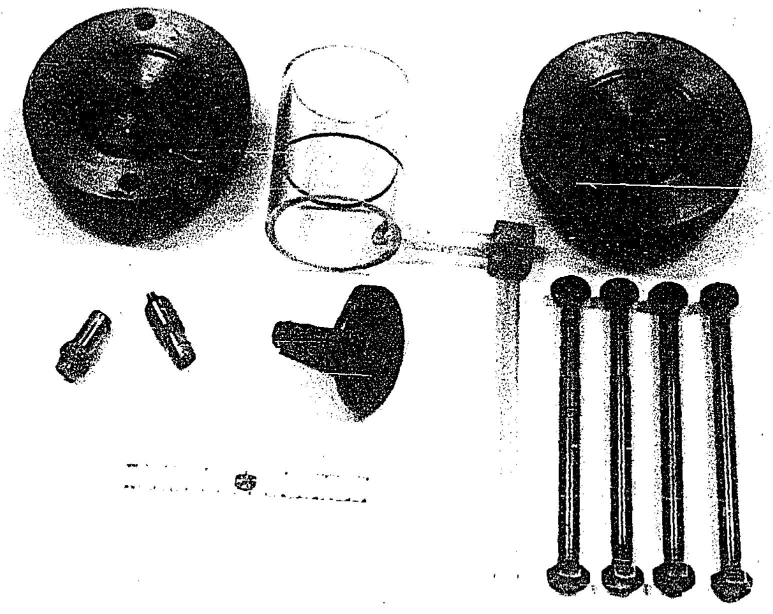

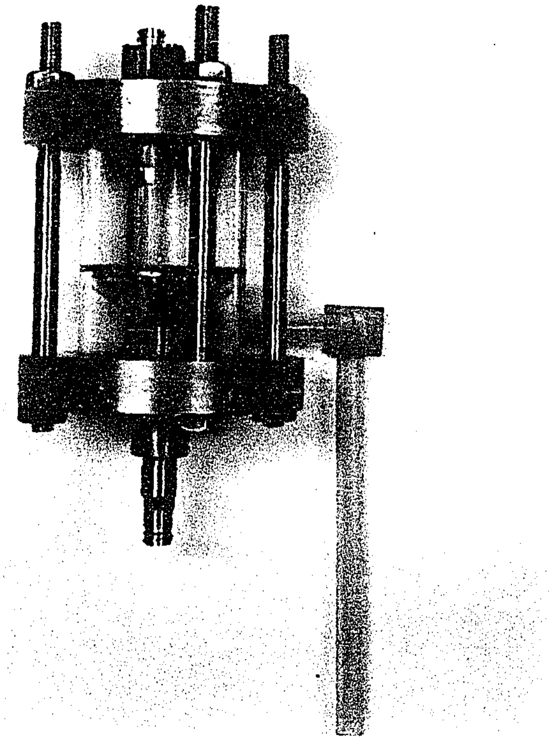

Figure 6. Photograph of balance for measuring filtrate volume as a function of time

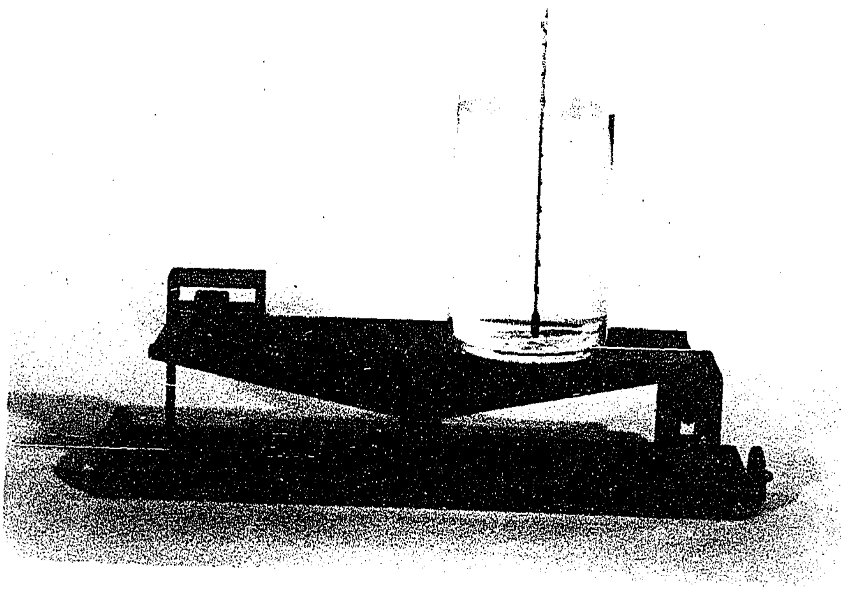

Bristol recorder was variable from 0-5 mv and to 0-50 mv and the chart speed was 0.25 inch per second.

Front and back photographs of the assembled filtration apparatus ready for use are shown in Figure 7.

Operating procedure for the filtration apparatus

A slurry of known solids content was introduced into the slurry tank. The valves were adjusted so that the slurry tank was pressurized and one of the two pressure gages was registering the pressure. The Jamesbury ball valve in the slurry line from the bottom of the slurry tank was opened. Slurry was prevented from entering the filter chamber at this time by a solenoid controlled, air-operated Jamesbury ball valve immediately before the filter chamber. The regulated air supply at 50 psi to operate the solenoid controlled ball valve was turned on. Cooling water to the slurry tank stirrer was turned on. The filter chamber had been filled with water and was attached to the slurry line. The 5-volt direct current transducer excitation voltage, recorders and stirrer were turned on. The balance had been assembled and was placed beneath the clear filtrate outlet. The recorders were zeroed. (The recorders must be zeroed because the transducers are strain-gages and due to the tightening torque, there is a small millivoltage which must be nulled.) The last switch thrown was the start filtration switch which controlled

Figure 7. Photographs of the front and back views of the constant pressure filtration apparatus

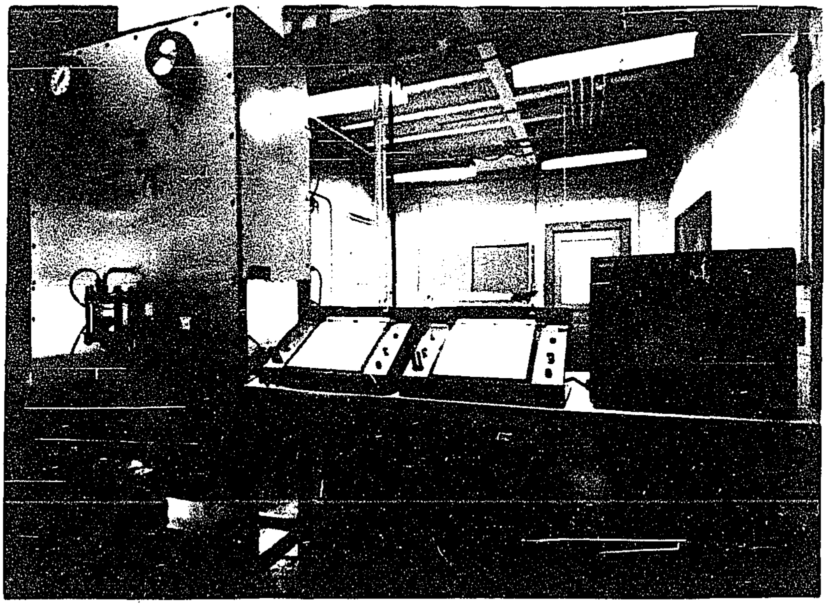

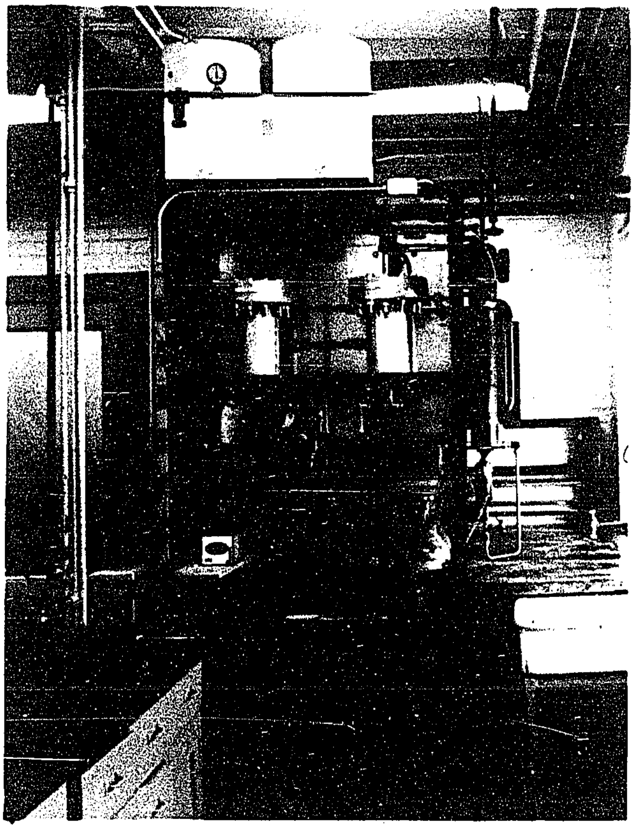

current to the solenoid operated ball valve. The volume of filtrate, septum solids pressure and liquid pressure at the cake septum interface are measured on the recorders simultaneously as a function of time. The temperature is obtained from a thermometer attached to the wall of the Lucite filtrate collection vessel. The constant pressure is obtained from one of the Marshalltown gages.

RESULTS AND DISCUSSION

Porosity-Time Determination

In the previous section the assumptions which are necessary if compression-permeability data is to be used for predicting filtration data were presented. Three experiments were proposed to determine the validity of these assumptions. In this section, the results of the first experiment are given.

Experimental procedure

Eight samples of calcium carbonate were thoroughly wetted with distilled water. Each sample had approximately the same weight of solids, W_c.

One of the samples was placed in the compression-permeability test cell under a solids compressive pressure of 8.69 psi. After about 3-minutes, a step change of 9.63 psi was applied to the piston. A Kodak Cine Special camera was set up to take pictures of the Ames dial and stop watch. An effective exposure of 1/400 second per frame was obtained by using a lens opening of F-8 and a speed of 64 frames per second. The camera was started a few seconds before the step change in pressure was applied. Measurements of cake height, L, and time, θ , were then obtained from the film strip by using a stop-motion movie projector.

This procedure was repeated for each sample using step changes in pressure of 19.25 psi, 29.31 psi, 39.07 psi, 49.21 psi, 58.83 psi, 68.89 psi and 78.52 psi. Each determination was made from the same initial value, 8.69 psi. Values of porosity were calculated from

$$(1-\epsilon_x) = \frac{W_c}{\rho_s A_c L} \tag{62}$$

where A_c = 2.074 in^2 and ρ_s = 2.711 gms per cm^3.

Results and discussion

The assumption tested in the first experiment was assumption 1 given on page 28:

> Since at a point, x, in a filter cake, the solids pressure, P_{sx}, and the porosity, ϵ_x are changing with time, then as P_{sx} increases by small increments, $P_{sx}(\theta_2)-P_{sx}(\theta_1) = \Delta P_{sx}(\theta)$, the porosity $\epsilon_x(\theta)$ has no time lag between $\epsilon_x(\theta_2)$, corresponding to $P_{sx}(\theta_2)$, and $\epsilon_x(\theta_1)$, corresponding to $P_{sx}(\theta_1)$.

The numerical data taken from the film strip is given in Tables 4 through 11 in the Appendix. These results are shown graphically in Figures 8 and 9 as log 10ϵ versus time in seconds. The slope, m', at the moment the step-change in pressure was applied, was taken from the graphs. The initial slope m' was plotted against the step-change in pressure, ΔP_{sx}, in Figure 10.

Figure 10 indicates that a ΔP_{sx} at least greater than 5 psi is necessary before any change in porosity occurs. Therefore at a point x in the filter cake where the solids

Figure 8. Plot of log 10ϵ versus time for initial slope determination

Run No. 2 ΔP_{sx} = 9.63 psi W_c = 19.5761 gms
Run No. 1 ΔP_{sx} = 19.25 psi W_c = 17.7966 gms
Run No. 8 ΔP_{sx} = 68.89 psi W_c = 19.4433 gms
Run No. 9 ΔP_{sx} = 78.52 psi W_c = 18.5493 gms

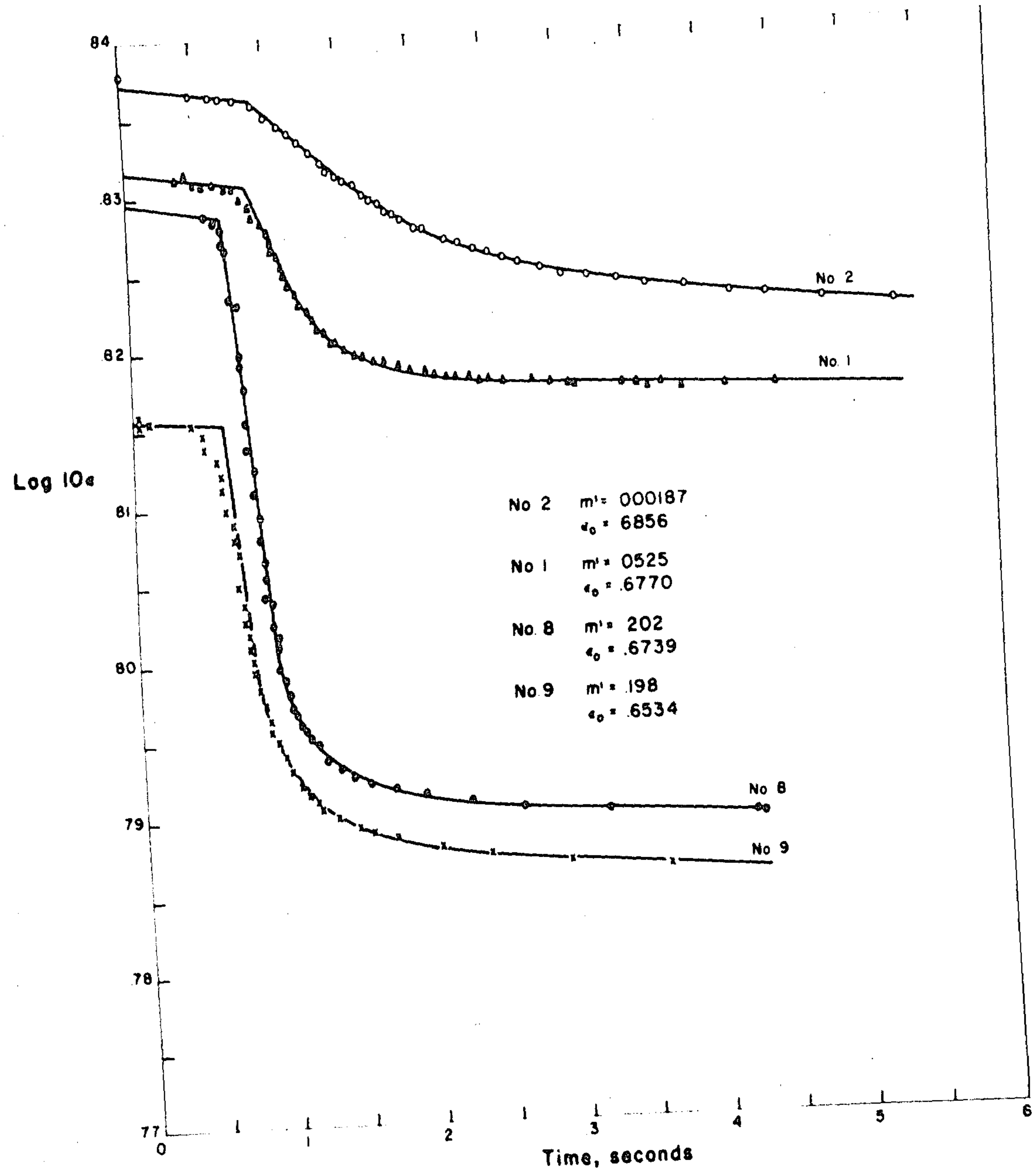
84
.83
.82
.81
.80
.79
.78
.77
Log 10e
No 2
No 1
No 8
No 9
No 2 m' = 000187 ϵ_0 = 6856
No 1 m' = 0525 ϵ_0 = .6770
No 8 m' = 202 ϵ_0 = .6739
No 9 m' = .198 ϵ_0 = .6534
0
1
2
3
4
5
6
Time, seconds

Figure 9. Plot of log 10ϵ versus time for initial slope determination

Run No. 4	ΔP_{sx} = 29.31 psi	W_c = 19.4206 gms
Run No. 5	ΔP_{sx} = 39.07 psi	W_c = 19.3847 gms
Run No. 6	ΔP_{sx} = 49.21 psi	W_c = 18.3985 gms
Run No. 7	ΔP_{sx} = 58.83 psi	W_c = 19.2608 gms

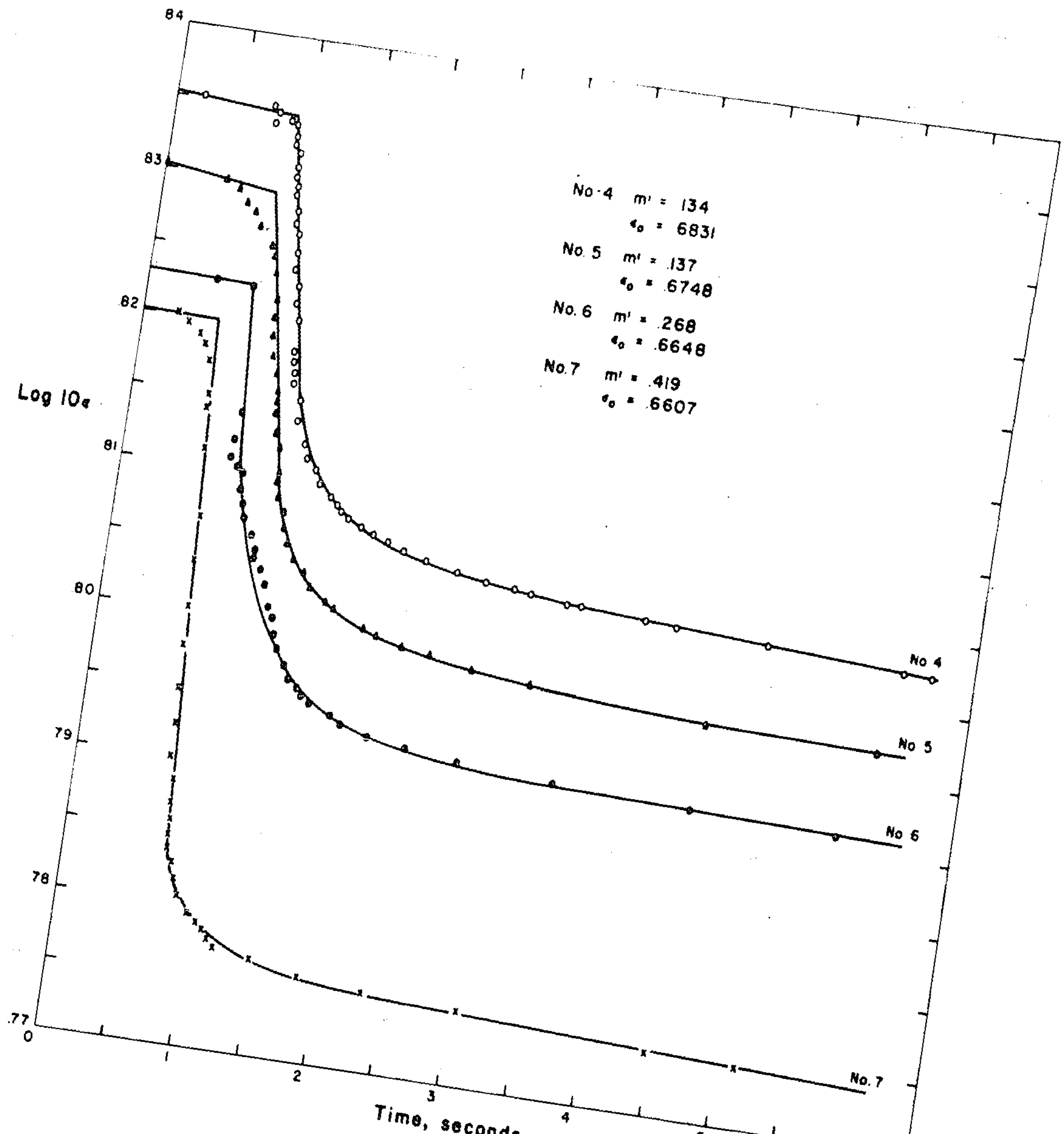
No.4 m' = .134
ϵ_0 = .6831
No. 5 m' = .137
ϵ_0 = .6748
No. 6 m' = .268
ϵ_0 = .6648
No.7 m' = .419
ϵ_0 = .6607
Log 10e
Time, seconds
No 4
No 5
No 6
No. 7
.84
.83
.82
.81
.80
.79
.78
.77
0
1
2
3
4
5
6

Figure 10. Plot of the initial slope, m', versus increment of solids pressure, ΔP_{sx}

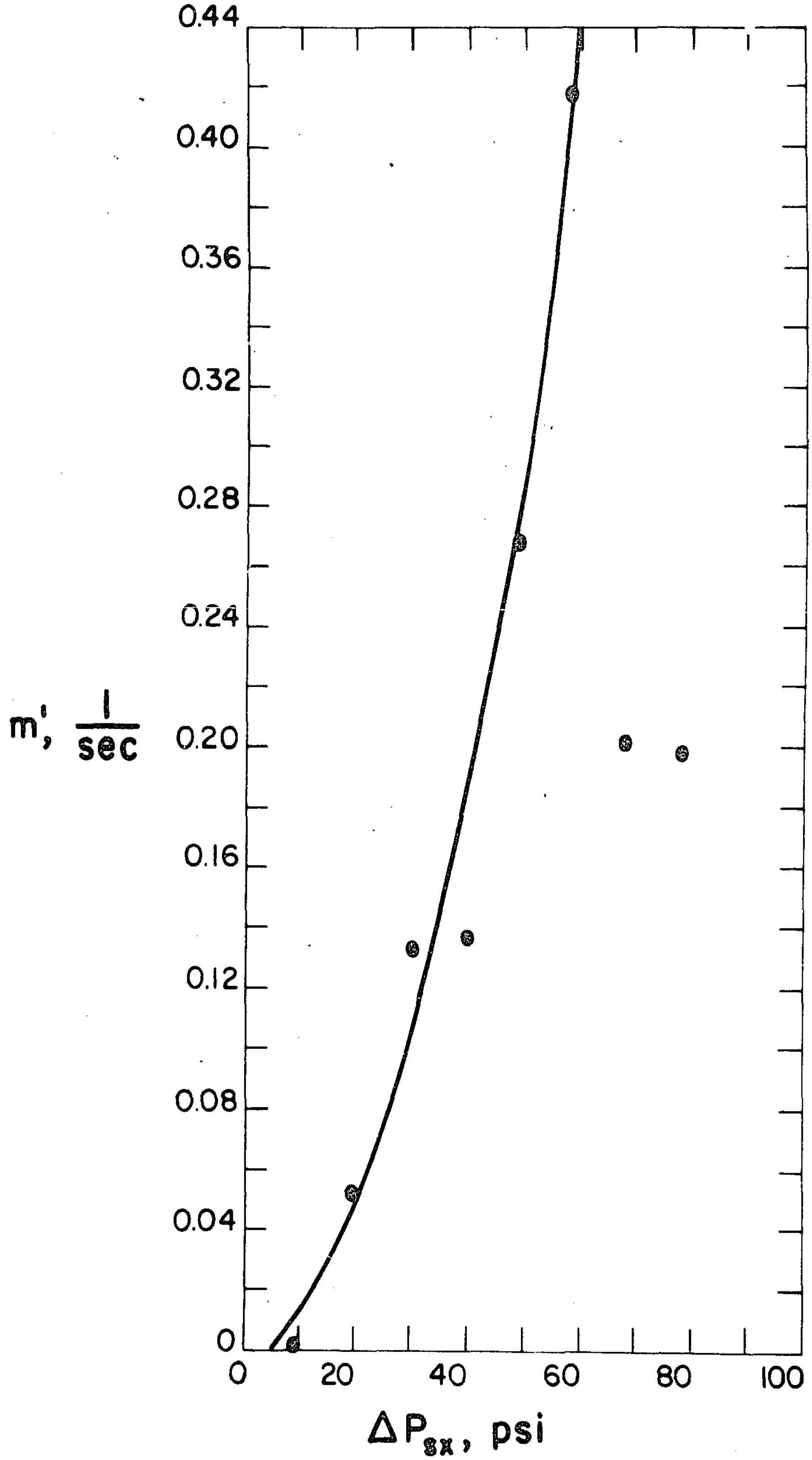
0.44
0.40
0.36
0.32
0.28
0.24
0.20
0.16
0.12
0.08
0.04
0
m', $\frac{1}{sec}$
0
20
40
60
80
100
ΔP_{sx}, psi

pressure is increasing continuously, there must be a total solids pressure increment of at least 5 psi before there is any change in porosity. Consequently assumption 1 is not valid for calcium carbonate. The time lag is at least the time necessary for P_{sx} to change 5 psi.

Assumption 1 would be valid if m' were zero or some positive value at $\Delta P_{sx}=0$. Other substances would probably have different curves but it is difficult to imagine a substance which would have a positive value of m' at $\Delta P_{sx}=0$. There may be materials which would have m'=0 at $\Delta P_{sx}=0$.

Determination of Relationship between P_{sx} and P_x

In this section, the results of the second experiment discussed in the Theory section are presented. This experiment was set up to test the second assumption necessary for the use of compression-permeability test data.

Experimental procedure

The constant pressure filtration apparatus and specially designed filter cell were used in these experiments. The material under study was calcium carbonate. The balance for measuring filtrate rate had ranges between 0-1 pound to 0-25 pounds capacity by moving the FT-5 force transducer to different positions under the right hand beam of the balance. The PT-25-50 pressure transducer, which measured P_1, had direct reading in pounds per square inch, after conversion from the millivolt reading by using the constant conversion factor of 2.1697 psi/mv.

Due to the O-ring seals, the PT-31-5C transducer does not read directly the septum pressure. The effect of all three O-rings was taken into account by removing only the top brass plate from the assembled filter cell and adding the weights to a cylinder placed inside the Lucite walls and resting on the porous stainless steel septum. This calibration force, F_c, was converted to pressure, p_c, by dividing by the septum area (7.0547 in^2). The transducer pressures, p_T, were recorded for known increases and decreases in p_c. The dead weight calibration pressures, p_c, and resulting transducer pressures p_T are given in Table 12 in the Appendix. This data is plotted as a calibration curve and used in subsequent filtration runs.

Due to the frictional flow of the filtrate through the septum itself, the PT-31-5C transducer measures not only the solids pressure, P_s, exerted by the cake solids on the septum but also the septum pressure, p_{sep}. Another calibration curve relating, P_1, the pressure at the cake septum interface to p_{sep}, the pressure due to the frictional flow of the filtrate through the septum is needed. This calibration curve was obtained by passing clear filtrate through the filter chamber and recording the values of P_1 and p_{sep}. This data is given in Table 13. The result of plotting this data is a straight line through the origin having a slope of 0.889. Therefore $p_{sep} = 0.889\ P_1$.

The millivolt reading from the PT-31-5C transducer was converted to pressure, p_T, using the conversion factor of 24.9501 psi/mv; this p_T was converted to the pressure on the septum using the dead-weight calibration curve. The resulting pressure was that due to the sum of the cake solids pressure and the pressure due to the flow through the septum, $(P_s + p_{sep})$. For any filtration, P_1 data is taken. By using the relation $p_{sep} = 0.889\ P_1$ the portion of the measured solids pressure attributable to the frictional flow through the septum can be subtracted from the sum, $(P_s + p_{sep})$.

Five filtrations were made at slurry concentrations, s, of .083, .134, .159, .193, and .231. The slurry concentrations were calculated from the total volume of filtrate collected and weight of solids in the filter chamber. The make-up slurries in the slurry tank had concentrations of .10, .15, .20, .25, and .30, respectively. These filtrations were run at constant pressures of 21.0 psi, 19.8 psi, 20.0 psi, 21.0 psi, and 21.0 psi, respectively.

The volume of filtrate was obtained by converting the millivolt reading of the FT-5 transducer to pounds using the constant .2713 lb_f/mv, and then to volume using the density of water at the temperature of the filtration.

Results and discussion

The assumption tested in the second experiment was assumption 2 given on page 29:

> The relationship, $dP_{sx} = -\epsilon_x dP_x$, between solids compressive pressure and liquid pressure is valid.

The data for the five filtrations are given in Tables 14 through 18 in the Appendix and are presented graphically in Figures 11 through 15. The volume-time data is plotted in the accepted manner as $\Delta\theta/\Delta V$ versus V in Figures 16 and 17.

Figures 11 through 15 show that the expression $dP_{sx} = -dP_x$ and consequently $P_s = P - P_l$ used by Tiller and others is not correct since P_s does not approach P as P_l approaches zero. The expression $dP_{sx} = -\epsilon_x dP_x$ seems to be correct and assumption 2 is considered valid.

The values of porosity obtained from the expression

$$\epsilon_{av} = \frac{P_s}{P-P_l} \tag{48}$$

are considered higher than they actually are since during a filtration, there is some blocking of the septum to flow. This results in a higher value of p_{sep} than that obtained from $p_{sep} = 0.889\ P_l$. Therefore the plot of p_{sep} versus P_l with a blocked septum would result in a value of slope greater than 0.889, which was obtained for the passage of clear filtrate. For more accurate values of ϵ_{av}, the calibration procedure used to obtain p_{sep} as a function of P_l should be slightly

Figure 11. Volume of filtrate V, applied pressure P, solids pressure P_s and hydraulic pressure, P_1, as functions of time for a constant pressure filtration

Run 1-F_{10}-20BA   s = .083   P = 21.0 psi

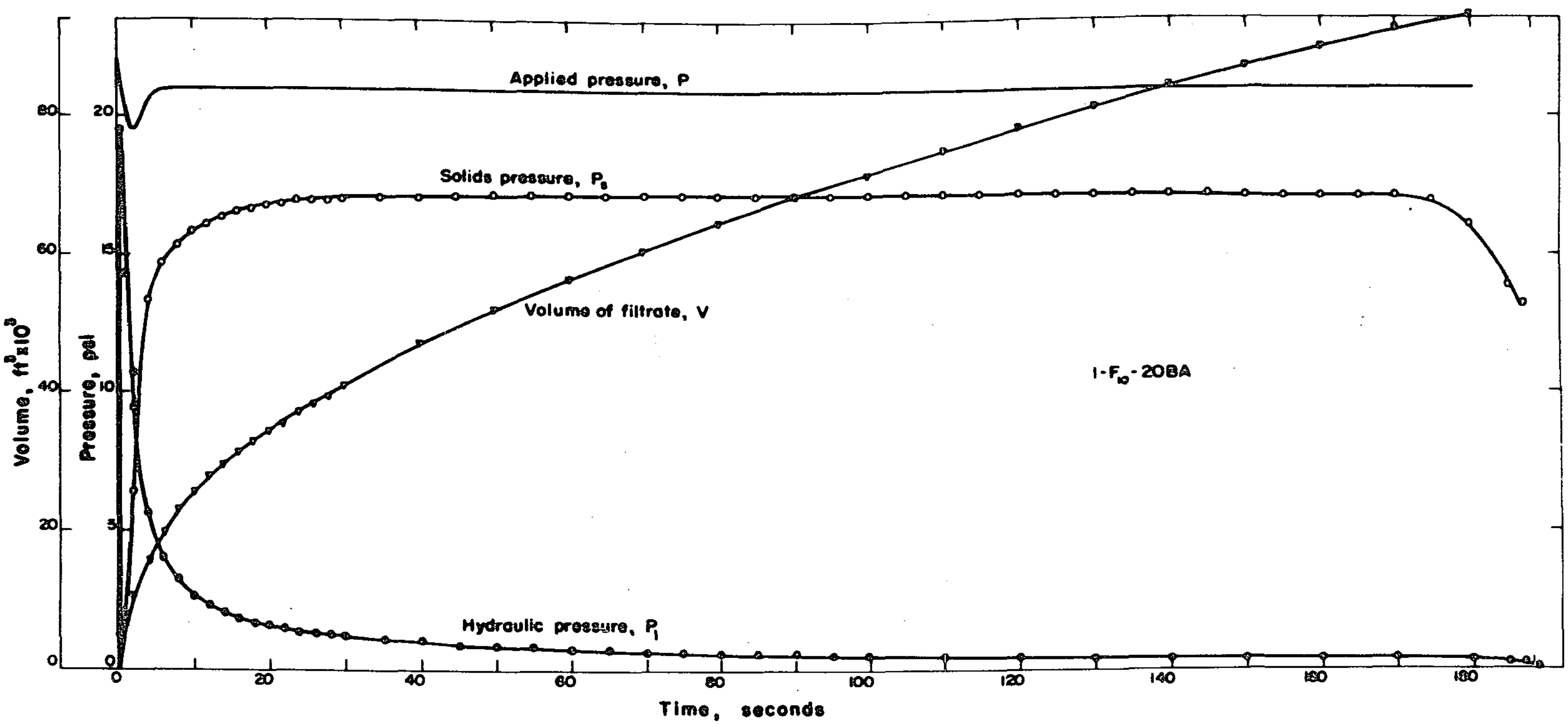
Applied pressure, P
Solids pressure, P_s
Volume of filtrate, V
Hydraulic pressure, P_l
1-F_{10}-20BA
Volume, $ft^3 \times 10^3$
Pressure, psi
Time, seconds
0
20
40
60
80
100
120
140
160
180
0
5
10
15
20
0
20
40
60
80

Figure 12. Volume of filtrate V, applied pressure P, solids pressure P_s, and hydraulic pressure P_1, as functions of time for a constant pressure filtration

Run 2-F_{15}-20BA s = .134 P = 19.8 psi

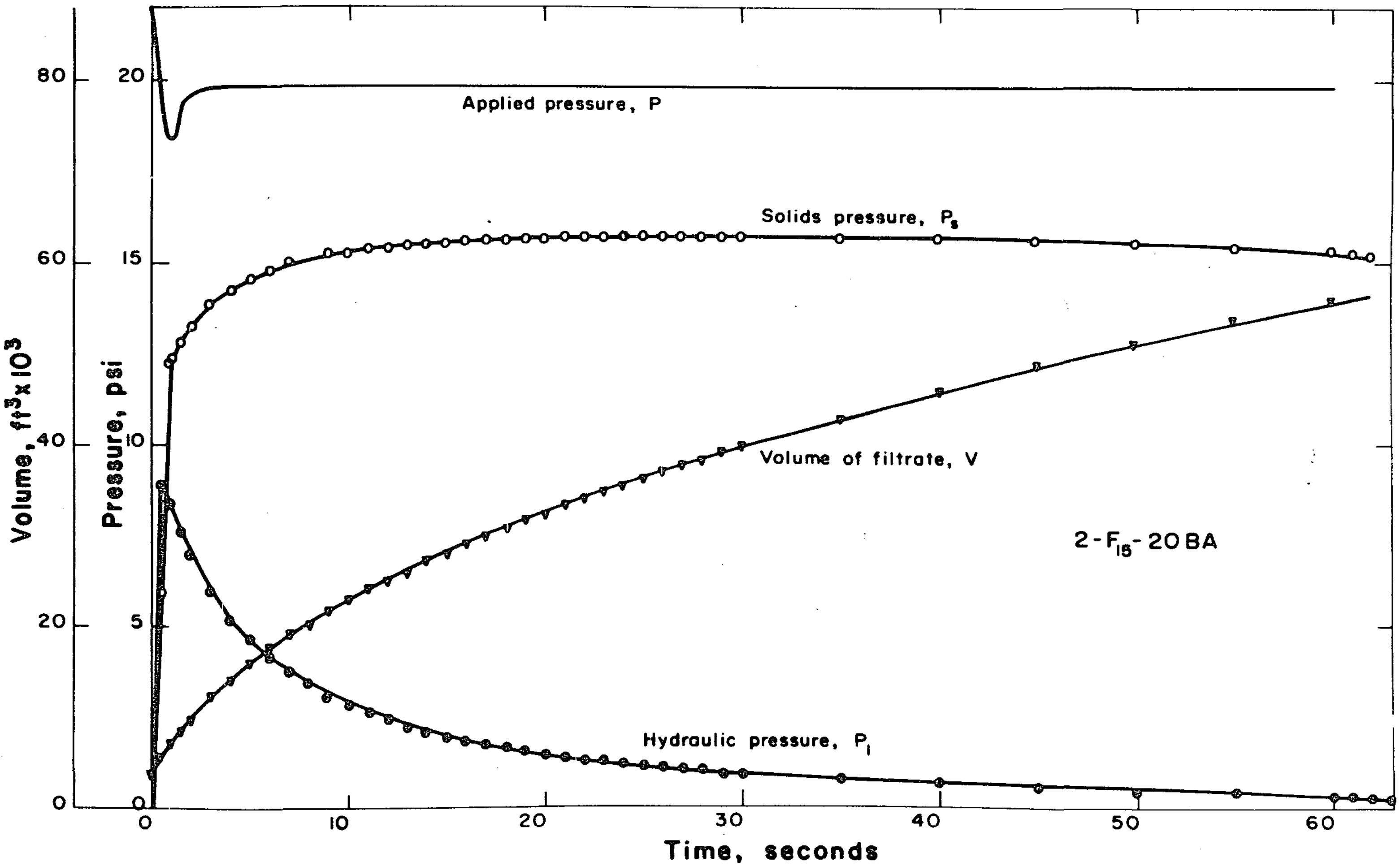
Applied pressure, P
Solids pressure, P_s
Volume of filtrate, V
Hydraulic pressure, P_l
2-F_{15}-20BA
Volume, $ft^3 \times 10^3$
Pressure, psi
Time, seconds
0
20
40
60
80
0
5
10
15
20
0
10
20
30
40
50
60

Figure 13. Volume of filtrate V, applied pressure P, solids pressure P_s, and hydraulic pressure P_l, as functions of time for a constant pressure filtration

Run $3\text{-}F_{20}\text{-}20BA$ $\quad s = .159 \quad P = 20.0$ psi

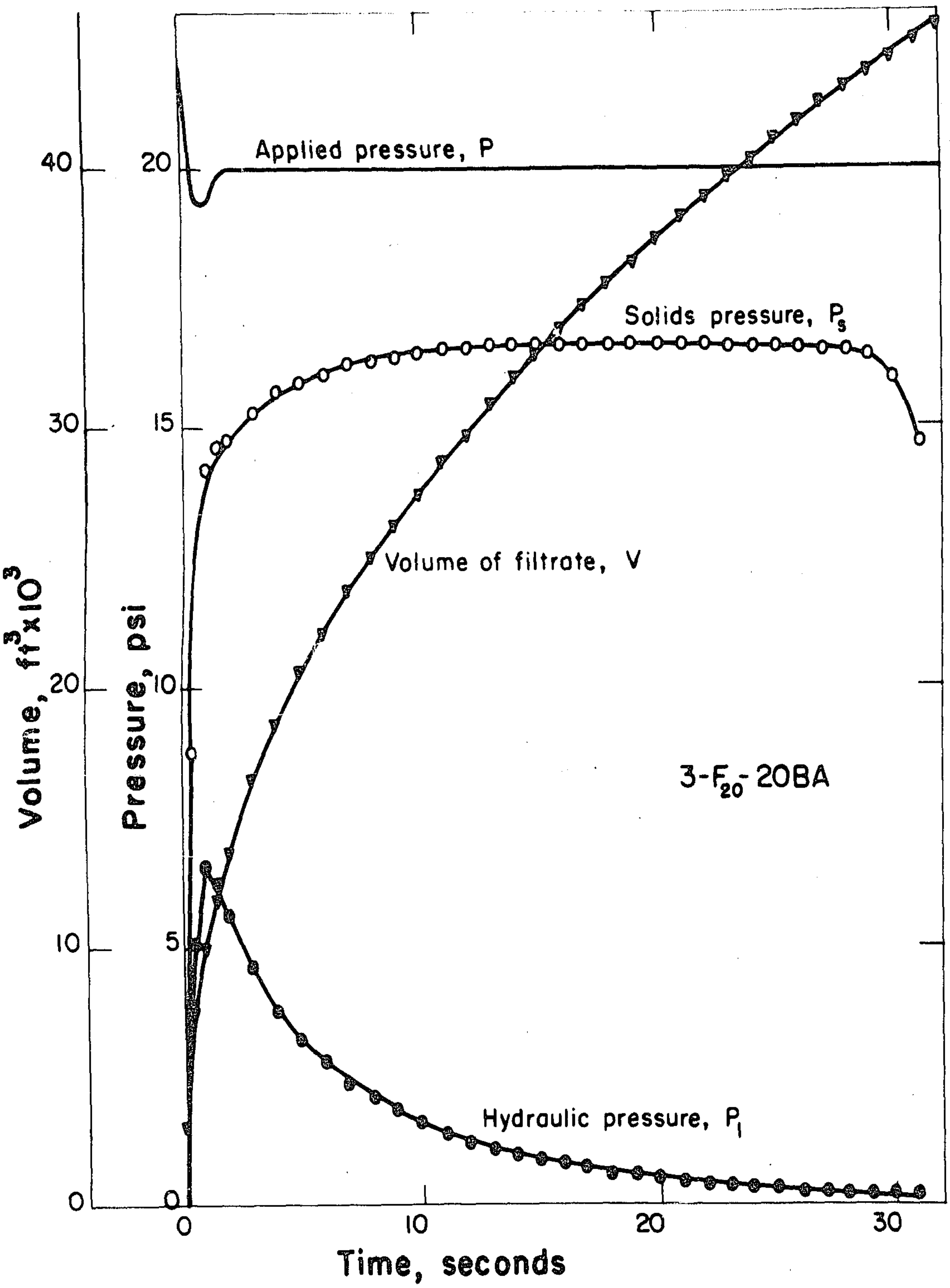
Applied pressure, P
Solids pressure, P_s
Volume of filtrate, V
Hydraulic pressure, P_l
3-F_{20}-20BA
Volume, $ft^3 \times 10^3$
Pressure, psi
Time, seconds
0
10
20
30
40
5
15

Figure 14. Volume of filtrate V, applied pressure P, solids pressure P_s, and hydraulic pressure P_l, as functions of time for a constant pressure filtration

Run 5-F_{25}-20BA   s = .193   P = 21.0 psi

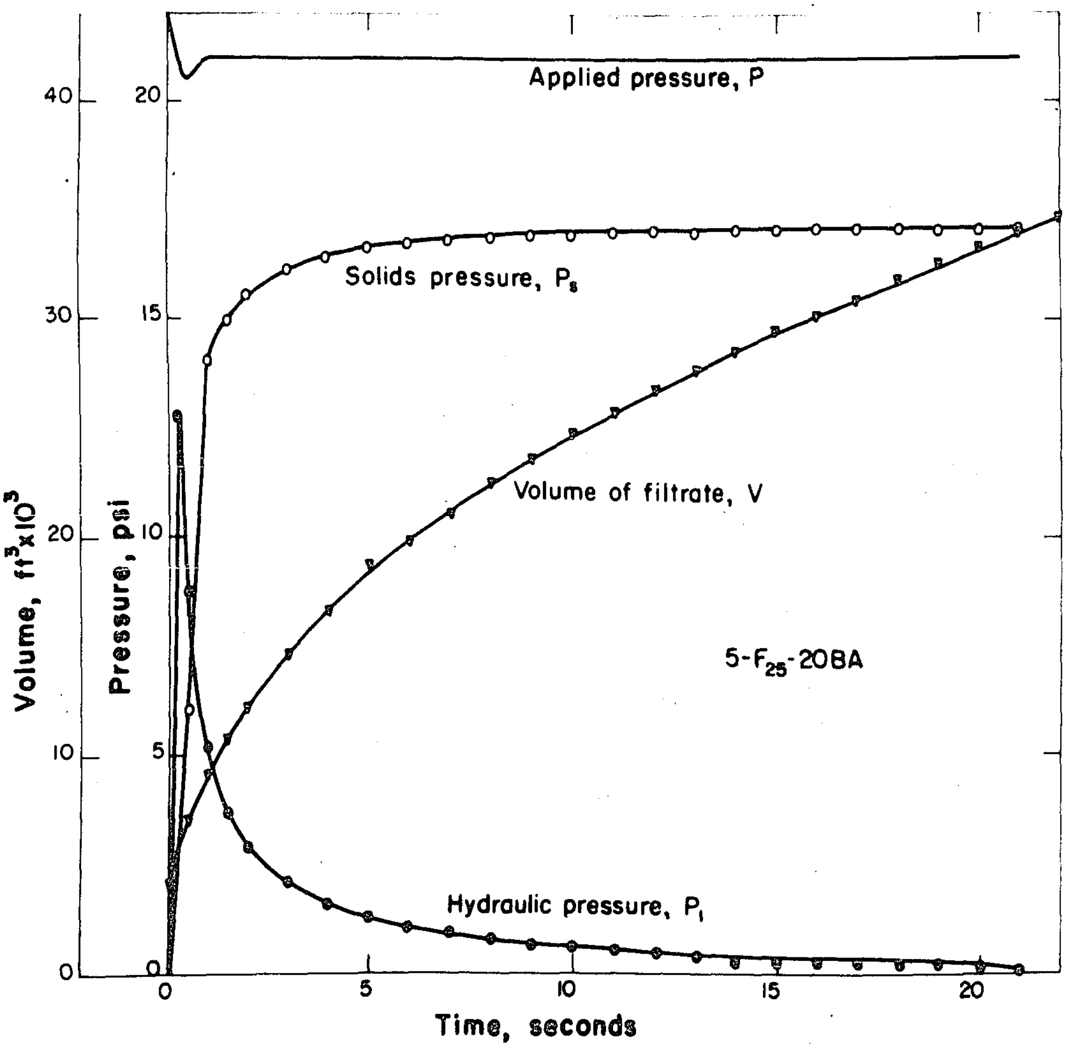
Applied pressure, P
Solids pressure, P_s
Volume of filtrate, V
$5\text{-}F_{25}\text{-}20BA$
Hydraulic pressure, P_l
Volume, $ft^3 \times 10^3$
Pressure, psi
Time, seconds
0
5
10
15
20
30
40

Figure 15. Volume of filtrate V, applied pressure P, solids pressure P_s, and hydraulic pressure P_1, as functions of time for a constant pressure filtration

Run 8-F_{30}-20BA   s = .231   P = 21.0 psi

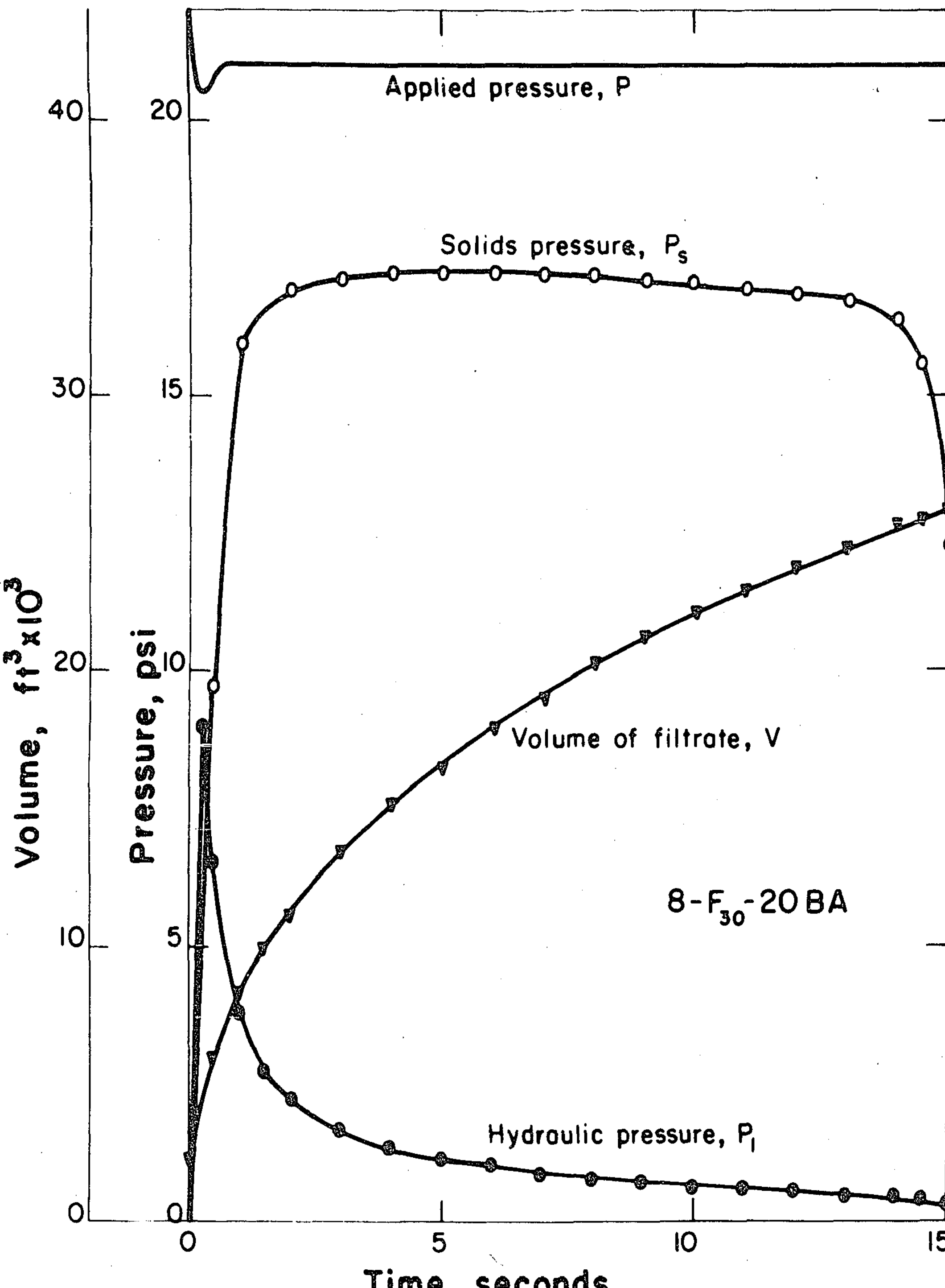
Applied pressure, P
Solids pressure, P_s
Volume of filtrate, V
Hydraulic pressure, P_l
8-F_{30}-20BA
Volume, $ft^3 \times 10^3$
Pressure, psi
Time, seconds
0
10
20
30
40
0
5
10
15
20
0
5
10
15

Figure 16. Plots of $\Delta\theta/\Delta V$ versus V for constant pressure filtrations

Run 1-F_{10}-20BA	Run 2-F_{15}-20BA
$W = .5747\ lb_m$	$W = .6056\ lb_m$
$\epsilon_{av} = .655$	$\epsilon_{av} = .632$

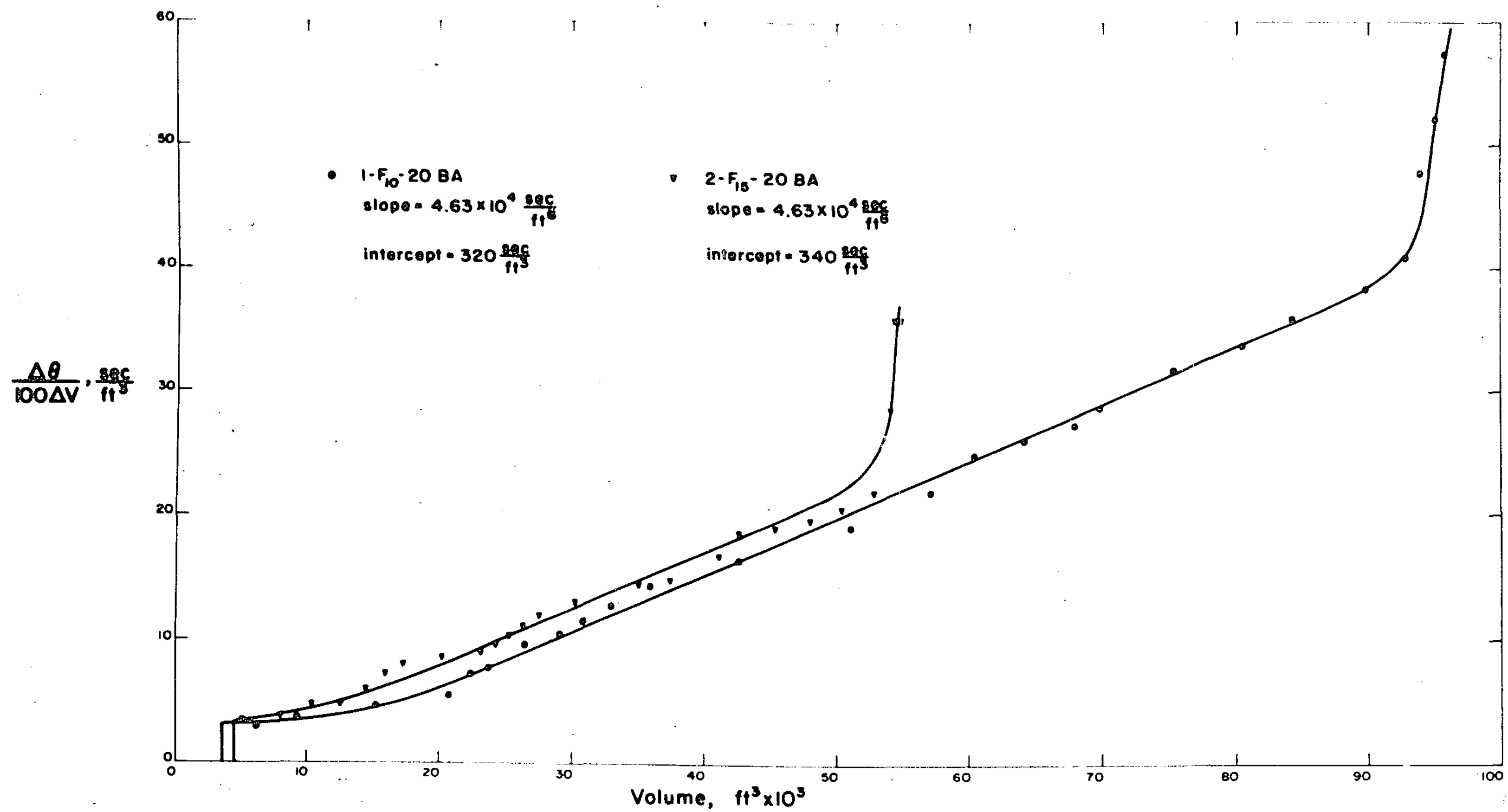

1-F10-20 BA
slope = 4.63 x 10^4 sec/ft^6
intercept = 320 sec/ft^3
2-F15-20 BA
slope = 4.63 x 10^4 sec/ft^6
intercept = 340 sec/ft^3
Δθ/100ΔV, sec/ft^3
Volume, ft^3 x 10^3
0
10
20
30
40
50
60
70
80
90
100

Figure 17. Plots of $\Delta\Theta/\Delta V$ versus V for constant pressure filtrations

Run 3-F_{20}-20BA	Run 5-F_{25}-20BA	Run 8-F_{30}-20BA
W = .6056 lb_m	W = .6121 lb_m	W = .6024 lb_m
ϵ_{av} = .632	ϵ_{av} = .632	ϵ_{av} = .638

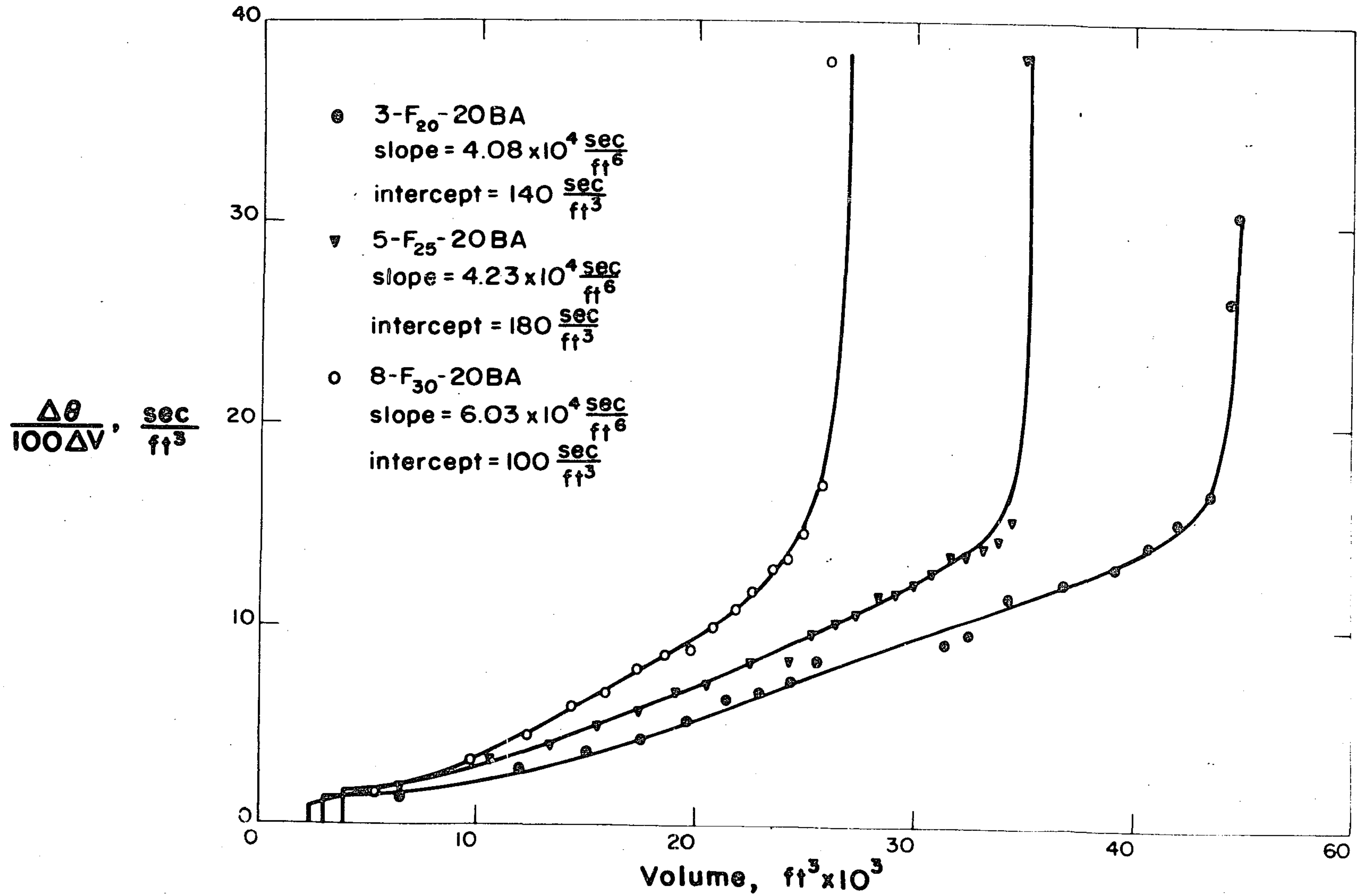

3-F20-20BA
slope = 4.08 x 10^4 sec/ft^6
intercept = 140 sec/ft^3
5-F25-20BA
slope = 4.23 x 10^4 sec/ft^6
intercept = 180 sec/ft^3
8-F30-20BA
slope = 6.03 x 10^4 sec/ft^6
intercept = 100 sec/ft^3
Δθ/100ΔV, sec/ft^3
Volume, ft^3 x 10^3
0
10
20
30
40
60

modified. This is the only place in the procedure where there is a possibility of recognized experimental error but even this error is in the proper direction to accept the relation $dP_{sx} = -\epsilon_x dP_x$ and the assumption. In addition, for the clear filtrate relationship $p_{sep} = 0.889\ P_1$, a much more severe test of the equation $dP_{sx} = -\epsilon_x dP_x$ is obtained.

The volume-time, when plotted in the usual manner and shown in Figures 16 and 17, confirms Tiller's prediction that $\Delta\theta/\Delta V$ versus V are curved lines for short filtrations. In addition, Figures 16 and 17 indicate that the initial phases of filtrations, plotted in this manner, are curved. Thus, the septum resistances, R_m, obtained from the intercept of a straight line extrapolation of $\Delta\theta/\Delta V$ versus V are low.

Determination of the Relationship between P_{sx}, ϵ_x, α_x by Statistical Analysis of Compression-Permeability Test Data

In this section, the third experiment which is described in the Theory section is discussed. This experiment evaluates the validity of the third assumption intrinsic to compression-permeability testing.

Experimental procedure

The assembly and operation of the compression-permeability test cell is described in the Equipment and Procedure section. The only exception to this operating procedure was that one-hour was allowed after the addition of weights to the piston before measurements of porosity and specific resistance were made. The total constant head was 63.80 cm of water. The head loss over the cake alone varied and was measured by the pressure probes and manometers. All determinations of porosity and specific resistance were made at the same solids pressure, 24.99 psi.

The following procedure was used in making up the calcium carbonate samples: the contents of a 5-pound jar of calcium carbonate were placed in a laboratory size V-mixer and allowed to mix for one-hour. From this mixture, five 200-gram portions were extracted and labeled M_i $(i = 1,..,5)$. From each of the M_i, 5-samples, W_k $(k = 1,..,5)$ of exactly 10, 15, 20, 25 and 30 grams were weighed out using an analytical balance.

A statistical analysis was necessary because each α_x and ϵ_x determined from compression-permeability measurements is affected by the test cell, the operator (time) and the material itself. The effect of the test cell is most likely to manifest itself through the geometry of the cake chamber. The simplest way to change the geometry of the cake chamber is to vary the cake weight. Consequently, weight was chosen as one of the components of variance. The time effect is that due to the proficiency of the operator at the time of a test. The effect of the material is due to sampling and to the shape, size, orientation and physical structure of the particles. Of these factors, provision was made for sampling variation and orientation. The orientation is taken into account by performing replications at the same P_{sx} on the same sample.

To analyze the specific resistance and porosity data, a Latin square analysis of variance was used. The rows of this design were designated M_i ($i = 1,..,5$) and the columns were designated T_j ($j = 1,..,5$) for time interval. Each weight was assigned at random within a row M_i and column T_j so that all weights appeared in each M_i and T_j. Thus the weights, W_k, were fixed by designating a M_i and T_j. To determine the significance of orientation or packing arrangements, five replications l ($l = 1,..,5$) were made for each W_k. At each replication l, two specific resistance determinations and one porosity measurement (two rate measurements at one cake height) were made.

Samples were designated as M_iT_j-W_k-l which refers to the lth replication of the kth W gram sample taken from the ith mixture, M_i and run in the jth time interval, T_j. Due to the order in which the samples were taken, k = i and hence the subscript on the W was dropped. A time interval was chosen as that length of time required to run one column of samples.

To make a replication at a given solids weight, the compression-permeability test cell was dismantled and the cake was removed, placed in a beaker of distilled water and stirred. The resulting slurry was then reintroduced into the test cell for another determination of specific resistance and porosity. During the course of the transfer, some solids were lost.

Therefore, at the end of a set of replications, the dried cake was again weighed. The total loss, usually about one-gram, was divided equally among the last four replications.

Results and discussion

The assumption tested in the third experiment was assumption 3 given on page 29:

> The point specific resistance, α_x, of a given solid is determined by the porosity, ϵ_x, which in turn depends upon the solids compressive, P_{sx}.

The results of the 250 specific resistance determinations and 125 porosity measurements are given in Table 19 in the Appendix. The Latin square analysis of variance for the specific resistances and porosities is given in Tables 1 and 2. The 10^9 for each α_x entry in Table 19 in the Appendix was dropped since it does not affect the analysis of variance calculations or conclusions.

Possibly the best way to interpret Table 1 is to consider the Latin square model used. Let the subscript m denote the determination (the other subscripts have been defined). The model is

$$(\alpha_x)_{ijklm} = \mu + \tau_k + A_i + B_j + \gamma_{ij(k)} + \eta_{ijkl} + \delta_{ijklm}$$

where μ is an over-all mean; τ_k is the true effect of the kth weight; the A_i's are random components associated with mixtures and have variance σ_A^2; the B_j's are random components associated with time (operator) and have variance σ_B^2, the

Table 1. Latin square analysis of variance for specific filtration resistances, α_x, obtained at a solids pressure of 24.99 psi

Source of variation	Degrees of freedom	Sum of squares	Mean square	Expected mean square
Mixture	4	95.558	23.890	$\sigma_\delta^2 + 2\ \sigma_\eta^2 + 10\ \sigma_\gamma^2 + 50\ \sigma_A^2$
Time	4	553.891	138.473	$\sigma_\delta^2 + 2\ \sigma_\eta^2 + 10\ \sigma_\gamma^2 + 50\ \sigma_B^2$
Weight	4	334.124	83.531	$\sigma_\delta^2 + 2\ \sigma_\eta^2 + 10\ \sigma_\gamma^2 + 50\ \sigma_\tau^2$
Error	12	1146.978	95.582	$\sigma_\delta^2 + 2\ \sigma_\eta^2 + 10\ \sigma_\gamma^2$
Packing (Repl.)	100	1633.017	16.330	$\sigma_\delta^2 + 2\ \sigma_\eta^2$
Determinations	125	2.159	.0173	σ_δ^2

Table 2. Latin square analysis of variance for porosities, ϵ_x obtained at a solids pressure of 24.99 psi

Source of variation	Degrees of freedom	Sum of squares	Mean square	Expected mean square
Mixture	4	.0005	1.25×10^{-4}	$\sigma_{\eta}^2 + 5\sigma_{\gamma}^2 + 25\sigma_{A}^2$
Time	4	.0048	24.0×10^{-4}	$\sigma_{\eta}^2 + 5\sigma_{\gamma}^2 + 25\sigma_{B}^2$
Weight	4	.0063	15.75×10^{-4}	$\sigma_{\eta}^2 + 5\sigma_{\gamma}^2 + 25\sigma_{\tau}^2$
Error	12	.0037	3.08×10^{-4}	$\sigma_{\eta}^2 + 5\sigma_{\gamma}^2$
Packing (Repl.)	100	.0272	2.72×10^{-4}	σ_{η}^2

η_{ijkl} are random components associated with packing and have variance σ_η^2 ; and the δ_{ijklm} are random components due to determination and have variance σ_δ^2.

The estimates of $\sum_k \tau_k^2$ and σ_A^2 are zero and the estimate for σ_δ is $\sqrt{.017} = .130$. The estimate of σ_B is

$$\hat{\sigma}_B = \sqrt{\frac{138.473 - 83.531}{50}} = 1.048$$

The estimate for σ_γ is

$$\hat{\sigma}_\gamma = \sqrt{\frac{95.582 - 16.330}{10}} = 2.815$$

The estimate for σ_η is

$$\hat{\sigma}_\eta = \sqrt{\frac{16.330 - .0173}{2}} = 2.868$$

The main sources of variation in $(\alpha_x)_{ijklm}$ were due to packing, σ_η , and what is termed experimental error, σ_γ. The standard deviation due to experimental error, σ_γ was due to sources of variation which have not been considered in the design of the experiment. For this reason, both of these sources of variation were considered attributable to the material. The standard deviation due to mixtures, σ_A, was zero, as expected, since the calcium carbonate was well mixed.

Before any conclusions were drawn, the analysis of variance for porosities was considered. The Latin square model for porosities is

$$(\epsilon_x)_{ijkl} = \mu + \gamma_k + A_i + B_j + \gamma_{ij(k)} + \eta_{ijkl}$$

where the symbols have the same meaning given previously, but in this case applied to porosity. Estimates of the standard deviations are

$$\hat{\sigma}_{\gamma} = \sqrt{\frac{15.75 \times 10^{-4} - 3.083 \times 10^{-4}}{25}} = 7.12 \times 10^{-3}$$

$$\hat{\sigma}_A = 0$$

$$\hat{\sigma}_B = \sqrt{\frac{24.0 \times 10^{-4} - 15.75 \times 10^{-4}}{25}} = 5.75 \times 10^{-3}$$

$$\hat{\sigma}_{\gamma} = \sqrt{\frac{3.083 \times 10^{-4} - 2.720 \times 10^{-4}}{5}} = 2.69 \times 10^{-3}$$

$$\hat{\sigma}_{\eta} = \sqrt{2.72 \times 10^{-4}} = 16.5 \times 10^{-3}$$

Even with the large packing standard deviation, σ_{η}, which in part might be explained by the weight loss in making replications, the F-test shows that the components of variance due to weight (cell geometry) and time were significant at the 5% level. Most important, the experimental error, σ_{γ}, was small which means that the Latin square model chosen does, in fact, account for the main sources of variation in determination of porosities from compression-permeability measurements.

Since the specific resistances, α_x, and porosities, ϵ_x, are related by measurement in a compression-permeability test cell, both of the analysis of variance tables must be considered together. The main conclusion is that the Latin square model chosen explains the major variations occurring in the measurement of porosities but not the variation occurring in specific resistance. Thus, the variability in α_x is due to other sources, in addition to those accounted for, which are not easily defined or practically controllable. On this basis then, the third assumption intrinsic to compression-permeability testing is not valid to the extent that α_x is determined by P_{sx}.

Since variance in weight was significant in the porosity measurements the data shown in Table 3 are, in fact, acceptable and there is a geometry effect on porosities due to the test cell itself.

Table 3. Average values of porosity taken over 25 measurements at each weight indicated

Weight in grams	Average ϵ_x
10.0	0.6188
15.0	0.6259
20.0	0.6328
25.0	0.6335
30.0	0.6394

Any effects of cell geometry on specific resistance determinations is masked by the large experimental error.

CONCLUSIONS

The direct comparison of compression-permeability data and filtration resistance data used by other investigators has not been conclusive in determining the validity of the compression-permeability technique because no resolution is possible when the data do not agree. As a result, the direct comparison method leads to a continued effort to take data until there is agreement. In this thesis, instead of direct comparison, each assumption necessary for the validity of compression-permeability testing was investigated by experiment.

The first experiment was to test the compression-permeability assumption that as $P_{sx}(\theta)$ varies with time, at a point in a filter cake, the porosity $\epsilon_x(\theta)$ at any instant is the equilibrium porosity at $P_{sx}(\theta)$. The data from this experiment indicates that the assumption is not valid and that some finite increment (about 5 psi for calcium carbonate) of ΔP_{sx} is necessary before there is any change in porosity. The time lag for porosity, $\epsilon_x(\theta)$, at some point in a filter cake is at least that amount of time necessary for $P_{sx}(\theta)$ to increase the finite amount necessary to cause any porosity change.

Thus far, this time dependency has not been accounted for in compression-permeability testing. Perhaps the way to perform compression-permeability testing is to pick a certain differential element in some filter cake and reproduce the

$P_{sx}(\theta)$ time history in a compression-permeability test cell in which the rate of applied mechanical pressure can be controlled. Then each succeeding element of the filter cake is considered until the data from the compression-permeability test cell reproduces a filter cake at any thickness, L, and at any time, θ.

The second experiment was to test the relation between liquid pressure, P_x, and solids compressive pressure, P_{sx}, at a point in a filter cake. The expressions considered were $dP_{sx} = -dP_x$ and $dP_{sx} = -\epsilon_x\, dP_x$. The second expression was arrived at by analogy with flow through an annulus. By using a specially designed filter chamber with a floating septum, the validity of these relationships was determined. It was concluded that the expression $dP_{sx} = -\epsilon_x\, dP_x$ seems to be correct and that $dP_{sx} = -dP_x$ is incorrect. As a result, the expression for α_{av} (Equation 52) and the differential equation describing a filtration when q_x and α_x vary have been changed to agree with the relationship $dP_{sx} = -\epsilon_x dP_x$. The filtration data were plotted in the usual manner and confirmed Tiller's prediction that $\Delta\theta/\Delta V$ versus V are curved lines for short filtrations.

The third experiment was to test the assumption that P_{sx} fixes both ϵ_x and α_x. A statistical analysis of 250 specific resistance determinations and 125 porosity determinations at the same solids pressure of 24.99 psi was made using a Latin square design. The conclusion reached was that the components of variance considered to be important in the determination of ϵ_x and α_x are sufficient to account for the variability in ϵ_x but not α_x. In other words, α_x is affected by sources of variation in addition to those considered in the Latin square design. These sources of variation are not easily defined or practically controllable. Thus, at present, it seems that α_x can not be considered to be determined solely by ϵ_x and P_{sx}. The assumption concerning the determination of ϵ_x by P_{sx} is considered to be valid but there is a geometry effect attributable to the test cell due to the significance of cake weight in the statistical analysis of porosity data.

In view of these experiments, the conclusion might be that compression-permeability testing should be discarded. If the time dependent nature of $\epsilon_x(\theta)$ and $P_{sx}(\theta)$ were accounted for then all the assumptions could be considered valid except the third one, which assumes that α_x and ϵ_x are determined solely by the solids pressure, P_{sx}. The interpretation of compression-permeability data collected in this manner would be that the behavior of some filtration is predicted, not a specific filtration.

The results of the compression-permeability testing technique up to this time can not be ignored. Compression-permeability testing has stimulated more progress in the last 7 to 8 years than in the previous 20 years. It has eliminated some of the hopelessness which previously existed in this important facet of chemical engineering.

REFERENCES

1. Adamson, J. E. Application of the Kozeny equation to consolidated porous media. Nature. (London) 166: 314-315. 1950.

2. Almy, C., Jr. and Lewis, W. K. Factors determining the capacity of a filter press. J. Ind. Eng. Chem. 4: 528-532. 1912.

3. Badger, W. L. and Banchero, J. T. Introduction to chemical engineering. N. Y., McGraw-Hill Book Co., Inc. 1955.

4. Baker, F. P. A study of the fundamental laws of filtration using plant-scale equipment. Ind. Eng. Chem. 13: 610-612. 1921.

5. Batchelor, G. K. The theory of homogeneous turbulence. London, England, Cambridge University Press. 1953.

6. Baver, L. D. Retention and movement of soil moisture. In Meinzer, O. E., ed. Physics of the earth-IX. Hydrology. pp. 364-384. N. Y., McGraw-Hill Book Co., Inc. 1942.

7. Bird, R. B. The equations of change and the macroscopic mass, momentum and energy balances. Chem. Eng. Sci. 6:123-131. 1957.

8. Blake, F. C. The resistance of packing to flow. Trans. Am. Inst. Chem. Engrs. 14:415-421. 1921.

9. Bonilla, C. F. Interpretation of constant rate filtration data. Trans. Am. Inst. Chem. Engrs. 34:243-250. 1938.

10. Brown, G. G., Foust, A. S., Katz, D. L., Schneidewind, R., White, R. R., Wood, W. P., Brown, G. M., Brownell, L. E., Martin, J. J., Williams, G. B., Banchero, J. T. and York, J. L. Unit operations. New York, John Wiley and Sons, Inc. 1950.

11. Brownell, L. E. and Katz, D. L. Flow of fluids through porous media. I. Single homogeneous fluids. Chem. Eng. Prog. 43:537-548. 1947.

12. Bulnes, A. C. and Fitting, R. U., Jr. Introductory discussion of the reservoir performance of limestone formations. Trans. Am. Inst. Mining and Met. Engrs. 160:179-201. 1945.

13. Cardwell, W. T., Jr. and Parsons, R. L. Average permeabilities of heterogeneous oil sands. Trans. Am. Inst. Mining and Met. Engrs. 160:34-42. 1945.

14. Carman, P. C. Fluid flow through granular beds. Trans. Inst. Chem. Engrs. (London) 15:150-166. 1937.

15. ________. Fundamental principles of industrial filtration. Trans. Inst. Chem. Engrs. (London) 16:168-188. 1938.

16. ________. A study of the mechanism of filtration, Part I. J. Soc. Chem. Ind. (London) 52:280T-282T. 1933.

17. ________. A study of the mechanism of filtration, Part II. J. Soc. Chem. Ind. (London) 52:301T-309T. 1934.

18. ________ and Malherbe, P. LeR. Routine measurements of surface of paint pigments and other fine powders. J. Soc. Chem. Ind. (London) 69:134-143. 1950.

19. Childs, E. C., Collis-George, N. and Holmes, J. W. Permeability measurements in the field as an assessment of anisotropy and structure development. J. Soil Sci. (London) 8:27-41. 1957.

20. Cloud, W. F. Effects of sand grain size distribution upon porosity and permeability. The Oil Weekly. 103: 26-30. October 27, 1941.

21. Coming, E. W. High pressure technology. New York, McGraw-Hill Book Co., Inc. 1956.

22. Comolet, R. Sur l'ecoulement laminaire dans un tube courbe. Comptes Rendus. Academie des Sciences. (Paris) 229:342-343. 1949.

23. Cooper, H. R. Analytical study of flow through compressible porous media. Unpublished M.S. Thesis. Houston, Texas, Library, University of Houston. 1958.

24. D'Arcy, H. P. G. Les fontaines publiques de la Ville de Dijon. Paris, Victor Dalamont. 1856. (Original not available; cited by Carman, P. C. Fundamental principles of filtration. Trans. Inst. Chem. Engrs. (London) 16: 168. 1938.)

25. Dupuit, A. J. Etudes theoretiques et practiques sur le mouvement des eaux. 1863. (Original not available; cited by Carman, P. C. Fundamental principles of filtration. Trans. Inst. Chem. Engrs. (London) 16:168. 1938.)

26. Eisenklam, P. Porous masses. In Cremer, Herbert W., ed. Chemical engineering practice. Vol. 2. pp. 342-463. London, England, Butterworths Scientific Publications. 1956.

27. Fair, G. H. and Hatch, L. P. Fundamental factors governing the streamline flow of water through sand. J. Am. Water-Works Assoc. 25:1551-1565. 1933.

28. Foust, A. S., Wenzel, L. A., Clump, C. W., Maus, L. and Andersen, L. B. Principles of unit operations. N. Y., John Wiley and Sons, Inc.

29. Gardner, W., Collier, T. R. and Farr, D. Fundamental principles governing the control of ground-water. Trans. Am. Geophys. Union. 15:563-566. 1934.

30. Grace, H. P. Resistance and compressibility of filter cakes. Chem. Eng. Prog. 49:303-318. 1953.

31. ________. Resistance and compressibility of filter cakes. II. Under conditions of pressure filtration. Chem. Eng. Prog. 49:367-377. 1953.

32. ________. Resistance and compressibility of filter cakes. III. Under conditions of centrifugal filtration. Chem. Eng. Prog. 49:427-436. 1953.

33. Heertjes, P. M. Industrial filtrations. Research 3: 254-259. June, 1950.

34. ________. Studies in filtration. The initial stages of the cake filtration. Chem. Eng. Sci. 6:269-276. 1957.

35. ________ and Nijman, J. Instability and inhomogeneity of filter cakes. Chem. Eng. Sci. 7:15-25. 1957.

36. Hinchley, J. W., Ure, S. G. M. and Clarke, B. W. Studies in filtration. J. Soc. Chem. Ind. (London) 45:1T-10T. 1926.

37. Hoffing, E. H. and Lockhart, F. J. Resistance to filtration. Chem. Eng. Prog. 47:3-10. 1951.

38. Hubbert, M. K. The theory of ground-water motion. J. Geol. 48:785-944. 1940.

39. Hutto, F. B., Jr. Distribution of porosity in filter cakes. Chem. Eng. Prog. 53:328-332. 1957.

40. ________ and Cummins, A. B. Filtration. In Weissberger, A., ed. Techniques of organic chemistry. Vol. 3. Part 1. pp. 607-786. N. Y., Interscience. 1956.

41. Igmanson, W. L. Drainage on the fourdrinier table roll section. J. Tech. Assoc. Pulp and Paper Ind. 42:449-454. 1959.

42. ________ and Andrews, B. D. The effect of beating on filtration resistance and its components of specific surface and specific volume. J. Tech. Assoc. Pulp and Paper Ind. 42:29-35. 1959.

43. ________, ________ and Johnson, R. C. Internal pressure distributions in compressible mats under fluid stress. J. Tech. Assoc. Pulp and Paper Ind. 42:840-849. 1959.

44. ________, Han, S. T., Wilder, H. D. and Myers, W. T., Jr. Resistance of wire screens to flow of water. J. Tech. Assoc. Pulp and Paper Ind. 44:47-54. 1961.

45. Kottwitz, F. A. Prediction of filtration resistance by compression-permeability techniques. Unpublished Ph.D. Thesis. Ames, Iowa, Library, Iowa State University of Science and Technology. 1955.

46. Kozeny, J. Kapillare Leitung des Wassers im Boden. Sitzber-Akad. Wiss. Wien. Math. naturw. Klasse, Abt. IIa, 136:271-282. 1927.

47. Kruger, E. Die Orundwasserbewegung. Internationale Mitteillungen fur Bodenkunde. 8:105-122. 1918.

48. LaMer, V. K., Smellie, R. H., Jr. and Lee, Pui-Kum. Flocculation, subsidence and filtration of phosphate slimes. V. The optimum filtration rate as a function of solid content and specific area. J. Colloid Sci. 12:566-574. 1957.

49. Michaels, A. S. and Lin, C. S. Permeability of kaolinite. Ind. Eng. Chem. 46:1239-1246. 1954.

50. Miller, S. A. Recent advances in filtration theory. Chem. Eng. Prog. 47:497-502. 1951.

51. ________. Filtration. Ind. Eng. Chem. 39:5. 1947.

52. ________. Filtration. Ind. Eng. Chem. 40:25. 1948.

53. ________. Filtration. Ind. Eng. Chem. 41:38. 1949.

54. ________. Filtration. Ind. Eng. Chem. 42:52. 1950.

55. ________. Filtration. Ind. Eng. Chem. 43:85. 1951.

56. ________. Filtration. Ind. Eng. Chem. 44:63. 1952.

57. ________. Filtration. Ind. Eng. Chem. 45:68. 1953.

58. ________. Filtration. Ind. Eng. Chem. 46:100. 1954.

59. ________. Filtration. Ind. Eng. Chem. 47:546. 1955.

60. Oppenheim, A. K. and Hughes, R. R. Fluid dynamics. Ind. Eng. Chem. 47:632-647. 1955.

61. ________ and ________. Fluid dynamics. Ind. Eng. Chem. 48:633-654. 1956.

62. Prandlt, L. The mechanics of viscous fluids. In Durand, W. F. Aerodynamic theory. Vol. 3. pp. 35-40. Berlin, Julius Springer. 1935.

63. Purchas, D. B. Filtration theory can be useful. Chem. Prods. and Chem. News. (London) 20:149-151. 1957.

64. Richardson, J. G. Flow through porous media. In Streeter, V. L., ed. Handbook of fluid dynamics. pp. 16-1 - 16-112. New York, McGraw-Hill Book Co., Inc. 1961.

65. Rietema, K. Stabilizing effects in compressible filter cakes. Chem. Eng. Sci. 2:88-94. 1953.

66. Ruth, B. F. Correlating filtration theory with industrial practice. Ind. Eng. Chem. 38:564-571. 1946.

67. ________. Studies in filtration. Unpublished Ph.D. Thesis. Minneapolis, Minnesota, Library, University of Minnesota. 1931.

68. ________. Studies in filtration. III. Derivation of general filtration equation. Ind. Eng. Chem. 27:708-723. 1945.

69. ________, Montillon, G. A. and Montanna, R. E. Comments upon recent developments in theory of filtration. Ind. Eng. Chem. 23:850-851. 1931.

70. ________, ________ and ________. Studies in filtration. I. Critical analysis of filtration theory. Ind. Eng. Chem. 25:76-82. 1933.

71. ________, ________ and ________. Studies in filtration. II. Fundamental axiom of constant-pressure filtration. Ind. Eng. Chem. 25:153-161. 1933.

72. Scheidegger, A. E. The physics of flow through porous media. New York, Macmillan. 1957.

73. Seelheim, F. Methoden zur Bestimmung der Durchlassigkeit des Bodens. Zeitschrift analytische Chemie. 19:387,418. 1880.

74. Shirato, M. Recent filtration theory and practice. Soc. of Chem. Engrs. (Japan) 23:823-830. 1959.

75. ________ and Okamura, S. The ageing and accuracy of the predictions of filtration of the ignition-plug slurries. Soc. of Chem. Engrs. (Japan) 20:98-105. 1956.

76. ________ and ________. Behaviors of gairome-clay slurries at constant pressure filtrations. Soc. of Chem. Engrs. (Japan) 20:678-684. 1956.

77. ________ and ________. Liquid pressure distribution within cakes in constant-pressure filtration. Soc. of Chem. Engrs. (Japan) 19:104-110. 1955.

78. ________ and ________. p_x distribution within cakes in the compression-permeability experiments. Soc. of Chem. Engrs. (Japan) 19:111-118. 1955.

79. Siemon, K. Manual for design of ferrous and non-ferrous pressure vessels and tanks. Ann Arbor, Michigan, Edwards Bros., Inc. 1952.

80. Sjenitzer, F. Contribution to the theory of filtration. Trans. Inst. Chem. Engrs. 33:289-302. 1955.

81. Sperry, D. R. Analysis of filtration data. Ind. Eng. Chem. 36:323-329. 1944.

82. ________. Effect of pressure on fundamental filtration equation when solids are non rigid or deformable. Ind. Eng. Chem. 20:892-895. 1928.

83. ________. A new method of conducting filtration tests. Ind. Eng. Chem. 18:276-278. 1926.

84. ________. A study of the fundamental law of filtration using plant-scale equipment. I. Ind. Eng. Chem. 13: 1163-1165. 1921.

85. Suttle, H. K. Filtration. Chem. and Process Eng. 39: 125-131. 1958.

86. Tiller, F. M. The role of porosity in filtration. I. Chem. Eng. Prog. 49:467-479. 1953.

87. ________. The role of porosity in filtration. II. Chem. Eng. Prog. 51:282-290. 1955.

88. ________. The role of porosity in filtration. III. Am. Inst. Chem. Eng. J. 4:170-174. 1958.

89. ________ and Cooper, H. R. The role of porosity in filtration. Am. Inst. Chem. Eng. J. 6:595-601. 1960.

90. ________ and Huang, C. J. Filtration equipment, theory. Ind. Eng. Chem. 53:529-537. 1961.

91. Valeroy, V. V. Comparison of resistances furnished by porous beds to liquid flow as measured by a permeability cell, a vacuum test filter and an experimental centrifugal filter. Unpublished Ph.D. Thesis, Lawrence, Kansas, Library, University of Kansas. 1956.

92. Van Gilse, J. P. M., Van Ginneken, P. J. H. and Waterman, H. I. Studies in filtration. I. J. Soc. Chem. Ind. (London) 49:444T-446T. 1930.

93. ________, ________ and ________. Studies in filtration. II. J. Soc. Chem. Ind. (London) 49:483T-490T. 1930.

94. ________, ________ and ________. Studies in filtration. III. J. Soc. Chem. Ind. (London) 50:41T-44T. 1931.

95. ________, ________ and ________. Studies in filtration. IV. J. Soc. Chem. Ind. (London) 50:95T-100T. 1931.

96. Volk, W. Applied statistics for engineers. New York, McGraw-Hill Book Co., Inc. 1958.

97. Walas, S. M. Resistance to filtration. Trans. Am. Inst. Chem. Engrs. 42:783-793. 1946.

98. Webber, H. C. and Herschey, R. L. Some practical applications of the Lewis filtration equations. Ind. Eng. Chem. 18:341-344. 1926.

99. Whitney, R. P., Ingmanson, W. L. and Han, S. T. Some aspects of permeation, filtration and fluidization. J. Tech. Assoc. Pulp and Paper Ind. 38:157-166. 1955.

100. Willis, M. S. Compression-permeability testing with calcium carbonate. Unpublished M.S. Thesis. Ames, Iowa, Library, Iowa State University of Science and Technology. 1959.

ACKNOWLEDGEMENTS

This thesis is part of the continuing work at the Iowa State University Engineering Experiment Station in the general field of flow through porous media. I am grateful to the Engineering Experiment Station for equipment funds and a Graduate Research Assistantship. Dr. D. R. Boylan directed this research and appreciation is expressed to him for his guidance.

Appreciation is also extended to:

Dr. Herbert T. David of the Statistics Department who gave freely of his time and effort in consultation with me on the statistical analysis.

Mr. N. C. Spicer, whose comments on the construction of equipment were invaluable.

Mr. R. C. Riedesel, who did the major task of building the compression-permeability test cell.

Mr. Robert Loudon, who machined the floating septum filtration chamber.

Mr. Robert Johns, who constructed the filtrate collection balance.

Mr. Del Whitmer, who assisted considerably in the electronics portion of the equipment.

My wife and son, who sometimes bore the brunt of my frustrations.

APPENDIX

Table 4. Porosity-time data for initial slope determination

Run No. 2

ΔP_{sx} = 9.63psi m' = .000187 (1/sec)

W_c = 19.5761 gms ϵ_o = .6856

Time sec.	L inch	1- ϵ	ϵ	log 10 ϵ	Time sec.	L inch	1- ϵ	ϵ	log 10 ϵ
0.00	.6818	.3115	.6885	.8379	1.41	.6600	.3218	.6782	.8314
0.44	.6818	.3115	.6885	.8379	1.46	.6591	.3223	.6777	.8310
0.44	.6710	.3165	.6835	.8347	1.52	.6580	.3228	.6772	.8307
0.49	.6760	.3142	.6858	.8362	1.60	.6570	.3233	.6767	.8304
0.49	.6770	.3137	.6863	.8365	1.61	.6560	.3238	.6762	.8301
0.62	.6769	.3138	.6862	.8365	1.66	.6550	.3243	.6757	.8298
0.68	.6766	.3139	.6861	.8364	1.71	.6540	.3248	.6752	.8294
0.69	.6765	.3140	.6860	.8363	1.76	.6530	.3253	.6747	.8291
0.73	.6762	.3141	.6859	.8363	1.81	.6520	.3258	.6742	.8288
0.73	.6760	.3142	.6858	.8362	1.86	.6510	.3263	.6737	.8285
0.80	.6758	.3143	.6857	.8361	1.92	.6500	.3268	.6732	.8281
0.82	.6752	.3146	.6854	.8360	2.01	.6490	.3273	.6727	.8278
0.83	.6750	.3147	.6853	.8359	2.06	.6480	.3278	.6722	.8275
0.87	.6745	.3149	.6851	.8358	2.11	.6470	.3283	.6727	.8278
0.90	.6743	.3150	.6850	.8357	2.21	.6460	.3288	.6712	.8269
0.93	.6732	.3155	.6845	.8354	2.31	.6450	.3293	.6707	.8265
0.96	.6725	.3158	.6842	.8352	2.40	.6440	.3298	.6702	.8262
1.01	.6720	.3161	.6839	.8350	2.50	.6430	.3303	.6697	.8259
1.03	.6714	.3164	.6836	.8348	2.60	.6420	.3308	.6692	.8256
1.06	.6705	.3168	.6832	.8346	2.71	.6410	.3314	.6686	.8252
1.10	.6700	.3170	.6830	.8344	2.86	.6400	.3319	.6681	.8248
1.13	.6696	.3172	.6828	.8343	3.01	.6390	.3324	.6676	.8245
1.13	.6690	.3175	.6825	.8341	3.19	.6380	.3329	.6671	.8242
1.16	.6684	.3178	.6822	.8339	3.40	.6370	.3334	.6666	.8239
1.16	.6680	.3180	.6820	.8338	3.60	.6360	.3340	.6660	.8235
1.20	.6675	.3182	.6818	.8337	3.86	.6350	.3345	.6655	.8232
1.22	.6665	.3187	.6813	.8333	4.19	.6340	.3350	.6650	.8228
1.22	.6660	.3189	.6811	.8332	4.43	.6330	.3355	.6645	.8225
1.26	.6650	.3194	.6806	.8329	4.83	.6320	.3361	.6639	.8221
1.26	.6645	.3196	.6804	.8328	5.33	.6310	.3366	.6634	.8218
1.30	.6640	.3199	.6801	.8326	5.91	.6300	.3371	.6629	.8215
1.31	.6630	.3204	.6796	.8323	6.57	.6290	.3377	.6623	.8211
1.36	.6620	.3209	.6791	.8319	7.43	.6280	.3382	.6618	.8207
1.41	.6610	.3213	.6787	.8317	8.61	.6270	.3388	.6612	.8203

Table 5. Porosity-time data for initial slope determination

Run No. 1

ΔP_{sx} = 19.25 psi m' = .0525 (1/sec)

W_c = 17.7966 gms ϵ_o = .6770

Time sec.	L inch	1- ε		log 10ε	Time sec.	L inch	1- ε	ε	log 10ε
0.35	.5995	.3221	.6779	.8312	1.00	.5863	.3294	.6706	.8264
0.38	.6010	.3213	.6787	.8317	1.04	.5852	.3300	.6700	.8261
0.38	.6006	.3215	.6785	.8316	1.04	.5851	.3300	.6700	.8261
0.41	.6000	.3218	.6782	.8314	1.06	.5840	.3307	.6693	.8256
0.44	.5993	.3222	.6778	.8311	1.07	.5830	.3312	.6688	.8253
0.48	.5990	.3224	.6776	.8310	1.08	.5820	.3318	.6682	.8249
0.48	.5988	.3225	.6775	.8309	1.08	.5810	.3324	.6676	.8245
0.50	.5984	.3227	.6773	.8308	1.11	.5800	.3329	.6671	.8242
0.50	.5981	.3229	.6771	.8307	1.11	.5794	.3333	.6667	.8239
0.54	.5980	.3229	.6771	.8309	1.14	.5789	.3336	.6664	.8237
0.56	.5981	.3229	.6771	.8307	1.16	.5781	.3340	.6660	.8235
0.58	.5984	.3227	.6773	.8308	1.17	.5776	.3343	.6657	.8233
0.58	.5987	.3225	.6775	.8309	1.18	.5770	.3347	.6653	.8230
0.62	.5985	.3226	.6774	.8309	1.18	.5762	.3351	.6649	.8228
0.64	.5981	.3229	.6771	.8307	1.20	.5759	.3353	.6647	.8226
0.65	.5980	.3229	.6771	.8307	1.20	.5752	.3357	.6643	.8224
0.68	.5978	.3230	.6770	.8306	1.25	.5750	.3358	.6642	.8223
0.70	.5975	.3232	.6768	.8305	1.25	.5744	.3362	.6638	.8220
0.73	.5973	.3233	.6767	.8304	1.28	.5739	.3365	.6635	.8218
0.74	.5971	.3234	.6766	.8303	1.28	.5737	.3366	.6634	.8218
0.75	.5970	.3235	.6765	.8303	1.28	.5731	.3369	.6631	.8216
0.78	.5968	.3236	.6764	.8302	1.30	.5730	.3370	.6630	.8215
0.79	.5972	.3233	.6767	.8304	1.30	.5724	.3374	.6626	.8213
0.80	.5957	.3242	.6758	.8298	1.35	.5720	.3376	.6624	.8211
0.84	.5949	.3246	.6754	.8296	1.35	.5717	.3378	.6622	.8210
0.86	.5940	.3251	.6749	.8292	1.38	.5712	.3381	.6619	.8208
0.87	.5933	.3255	.6745	.8290	1.38	.5710	.3382	.6618	.8207
0.88	.5928	.3257	.6743	.8289	1.38	.5707	.3384	.6616	.8206
0.88	.5920	.3262	.6738	.8285	1.39	.5702	.3387	.6613	.8204
0.91	.5914	.3265	.6735	.8283	1.39	.5700	.3388	.6612	.8203
0.91	.5910	.3267	.6733	.8282	1.43	.5696	.3390	.6610	.8203
0.94	.5905	.3270	.6730	.8280	1.48	.5693	.3392	.6608	.8201
0.94	.5900	.3273	.6727	.8278	1.48	.5691	.3393	.6607	.8200
0.95	.5895	.3276	.6724	.8276	1.48	.5690	.3394	.6606	.8199
0.98	.5890	.3278	.6722	.8275	1.49	.5689	.3394	.6606	.8199
0.98	.5880	.3284	.6716	.8271	1.50	.5686	.3396	.6604	.8198
1.00	.5873	.3288	.6712	.8269	1.53	.5684	.3397	.6603	.8197

Table 5. (Continued)

Time sec.	L inch	1- ε	ε	log 10 ε	Time sec.	L inch	1- ε	ε	log 10 ε
1.53	.5682	.3398	.6602	.8197	2.19	.5641	.3423	.6577	.8180
1.57	.5680	.3400	.6600	.8195	2.25	.5640	.3424	.6576	.8180
1.59	.5677	.3401	.6599	.8195	2.35	.5639	.3424	.6576	.8180
1.63	.5672	.3404	.6596	.8193	2.38	.5637	.3426	.6574	.8178
1.65	.5671	.3405	.6595	.8192	2.35	.5636	.3426	.6574	.8178
1.68	.5670	.3406	.6594	.8192	2.41	.5635	.3427	.6573	.8178
1.69	.5669	.3406	.6594	.8192	2.47	.5634	.3427	.6573	.8178
1.69	.5667	.3407	.6593	.8191	2.48	.5632	.3429	.6571	.8176
1.76	.5665	.3409	.6591	.8190	2.57	.5631	.3429	.6571	.8176
1.78	.5663	.3410	.6590	.8189	2.57	.5630	.3430	.6570	.8176
1.78	.5662	.3411	.6589	.8188	2.77	.5629	.3431	.6569	.8175
1.80	.5661	.3411	.6589	.8188	2.83	.5628	.3431	.6569	.8175
1.80	.5660	.3412	.6588	.8188	2.89	.5626	.3432	.6568	.8174
1.86	.5659	.3412	.6588	.8188	2.94	.5625	.3433	.6567	.8174
1.86	.5657	.3414	.6586	.8186	3.03	.5624	.3434	.6566	.8173
1.90	.5655	.3415	.6585	.8186	3.06	.5622	.3435	.6565	.8172
1.90	.5653	.3416	.6584	.8185	3.41	.5619	.3437	.6563	.8171
1.95	.5652	.3417	.6583	.8184	3.51	.5618	.3437	.6563	.8171
1.95	.5651	.3417	.6583	.8184	3.58	.5616	.3438	.6562	.8170
1.98	.5650	.3418	.6582	.8184	3.67	.5615	.3439	.6561	.8170
2.05	.5649	.3418	.6582	.8184	3.82	.5612	.3441	.6559	.8168
2.08	.5648	.3419	.6581	.8183	3.98	.5611	.3441	.6559	.8168
2.10	.5646	.3420	.6580	.8182	4.12	.5610	.3442	.6558	.8168
2.14	.5643	.3422	.6578	.8181	4.48	.5609	.3443	.6557	.8167
2.18	.5642	.3423	.6577	.8180					

Table 6. Porosity-time data for initial slope determination

Run No. 4

ΔP_{sx} = 29.31 psi m' = .134 (1/sec)

W_c = 19.4206 gms ϵ_0 = .6831

Time sec.	L inch	1- ϵ	ϵ	log 10ϵ	Time sec.	L inch	1- ϵ	ϵ	log 10ϵ
0.20	.6672	.3158	.6842	.8352	1.30	.6012	.3505	.6495	.8126
0.73	.6670	.3159	.6841	.8351	1.33	.6006	.3508	.6492	.8124
0.76	.6630	.3178	.6822	.8339	1.34	.6000	.3512	.6488	.8121
0.77	.6655	.3166	.6834	.8347	1.36	.5992	.3516	.6484	.8118
0.80	.6650	.3168	.6832	.8346	1.37	.5980	.3523	.6477	.8114
0.86	.6640	.3173	.6827	.8342	1.40	.5975	.3526	.6474	.8112
0.90	.6637	.3175	.6825	.8341	1.40	.5970	.3529	.6471	.8110
0.92	.6608	.3189	.6811	.8332	1.43	.5965	.3532	.6468	.8108
0.93	.6590	.3197	.6803	.8327	1.43	.5960	.3535	.6465	.8106
0.97	.6570	.3207	.6793	.8321	1.46	.5955	.3538	.6462	.8104
0.97	.6540	.3222	.6778	.8311	1.46	.5950	.3541	.6459	.8102
0.98	.6522	.3231	.6769	.8305	1.48	.5940	.3547	.6453	.8098
1.00	.6498	.3243	.6757	.8298	1.53	.5930	.3553	.6447	.8094
1.00	.6482	.3251	.6749	.8292	1.57	.5920	.3559	.6441	.8090
1.03	.6450	.3267	.6733	.8282	1.64	.5910	.3565	.6435	.8086
1.03	.6425	.3279	.6721	.8274	1.67	.5900	.3571	.6429	.8081
1.06	.6400	.3292	.6708	.8266	1.73	.5890	.3577	.6423	.8077
1.06	.6368	.3309	.6691	.8255	1.83	.5880	.3583	.6417	.8073
1.07	.6330	.3329	.6671	.8242	1.93	.5870	.3589	.6411	.8069
1.11	.6296	.3347	.6653	.8230	2.05	.5860	.3596	.6404	.8065
1.11	.6260	.3366	.6634	.8218	2.18	.5850	.3602	.6398	.8060
1.14	.6230	.3382	.6618	.8207	2.35	.5840	.3608	.6392	.8056
1.14	.6120	.3443	.6557	.8167	2.60	.5830	.3614	.6386	.8052
1.15	.6172	.3414	.6586	.8186	2.83	.5820	.3620	.6380	.8048
1.16	.6150	.3426	.6574	.8178	3.03	.5815	.3623	.6377	.8046
1.17	.6130	.3437	.6563	.8171	3.15	.5810	.3627	.6373	.8043
1.18	.6110	.3448	.6552	.8164	3.44	.5805	.3630	.6370	.8041
1.18	.6195	.3401	.6599	.8195	3.55	.5801	.3632	.6368	.8040
1.25	.6080	.3465	.6535	.8153	4.02	.5795	.3636	.6364	.8037
1.25	.6070	.3471	.6529	.8149	4.25	.5790	.3639	.6361	.8035
1.26	.6052	.3481	.6519	.8142	4.95	.5780	.3645	.6355	.8031
1.26	.6042	.3487	.6513	.8138	5.97	.5770	.3652	.6348	.8026
1.27	.6031	.3494	.6506	.8133	6.18	.5770	.3652	.6348	.8026

Table 7. Porosity-time data for initial slope determination

Run No. 5

ΔP_{SX} = 39.07 psi   m' = 0.137 (1/sec)

W_c = 19.3847 gms ϵ_o = 0.6748

Time sec.	L inch	1- ϵ	ϵ	log 10ϵ	Time sec.	L inch	1- ϵ	ϵ	log 10 ϵ
0.00	.6570	.3201	.6799	.8325	1.11	.6000	.3505	.6495	.8127
0.47	.6470	.3250	.6750	.8293	1.15	.5980	.3517	.6483	.8118
0.47	.6490	.3240	.6760	.8300	1.16	.5960	.3529	.6471	.8110
0.47	.6480	.3245	.6755	.8296	1.17	.5940	.3540	.6460	.8102
0.53	.6475	.3248	.6752	.8294	1.17	.5922	.3551	.6449	.8095
0.53	.6470	.3250	.6750	.8293	1.18	.5908	.3560	.6440	.8089
0.58	.6460	.3255	.6745	.8290	1.20	.5894	.3568	.6432	.8084
0.64	.6450	.3260	.6740	.8287	1.25	.5870	.3583	.6419	.8075
0.65	.6440	.3266	.6734	.8283	1.26	.5860	.3589	.6411	.8069
0.69	.6430	.3271	.6729	.8280	1.27	.5850	.3595	.6405	.8065
0.72	.6420	.3276	.6724	.8276	1.27	.5843	.3599	.6401	.8063
0.76	.6410	.3281	.6719	.8273	1.29	.5836	.3603	.6397	.8060
0.77	.6400	.3286	.6714	.8270	1.30	.5830	.3607	.6393	.8057
0.77	.6390	.3291	.6709	.8267	1.31	.5820	.3613	.6387	.8053
0.80	.6380	.3296	.6704	.8263	1.36	.5810	.3620	.6380	.8048
0.82	.6370	.3301	.6699	.8260	1.37	.5800	.3626	.6374	.8044
0.87	.6355	.3309	.6691	.8255	1.42	.5790	.3632	.6368	.8040
0.87	.6340	.3317	.6683	.8250	1.46	.5780	.3638	.6362	.8036
0.89	.6337	.3319	.6681	.8248	1.47	.5770	.3645	.6355	.8031
0.89	.6310	.3333	.6667	.8239	1.51	.5760	.3651	.6349	.8027
0.92	.6297	.3340	.6660	.8235	1.57	.5750	.3657	.6343	.8023
0.93	.6276	.3351	.6649	.8228	1.65	.5740	.3664	.6336	.8018
0.97	.6255	.3362	.6638	.8220	1.72	.5730	.3670	.6330	.8014
0.97	.6235	.3373	.6627	.8213	1.72	.5720	.3677	.6323	.8009
0.97	.6215	.3384	.6616	.8206	1.97	.5710	.3683	.6317	.8005
0.98	.6196	.3394	.6606	.8199	2.07	.5700	.3689	.6311	.8000
0.98	.6180	.3403	.6597	.8194	2.27	.5690	.3696	.6304	.7996
0.99	.6160	.3414	.6586	.8186	2.47	.5680	.3702	.6298	.7992
1.00	.6140	.3425	.6575	.8179	2.80	.5670	.3709	.6291	.7987
1.05	.6120	.3436	.6564	.8172	3.25	.5660	.3716	.6284	.7982
1.05	.6110	.3442	.6558	.8168	3.77	.5650	.3722	.6278	.7978
1.07	.6080	.3459	.6541	.8156	4.57	.5640	.3729	.6271	.7973
1.08	.6060	.3470	.6530	.8149	5.85	.5630	.3735	.6265	.7969
1.08	.6040	.3482	.6518	.8141	6.92	.5626	.3738	.6262	.7967
1.11	.6020	.3493	.6507	.8135					

Table 8. Porosity-time data for initial slope determination

Run No. 6

ΔP_{sx} = 49.21 psi   m' = 0.268 (1/sec)

W_c = 18.3985 gms ϵ_o = 0.6648

Time sec.	L inch	$1-\epsilon$	ϵ	log 10ϵ	Time sec.	L inch	$1-\epsilon$	ϵ	log 10ϵ
0.50	.5955	.3352	.6648	.8227	1.22	.5445	.3666	.6334	.8017
0.79	.5955	.3352	.6648	.8227	1.25	.5430	.3676	.6324	.8010
0.80	.5650	.3533	.6467	.8107	1.25	.5421	.3682	.6318	.8006
0.82	.5730	.3483	.6517	.8141	1.27	.5415	.3686	.6314	.8003
0.82	.5680	.3514	.6486	.8120	1.30	.5400	.3696	.6304	.7996
0.83	.5725	.3486	.6514	.8139	1.32	.5390	.3703	.6297	.7991
0.83	.5660	.3527	.6473	.8111	1.34	.5380	.3710	.6290	.7987
0.87	.5640	.3539	.6461	.8103	1.34	.5370	.3717	.6283	.7982
0.91	.5630	.3545	.6455	.8099	1.38	.5360	.3724	.6276	.7977
0.91	.5600	.3564	.6436	.8086	1.42	.5350	.3731	.6269	.7972
0.94	.5590	.3571	.6429	.8081	1.46	.5340	.3738	.6262	.7967
0.94	.5580	.3577	.6423	.8077	1.46	.5330	.3745	.6255	.7962
0.97	.5570	.3583	.6417	.8073	1.52	.5320	.3752	.6248	.7957
0.97	.5556	.3593	.6407	.8067	1.57	.5310	.3759	.6241	.7953
1.01	.5552	.3595	.6405	.8065	1.64	.5300	.3766	.6234	.7948
1.04	.5532	.3608	.6392	.8056	1.80	.5290	.3773	.6227	.7943
1.04	.5520	.3616	.6384	.8051	1.90	.5280	.3780	.6220	.7938
1.08	.5510	.3623	.6377	.8046	2.10	.5270	.3788	.6212	.7932
1.08	.5500	.3629	.6371	.8042	2.40	.5260	.3795	.6205	.7927
1.12	.5490	.3636	.6364	.8037	2.80	.5250	.3802	.6198	.7923
1.15	.5482	.3641	.6359	.8034	3.52	.5240	.3809	.6191	.7918
1.15	.5475	.3646	.6354	.8031	4.57	.5230	.3816	.6184	.7913
1.15	.5468	.3650	.6350	.8028	5.62	.5225	.3820	.6180	.7910
1.18	.5460	.3656	.6344	.8024					

Table 9. Porosity-time data for initial slope determination

Run No. 7

ΔP_{sx} = 58.83 psi m' = 0.419 (1/sec)

W_c = 19.2608 gms ϵ_o = 0.6607

Time sec.	L inch	1-ϵ	ϵ	log 10ϵ	Time sec.	L inch	1-ϵ	ϵ	log 10ϵ
0.30	.6161	.3392	.6608	.8201	0.75	.5390	.3878	.6122	.7869
0.27	.6160	.3393	.6607	.8200	0.76	.5365	.3896	.6104	.7856
0.35	.6150	.3398	.6602	.8197	0.77	.5342	.3912	.6088	.7845
0.37	.6140	.3404	.6596	.8193	0.77	.5326	.3924	.6076	.7836
0.44	.6130	.3410	.6590	.8189	0.82	.5312	.3935	.6065	.7828
0.50	.6120	.3415	.6585	.8186	0.82	.5305	.3940	.6060	.7825
0.50	.6107	.3422	.6578	.8181	0.85	.5300	.3943	.6057	.7823
0.55	.6100	.3426	.6574	.8178	0.85	.5290	.3951	.6049	.7817
0.55	.6090	.3432	.6578	.8181	0.86	.5280	.3958	.6042	.7812
0.56	.6070	.3443	.6557	.8167	0.90	.5270	.3966	.6034	.7806
0.57	.6022	.3471	.6529	.8149	0.94	.5260	.3973	.6027	.7801
0.57	.5975	.3498	.6502	.8131	0.98	.5250	.3981	.6019	.7795
0.61	.5927	.3526	.6474	.8112	1.06	.5240	.3989	.6011	.7790
0.61	.5875	.3558	.6442	.8090	1.11	.5230	.3996	.6004	.7784
0.65	.5810	.3597	.6403	.8064	1.16	.5220	.4004	.5996	.7779
0.65	.5740	.3641	.6359	.8034	1.31	.5210	.4012	.5988	.7773
0.66	.5670	.3686	.6314	.8003	1.49	.5200	.4019	.5981	.7768
0.67	.5610	.3725	.6275	.7976	1.86	.5190	.4027	.5973	.7762
0.68	.5550	.3766	.6234	.7948	2.35	.5180	.4035	.5965	.7756
0.70	.5497	.3802	.6198	.7923	3.06	.5170	.4043	.5957	.7750
0.70	.5450	.3835	.6165	.7899	4.47	.5160	.4050	.5950	.7745
0.75	.5420	.3856	.6144	.7885	5.14	.5158	.4052	.5948	.7744

Table 10. Porosity-time data for initial slope determination

Run No. 8

ΔP_{sx} = 68.89 psi   m' = .202 (1/sec)

W_c = 19.4433 gms ϵ_o = .6739

Time sec.	L inch	1- ϵ	ϵ	log 10 ϵ	Time sec.	L inch	1- ϵ	ϵ	log 10 ϵ
0.55	.6480	.3256	.6744	.8289	0.97	.5740	.3676	.6324	.8010
0.55	.6475	.3259	.6741	.8287	0.99	.5710	.3695	.6305	.7997
0.57	.6466	.3263	.6737	.8285	1.01	.5697	.3704	.6296	.7991
0.60	.6460	.3266	.6734	.8283	1.05	.5684	.3712	.6288	.7985
0.65	.6448	.3272	.6728	.8279	1.05	.5672	.3720	.6280	.7980
0.67	.6432	.3281	.6719	.8273	1.07	.5660	.3728	.6272	.7974
0.67	.6420	.3287	.6713	.8269	1.07	.5652	.3733	.6267	.7971
0.67	.6408	.3293	.6707	.8265	1.09	.5645	.3738	.6262	.7967
0.70	.6320	.3339	.6661	.8235	1.10	.5648	.3736	.6264	.7969
0.75	.6305	.3347	.6653	.8230	1.12	.5630	.3748	.6252	.7960
0.76	.6210	.3398	.6602	.8197	1.15	.5620	.3754	.6246	.7956
0.77	.6200	.3403	.6597	.8194	1.17	.5610	.3761	.6239	.7951
0.77	.6190	.3409	.6591	.8190	1.23	.5600	.3768	.6232	.7946
0.79	.6153	.3429	.6571	.8176	1.27	.5590	.3775	.6225	.7941
0.79	.6090	.3465	.6535	.8153	1.28	.5580	.3781	.6219	.7937
0.80	.6050	.3488	.6512	.8137	1.37	.5570	.3788	.6212	.7932
0.84	.6017	.3507	.6493	.8125	1.47	.5560	.3795	.6205	.7927
0.84	.5980	.3528	.6472	.8110	1.58	.5550	.3802	.6198	.7923
0.87	.5937	.3554	.6446	.8093	1.75	.5540	.3809	.6191	.7918
0.87	.5900	.3576	.6424	.8078	1.95	.5530	.3816	.6184	.7913
0.89	.5870	.3595	.6405	.8065	2.27	.5520	.3822	.6178	.7909
0.90	.5844	.3611	.6389	.8054	2.62	.5510	.3829	.6171	.7904
0.90	.5819	.3626	.6374	.8044	3.22	.5500	.3836	.6164	.7899
0.93	.5794	.3642	.6368	.8040	4.25	.5490	.3843	.6157	.7894
0.94	.5772	.3656	.6344	.8024	4.29	.5490	.3843	.6157	.7894
0.97	.5756	.3666	.6334	.8017					

Table 11. Porosity-time data for initial slope determination

Run No. 9

ΔP_{sx} = 78.52 psi m' = 0.198 (1/sec)

W_c = 18.5493 gms ϵ_o = 0.6534

Time sec.	L inch	$1-\epsilon$	ϵ	log 10ϵ	Time sec.	L inch	$1-\epsilon$	ϵ	log 10ϵ
0.04	.5810	.3465	.6535	.8153	0.84	.5407	.3723	.6277	.7978
0.04	.5826	.3455	.6545	.8159	0.88	.5400	.3728	.6272	.7974
0.10	.5820	.3459	.6541	.8156	0.88	.5390	.3735	.6265	.7969
0.40	.5810	.3465	.6535	.8153	0.90	.5380	.3742	.6258	.7964
0.44	.5800	.3471	.6529	.8149	0.91	.5370	.3749	.6251	.7960
0.48	.5790	.3477	.6523	.8146	0.91	.5362	.3754	.6246	.7956
0.49	.5780	.3483	.6517	.8141	0.96	.5357	.3758	.6242	.7953
0.50	.5770	.3489	.6511	.8137	0.96	.5350	.3763	.6237	.7950
0.53	.5760	.3495	.6505	.8133	0.98	.5340	.3770	.6230	.7945
0.58	.5750	.3501	.6499	.8129	1.00	.5330	.3777	.6223	.7940
0.58	.5740	.3507	.6493	.8125	1.01	.5322	.3782	.6218	.7937
0.61	.5730	.3513	.6487	.8120	1.01	.5320	.3784	.6216	.7935
0.61	.5720	.3519	.6481	.8116	1.04	.5310	.3791	.6209	.7930
0.61	.5710	.3525	.6475	.8112	1.09	.5302	.3797	.6203	.7926
0.63	.5695	.3535	.6465	.8106	1.09	.5300	.3798	.6202	.7925
0.63	.5678	.3545	.6455	.8099	1.10	.5290	.3805	.6195	.7920
0.68	.5657	.3558	.6442	.8090	1.14	.5280	.3813	.6187	.7915
0.69	.5635	.3572	.6428	.8080	1.21	.5270	.3820	.6180	.7910
0.71	.5610	.3588	.6412	.8070	1.24	.5260	.3827	.6173	.7905
0.71	.5585	.3604	.6396	.8059	1.35	.5250	.3834	.6166	.7900
0.71	.5560	.3621	.6379	.8048	1.49	.5240	.3842	.6158	.7894
0.75	.5536	.3636	.6364	.8037	1.59	.5230	.3849	.6151	.7890
0.75	.5512	.3652	.6348	.8026	1.75	.5220	.3856	.6144	.7885
0.78	.5493	.3665	.6335	.8018	2.05	.5210	.3864	.6136	.7879
0.78	.5476	.3676	.6324	.8010	2.39	.5200	.3871	.6129	.7874
0.80	.5460	.3687	.6313	.8002	2.93	.5190	.3879	.6121	.7868
0.80	.5442	.3699	.6301	.7994	3.64	.5180	.3886	.6114	.7863
0.81	.5430	.3707	.6293	.7989	4.20	.5176	.3889	.6111	.7861
0.84	.5420	.3714	.6286	.7984					

Table 12. Dead-weight calibration of the movable septum

Septum area = 7.0547 in^2

Septum piston area = 0.3662 in^2

F_c[a] lb_f	p_c[b] psi	increasing p_T[c] psi	decreasing p_T psi
0	0	0	2.50
10.02	1.45	14.97	20.71
20.01	2.85	39.42	45.66
30.00	4.25	63.12	72.60
39.98	5.67	92.56	99.80
49.96	7.08	119.51	126.75
59.93	8.50	146.21	152.20
69.91	9.91	169.66	180.89
80.69	11.44	200.85	207.83
90.68	12.85	225.55	234.53
100.65	14.27	252.00	261.23
110.64	15.68	276.95	285.18
120.61	17.10	303.39	311.38
130.72	18.53	331.84	339.32
141.44	20.08	363.02	368.51
151.62	21.49	385.73	393.21
161.81	22.94	410.68	420.16
172.48	22.45	438.37	443.86
182.76	25.91	463.82	463.82

[a] F_c = dead-weight calibration force.

[b] p_c = dead-weight calibration pressure, $p_c = F_c$/septum area.

[c] p_T = pressure reading of PT-31-5C pressure transducer after conversion from millivolt reading using 24.9501 psi/mv.

Table 13. Clear filtrate calibration data for relating P_1 to p_{sep}[a]

P_1 psi	p_{sep}[b] psi	P_1 psi	p_{sep} psi
5.38	4.62	17.03	15.36
5.42	4.84	17.03	15.45
5.71	5.05	17.79	15.81
6.90	5.90	18.03	15.97
9.26	8.34	18.42	16.70
9.35	8.61	21.26	18.43
9.61	8.94	21.31	18.25
10.20	9.18	21.83	19.22
12.67	11.31	22.83	19.34
12.98	11.72	23.43	20.94
13.67	12.08	23.65	21.58
16.71	14.93		

[a]From this data the relation $p_{sep} = .889\ P_1$ is obtained.

[b]p_{sep} = pressure exerted by fluid passing through the septum.

Table 14. Constant pressure filtration data

Run No. 1-F_{10}-20BA

P = 21.0 psi   s = .083   W = .5747 lb_m

m = 1.695 ϵ_{av} = .655 $\frac{2}{K}$ = 4.63 x 10^4

θ sec.	$10^3 V$ ft^3	$10^{-2}\frac{\Delta\theta}{\Delta V}$ sec/ft^3	P_1 psi	p_T[a] psi	(P_s + P_{sep}) psi	P_{sep}[b] psi	P_s psi	$\frac{P_s}{P-P_1}$
0.0	4.53	-	0.0	0.0	0.0	0.0	0.0	0.0
0.51	-	-	19.53	349.30	19.40	17.36	2.04	1.388
1.0	8.01	2.87	14.32	343.56	19.13	12.73	6.40	.958
2.0	10.71	3.71	9.44	343.56	19.13	8.39	10.74	.929
3.0	13.33	4.59	7.03	339.57	18.52	6.25	12.27	.878
4.0	15.50	4.59	5.64	337.08	18.40	5.01	13.39	.872
5.0	17.68	4.59	4.73	335.58	18.33	4.21	14.12	.868
6.0	19.86	4.59	4.01	334.33	18.28	3.57	14.71	.866
7.0	21.69	5.47	3.54	333.83	18.25	3.15	15.10	.865
8.0	23.08	7.18	3.21	333.08	18.20	2.85	15.35	.863
9.0	24.39	7.66	2.91	332.09	18.20	2.59	15.61	.863
10.0	25.43	9.57	2.65	332.09	18.20	2.36	15.84	.863
11.0	26.48	9.57	2.45	331.84	18.12	2.18	15.94	.859
12.0	27.52	9.57	2.32	332.09	18.13	2.06	16.07	.860
13.0	28.57	9.57	2.17	332.34	18.16	1.93	16.23	.862
14.0	29.52	10.44	2.08	332.83	18.20	1.85	16.35	.864
15.0	30.39	11.48	1.95	333.08	18.20	1.73	16.47	.865
16.0	31.27	11.48	1.84	333.33	18.21	1.64	16.57	.865
17.0	32.14	11.48	1.74	333.58	18.23	1.55	16.68	.866
18.0	32.92	12.76	1.71	333.83	18.23	1.52	16.71	.866
19.0	33.70	12.76	1.65	333.83	18.23	1.47	16.76	.866
20.0	34.40	14.35	1.61	333.83	18.23	1.43	16.80	.866
21.0	35.10	14.35	1.56	333.83	18.23	1.39	16.84	.866
22.0	35.79	14.35	1.52	333.83	18.23	1.35	16.88	.867
23.0	36.49	14.35	1.48	333.58	18.23	1.32	16.91	.866
24.0	37.19	14.35	1.37	333.58	18.23	1.22	17.01	.867
25.0	37.88	14.35	1.35	332.83	18.19	1.20	16.99	.865
26.0	38.49	16.39	1.32	332.34	18.17	1.17	17.00	.864
27.0	39.10	16.39	1.30	332.34	18.17	1.16	17.01	.864

[a] p_T = pressure reading of PT-31-5C pressure transducer after conversion from millivolt reading using 24.9501 psi/mv.

[b] p_{sep} = pressure exerted by fluid passing through the septum.

Table 14. (Continued)

θ sec.	10^3V ft^3	$10^{-2}\frac{\Delta\theta}{\Delta V}$ sec/ft^3	P_1 psi	p_T[a] psi	(P_s + p_{sep}) psi	p_{sep}[b] psi	P_s psi	$\frac{P_s}{P-P_1}$
28.0	39.71	16.39	1.28	332.08	18.15	1.14	17.01	.863
29.0	40.32	16.39	1.26	332.08	18.15	1.12	17.03	.863
30.0	40.93	16.39	1.24	332.08	18.15	1.10	17.05	.863
35.0	43.98	16.40	1.08	331.34	18.12	0.96	17.16	.861
40.0	47.03	16.40	1.04	330.34	18.08	0.93	17.15	.859
45.0	49.64	19.14	0.89	329.59	18.01	0.79	17.22	.856
50.0	52.25	19.14	0.87	329.09	18.00	0.77	17.23	.856
55.0	54.87	19.14	0.87	328.59	17.98	0.77	17.21	.855
60.0	57.04	22.97	0.78	328.34	17.96	0.69	17.27	.854
65.0	59.22	22.97	0.76	326.85	17.90	0.68	17.23	.851
70.0	61.22	24.96	0.65	326.85	17.90	0.58	17.32	.851
75.0	63.14	26.10	0.65	326.35	17.87	0.58	17.29	.850
80.0	65.06	26.10	0.65	325.60	17.81	0.58	17.23	.847
85.0	66.97	26.10	0.61	325.10	17.80	0.54	17.26	.847
90.0	68.80	27.34	0.61	324.60	17.79	0.54	17.25	.846
95.0	70.54	28.70	0.56	324.35	17.78	0.50	17.28	.845
100.0	72.11	31.89	0.54	324.10	17.73	0.48	17.25	.843
105.0	73.68	31.89	0.50	323.85	17.72	0.45	17.27	.842
110.0	75.25	31.89	0.50	323.35	17.70	0.45	17.25	.842
115.0	76.81	31.89	0.46	322.61	17.68	0.41	17.27	.841
120.0	78.38	31.89	0.46	322.11	17.64	0.41	17.23	.839
125.0	79.86	33.76	0.46	321.86	17.62	0.41	17.21	.838
130.0	81.34	33.76	0.43	321.61	17.61	0.38	17.23	.838
135.0	82.74	35.89	0.43	321.11	17.60	0.38	17.22	.837
140.0	84.13	35.89	0.43	320.61	17.58	0.38	17.20	.836
145.0	85.52	35.89	0.43	320.11	17.57	0.38	17.19	.836
150.0	86.92	35.89	0.43	319.61	17.51	0.38	17.13	.833
155.0	88.22	38.29	0.43	319.36	17.50	0.38	17.12	.832
160.0	89.53	38.29	0.43	319.11	17.49	0.38	17.11	.832
165.0	90.84	38.29	0.43	318.86	17.49	0.38	17.11	.832
170.0	92.14	38.29	0.43	317.86	17.49	0.38	17.11	.832
175.0	93.36	41.02	0.39	315.62	17.31	0.35	16.96	.823
180.0	94.41	47.85	0.37	297.65	16.39	0.33	16.06	.779
185.0	95.36	52.19	0.22	256.99	14.05	0.20	13.85	.667
187.0	95.80	57.47	0.20	244.51	13.39	0.18	13.21	.635

Table 15. Constant pressure filtration data

Run No. 2-F_{15}-20BA

P = 19.8 psi   s = .134   W = .6056 lb_m

m = 1.641 ϵ_{av} = .632 $\frac{2}{K}$ = 4.63 x 10^4

θ sec.	10^3V ft^3	$10^{-2}\frac{\Delta\theta}{\Delta V}$ sec/ft^3	P_1 psi	p_T[a] psi	$(P_s + p_{sep})$ psi	p_{sep}[b] psi	P_s psi	$\frac{P_s}{P-P_1}$
0.0	3.62	-	0.0	0.0	0.0	0.0	0.0	0.0
0.5	-	-	8.87	242.52	13.78	7.89	5.89	.539
0.75	-	-	8.87	364.27	20.18	7.89	12.29	1.124
1.0	6.61	3.34	8.31	362.53	19.73	7.39	12.34	1.074
1.5	-	-	7.59	359.53	19.58	6.75	12.83	1.051
2.0	9.33	3.69	6.94	356.79	19.42	6.17	13.25	1.030
3.0	11.48	4.64	5.90	351.30	19.12	5.25	13.87	.998
4.0	13.57	4.79	5.16	346.31	18.88	4.59	14.29	.976
5.0	15.24	5.99	4.60	340.57	18.60	4.09	14.51	.955
6.0	16.63	7.18	4.12	336.83	18.40	3.66	14.74	.940
7.0	17.89	7.98	3.73	335.08	18.31	3.32	14.99	.933
8.0	19.07	8.45	3.41	329.34	18.01	3.03	14.98	.914
9.0	20.25	8.45	3.04	326.85	17.93	2.70	15.23	.909
10.0	21.43	8.45	2.82	323.35	17.70	2.51	15.19	.895
11.0	22.62	8.45	2.60	321.61	17.16	2.31	15.31	.890
12.0	23.73	8.99	2.41	319.11	17.50	2.14	15.36	.883
13.0	24.77	9.58	2.21	317.12	17.40	1.97	15.43	.877
14.0	25.75	10.27	2.08	315.12	17.30	1.85	15.45	.872
15.0	26.65	11.05	1.95	314.12	17.23	1.73	15.50	.868
16.0	27.49	11.98	1.82	312.38	17.15	1.62	15.53	.863
17.0	28.32	11.98	1.71	311.13	17.10	1.52	15.58	.861
18.0	29.09	13.06	1.61	309.63	17.00	1.43	15.57	.856
19.0	29.85	13.06	1.52	308.63	16.94	1.35	15.59	.853
20.0	30.62	13.06	1.45	307.64	16.90	1.29	15.61	.851
21.0	31.39	13.06	1.32	306.89	16.88	1.17	15.71	.850
22.0	32.15	13.06	1.28	306.14	16.82	1.14	15.68	.847
23.0	32.85	14.37	1.24	304.89	16.78	1.10	15.68	.845
24.0	33.54	14.37	1.13	304.39	16.72	1.01	15.72	.842
25.0	34.24	14.37	1.09	303.14	16.68	0.97	15.51	.840

[a] p_T = pressure reading of PT-31-5C pressure transducer after conversion from millivolt reading using 24.9501 psi/mv

[b] p_{sep} = pressure exerted by fluid passing through the septum.

Table 15. (Continued)

θ sec.	$10^3 V$ ft^3	$10^{-2}\frac{\Delta\theta}{\Delta V}$ sec/ft^3	P_1 psi	p_T[a] psi	$(P_s + p_{sep})$ psi	p_{sep}[b] psi	P_s psi	$\frac{P_s}{P-P_1}$
26.0	34.93	14.37	1.09	302.65	16.64	0.97	15.67	.838
27.0	35.63	14.37	1.04	302.15	16.61	0.93	15.68	.836
28.0	36.33	14.37	0.96	301.40	16.59	0.85	15.74	.836
29.0	37.02	14.37	0.89	300.15	16.52	0.79	15.73	.831
30.0	37.72	14.37	0.87	299.65	16.49	0.77	15.72	.830
35.0	41.13	14.66	0.74	297.16	16.34	0.66	15.68	.823
40.0	43.84	18.42	0.63	294.66	16.20	0.56	15.64	.816
45.0	46.49	18.91	0.52	292.17	16.03	0.46	15.57	.808
50.0	49.06	19.42	0.43	289.67	15.90	0.38	15.52	.801
55.0	51.50	20.53	0.43	287.43	15.79	0.38	15.41	.796
60.0	53.79	21.77	0.28	284.18	15.59	0.25	15.34	.786
61.0	54.14	28.65	0.28	282.93	15.50	0.25	15.25	.781
62.0	54.42	35.97	0.26	281.94	15.43	0.23	15.20	.778
62.3	-	-	0.26	281.44	15.41	0.23	15.18	.777
63.0	54.70	35.97	-	280.19	15.36	-	-	-

Table 16. Constant pressure filtration data

Run No. 3-F_{20}-20BA

P = 20.0 psi s = .159 W = .6056 lb_m

m = 1.639 ϵ_{av} = .632 $\frac{2}{K}$ = 4.08 x 10^4

θ sec.	$10^3 V$ ft^3	$10^{-2}\frac{\Delta\theta}{\Delta V}$ sec/ft^3	P_1 psi	p_T[a] psi	(P_s + p_{sep}) psi	p_{sep}[b] psi	P_s psi	$\frac{P_s}{P-P_1}$
0.0	3.00	-	0.0	0.0	0.0	0.0	0.0	0.0
0.5	-	-	5.10	234.53	13.31	4.53	8.78	.589
1.0	10.14	1.40	6.51	361.78	20.05	5.79	14.26	1.057
1.5	-	-	6.25	365.02	20.24	5.56	14.68	1.068
2.0	13.68	2.82	5.62	363.77	19.80	5.00	14.80	1.029
3.0	16.35	3.75	4.67	358.28	19.50	4.15	15.35	1.001
4.0	18.69	4.27	3.84	351.55	19.14	3.41	15.73	.973
5.0	20.60	5.24	3.26	345.06	18.81	2.90	15.91	.950
6.0	22.18	6.33	2.82	340.32	18.58	2.51	16.07	.935
7.0	23.65	6.71	2.39	336.33	18.38	2.13	16.25	.923
8.0	25.01	7.34	2.13	333.33	18.21	1.89	16.32	.913
9.0	26.21	8.34	1.84	329.59	18.02	1.64	16.38	.902
10.0	27.35	8.74	1.63	327.35	17.90	1.45	16.45	.896
11.0	28.50	8.74	1.41	324.85	17.79	1.25	16.54	.890
12.0	29.64	8.74	1.26	323.35	17.70	1.12	16.58	.885
13.0	30.79	8.74	1.13	321.86	17.63	1.01	16.62	.881
14.0	31.88	9.17	1.04	319.86	17.55	0.93	16.62	.877
15.0	32.91	9.66	0.91	318.86	17.49	0.81	16.68	.874
16.0	33.78	11.47	0.85	317.37	17.40	0.76	16.64	.869
17.0	34.66	11.47	0.76	316.62	17.38	0.68	16.70	.868
18.0	35.53	11.47	0.65	314.62	17.28	0.58	16.70	.863
19.0	36.35	12.24	0.61	313.62	17.21	0.54	16.67	.860
20.0	37.16	12.24	0.54	312.38	17.14	0.48	16.66	.856
21.0	37.98	12.24	0.46	311.38	17.10	0.41	16.69	.854
22.0	38.74	13.11	0.43	310.13	17.03	0.38	16.65	.851
23.0	39.51	13.11	0.43	309.13	16.98	0.38	16.60	.848
24.0	40.27	13.11	0.41	307.88	16.92	0.36	16.56	.845
25.0	40.98	14.12	0.33	306.89	16.88	0.29	16.59	.834
26.0	41.63	15.29	0.30	305.89	16.81	0.27	16.54	.840
27.0	42.28	15.29	0.28	304.64	16.75	0.25	16.50	.837

[a]p_T = pressure reading of PT-31-5C pressure transducer after conversion from millivolt reading using 24.9501 psi/mv.

[b]p_{sep} = pressure exerted by fluid passing through the septum.

Table 16. (Continued)

θ sec.	10^3V ft^3	$10^{-2}\frac{\Delta\theta}{\Delta V}$ sec/ft^3	P_1 psi	p_T[a] psi	(P_s + p_{sep} psi	p_{sep}[b] psi	P_s psi	$\frac{P_s}{P-P_1}$
28.0	42.94	15.29	0.22	303.89	16.71	0.20	16.51	.835
29.0	43.54	16.70	0.22	302.40	16.62	0.20	16.42	.830
30.0	44.14	16.70	0.22	294.41	16.18	0.20	15.98	.808
31.0	44.52	26.25	0.20	264.47	14.43	0.20	14.23	.719
32.0	44.85	30.58	-	-	-	-	-	-
33.0	45.12	36.63	-	-	-	-	-	-

Table 17. Constant pressure filtration data

Run No. $5\text{-}F_{25}\text{-}20BA$

$P = 21.0$ psi $\quad s = .193 \quad W = .6121\ lb_m$

$m = 1.632 \quad \epsilon_{av} = .632 \quad \frac{2}{K} = 4.23 \times 10^4$

θ sec.	$10^3 V$ ft^3	$10^{-2}\frac{\Delta\theta}{\Delta V}$ sec/ft^3	P_1 psi	p_T[a] psi	$(P_s + p_{sep})$ psi	p_{sep}[b] psi	P_s psi	$\frac{P_s}{P-P_1}$
0.0	3.92	-	0.0	0.0	0.0	0.0	0.0	0.0
0.25	-	-	12.80	126.00	7.40	-	-	-
0.5	-	-	8.79	244.51	13.88	7.81	6.07	.497
1.0	9.11	1.93	5.21	335.08	18.70	4.63	14.07	.891
1.5	-	-	3.69	334.08	18.25	3.28	14.97	.865
2.0	12.12	3.33	2.86	331.34	18.12	2.54	15.58	.859
3.0	14.60	4.03	2.04	327.84	17.92	1.81	16.11	.850
4.0	16.60	4.99	1.58	325.60	17.82	1.41	16.41	.845
5.0	18.35	5.74	1.28	324.35	17.78	1.14	16.64	.844
6.0	19.83	6.75	1.09	322.61	17.68	0.97	16.71	.839
7.0	21.25	7.06	0.93	321.86	17.63	0.83	16.80	.837
8.0	22.47	8.20	0.78	320.86	17.59	0.69	16.90	.836
9.0	23.69	8.20	0.65	319.86	17.53	0.58	16.95	.833
10.0	24.88	8.34	0.61	319.61	17.51	0.54	16.97	.832
11.0	25.93	9.56	0.52	319.36	17.50	0.46	17.04	.832
12.0	26.91	10.19	0.46	318.61	17.47	0.41	17.06	.831
13.0	27.85	10.67	0.39	317.86	17.43	0.35	17.08	.829
14.0	28.72	11.47	0.28	317.62	17.41	0.25	17.16	.828
15.0	29.57	11.77	0.24	317.37	17.40	0.21	17.19	.820
16.0	30.40	12.08	0.24	316.87	17.39	0.21	17.18	.828
17.0	31.18	12.76	0.22	316.37	17.35	0.20	17.15	.825
18.0	31.92	13.50	0.22	315.87	17.33	0.20	17.13	.824
19.0	32.66	13.50	0.22	315.12	17.30	0.20	17.10	.823
20.0	33.38	13.91	0.17	314.87	17.28	0.15	17.13	.822
21.0	34.08	14.35	0.09	313.87	17.22	0.08	17.14	.820
22.0	34.73	15.29	-	-	-	-	-	-
23.0	34.86	38.31	-	-	-	-	-	-

[a] p_T = pressure reading of PT-31-5C pressure transducer after conversion from millivolt reading using 24.9501 psi/mv.

[b] p_{sep} = pressure exerted by fluid passing through the septum.

Table 18. Constant pressure filtration data

Run No. $8\text{-}F_{30}\text{-}20BA$

$P = 21.0$ psi $s = .231$ $W = .6024\ lb_m$

$m = 1.649$ $\epsilon_{av} = .638$ $\frac{2}{K} = 6.03 \times 10^4$

θ sec.	$10^3 V$ ft^3	$10^{-2}\frac{\Delta\theta}{\Delta V}$ sec/ft^3	P_1 psi	p_T[a] psi	$(P_s + p_{sep})$ psi	p_{sep}[b] psi	P_s psi	$\frac{P_s}{P-P_1}$
0.0	2.29	-	0.0	0.0	0.0	0.0	0.0	0.0
0.25	-	-	9.00	127.25	7.48	-	-	-
0.5	-	-	6.51	274.45	15.52	5.79	9.73	.672
1.0	8.23	1.68	3.80	347.31	19.30	3.38	15.92	.926
1.5	-	-	2.78	349.30	19.40	2.47	16.93	.929
2.0	11.24	3.33	2.24	348.05	18.94	1.99	16.95	.904
3.0	13.46	4.50	1.67	342.81	18.68	1.49	17.19	.889
4.0	15.12	6.00	1.37	339.07	18.50	1.22	17.28	.880
5.0	16.62	6.66	1.15	335.08	18.30	1.02	17.28	.871
6.0	17.90	7.85	1.02	332.09	18.15	0.91	17.24	.863
7.0	19.07	8.50	0.89	329.34	18.01	0.79	17.22	.856
8.0	20.22	8.75	0.78	326.85	17.89	0.69	17.20	.851
9.0	21.23	9.87	0.74	324.35	17.75	0.66	17.09	.844
10.0	22.14	10.93	0.65	321.86	17.64	0.58	17.06	.838
11.0	22.99	11.78	0.61	319.61	17.51	0.54	16.97	.832
12.0	23.78	12.76	0.56	317.37	17.40	0.50	16.90	.827
13.0	24.53	13.32	0.54	314.87	17.28	0.48	16.80	.821
14.0	25.21	14.58	0.50	306.89	16.88	0.45	16.43	.802
14.5	25.57	13.93	0.41	290.92	15.98	0.37	15.61	.758
15.0	25.87	17.01	0.30	228.29	12.57	0.27	12.30	.594
15.5	26.00	38.17	-	143.71	8.00	-	-	-

[a] p_T = pressure reading of PT-31-5C pressure transducer after conversion from millivolt reading using 24.9501 psi/mv.

[b] p_{sep} = pressure exerted by fluid passing through the septum.

Table 19. Specific resistance and porosity determinations for Latin square analysis of variance

P_{sx} = 24.99 psi   1 = 1,2,3,4,5

Temp. °C	ΔH cm	$(dV/d\theta)_1$ cm³/sec	$(dV/d\theta)_2$ cm³/sec	W_c gms	$10^{-9}\alpha_{x1}$ cm/gm	$10^{-9}\alpha_{x2}$ cm/gm	L inch	ϵ
				M_1T_1-10-1				
27.0	60.35	.0876	.0888	10.0000	1.412	1.393	.2879	.6231
27.0	61.55	.0407	.0408	9.6653	3.208	3.200	.2584	.5941
26.8	62.15	.0097	.0097	9.3306	14.032	14.032	.2560	.6045
26.4	60.30	.0906	.0920	8.9959	1.497	1.476	.2554	.6178
25.0	59.35	.1126	.1135	8.6612	1.192	1.182	.2303	.5919
				M_2T_1-30-1				
25.2	58.09	.1188	.1177	30.0000	3.206	3.236	.9109	.6426
25.5	59.45	.0815	.0830	29.2626	4.937	4.848	.8850	.6286
25.6	57.08	.0203	.0220	28.5252	19.566	18.054	.8414	.6321
25.5	60.75	.1002	.1007	27.7878	4.321	4.300	.8627	.6505
25.5	62.18	.0167	.0162	27.0504	27.257	27.296	.8361	.6489
				M_3T_1-25-1				
22.9	50.0	.1074	.1070	25.0000	0.3479	0.3492	.7368	.6318
24.1	58.37	.1068	.1073	24.3474	0.4309	0.429	.6965	.6207
24.5	58.30	.1116	.1118	23.6948	0.4270	0.426	.6835	.6238
25.0	58.35	.1378	.1382	23.0422	0.3598	0.359	.6488	.6146
24.9	57.20	.1541	.1546	22.3896	0.3239	0.323	.5816	.5823
				M_4T_1-20-1				
23.4	57.7	.1343	.1328	20.0000	0.4057	0.410	.5708	.6198
21.9	60.79	.09205	.09195	19.3355	0.6235	0.624	.5644	.6283
23.8	58.25	.1793	.1767	18.6710	0.3644	0.370	.5161	.6074
24.0	59.2	.1171	.1163	18.0065	0.5378	0.542	.5342	.6342
24.2	60.3	.10091	.1001	17.3420	0.6630	0.668	.5383	.6504
				M_5T_1-15-1				
23.7	56.50	.1429	.1420	15.0000	0.5016	0.505	.4269	.6187
24.0	56.25	.1592	.1573	14.7000	0.4604	0.466	.4029	.6041
24.0	59.45	.1174	.1154	14.4000	0.6736	0.685	.4029	.6121
24.0	61.29	.0333	.0325	14.1001	2.5005	2.562	.4039	.6212
24.0	53.80	.1253	.1253	13.8001	0.5960	0.596	.3680	.5931

Table 19. (Continued)

Temp. ^{o}C	ΔH cm	$(dV/d\theta)_1$ cm^3/sec	$(dV/d\theta)_2$ cm^3/sec	W_c gms	$10^{-9}\alpha_{x1}$ cm/gm	$10^{-9}\alpha_{x2}$ cm/gm	L inch	ϵ
				M_1T_2-15-1				
20.6	54.65	.2250	.2236	15.0000	0.287	0.288	.5113	.6817
20.8	58.37	.1291	.1270	14.8194	0.543	0.552	.4673	.6559
21.2	58.00	.1040	.1032	14.6388	0.684	0.689	.4390	.6382
22.0	55.60	.1812	.1795	14.4582	0.388	0.397	.3511	.5531
23.0	11.25	.2640	.2643	14.2777	0.056	0.056	.4808	.6778
				M_2T_2-10-1				
21.8	57.15	.1079	.1078	10.0000	0.097	0.097	.3031	.6420
22.0	58.70	.1356	.1347	9.8766	0.080	0.081	.2878	.6276
23.0	58.60	.1403	.1382	9.7532	0.075	0.076	.2579	.5896
25.0	61.80	.0164	.0154	9.6298	0.766	0.816	.2637	.6037
24.0	60.20	.0819	.0810	9.5063	0.148	0.150	.2558	.5967
				M_3T_2-30-1				
23.0	58.30	.0938	.0928	30.0000	0.389	0.392	.9456	.6557
24.3	61.45	.0223	.0222	29.7618	1.785	1.793	.9127	.6462
23.9	59.00	.1291	.1277	29.5235	0.296	0.299	.8760	.6343
24.9	59.55	.0896	.0884	29.2853	0.443	0.450	.8828	.6400
25.0	60.70	.0979	.0967	29.0470	0.418	0.423	.8675	.6367
				M_4T_2-25-1				
23.8	59.60	.1142	.1130	25.0000	0.398	0.402	.7719	.6486
24.1	57.89	.1772	.1760	24.7398	0.254	0.255	.7212	.6278
25.0	58.90	.1644	.1633	24.4796	0.287	0.289	.7715	.6557
26.0	60.60	.0615	.0611	24.2194	0.815	0.820	.7229	.6364
25.5	58.95	.1664	.1662	23.9593	0.293	0.293	.7079	.6327
				M_5T_2-20-1				
23.5	56.30	.1671	.1655	20.0000	0.319	0.322	.6308	.6560
24.0	58.40	.1302	.1298	19.9016	0.432	0.433	.6040	.6425
24.6	61.10	.0521	.5190	19.8033	1.150	1.154	.5803	.6297
25.4	59.40	.1200	.1196	19.7049	0.496	0.498	.5707	.6253
25.8	60.30	.0922	.0920	19.6066	0.665	0.667	.5869	.6375

Table 19. (Continued)

Temp. °C	ΔH cm	$(dV/d\theta)_1$ cm³/sec	$(dV/d\theta)_2$ cm³/sec	W_c gms	$10^{-9}\alpha_{x1}$ cm/gm	$10^{-9}\alpha_{x2}$ cm/gm	L inch	ϵ
				M_1T_3-20-1				
24.2	59.30	.0797	.0794	20.0000	0.716	0.718	.6042	.6583
25.1	59.05	.1060	.1052	19.6640	0.556	0.560	.5753	.6481
26.4	59.60	.0909	.0909	19.4960	0.681	0.681	.5630	.6242
25.8	59.10	.1304	.1276	19.3280	0.468	0.478	.5583	.6243
26.0	58.95	.1236	.1221	19.1600	0.499	0.505	.5423	.6159
				M_2T_3-15-1				
22.1	55.99	.1838	.1883	15.0000	0.372	0.363	.4412	.6311
22.8	57.15	.1479	.1494	14.6312	0.492	0.488	.4215	.6233
24.0	57.59	.1867	.1866	14.2624	0.414	0.415	.4118	.6242
24.0	58.50	.0957	.0943	13.8936	0.843	0.855	.4009	.6239
23.3	57.65	.1095	.1095	13.5248	0.733	0.733	.3590	.5912
				M_3T_3-10-1				
23.8	60.20	.0597	.0596	10.0000	1.923	1.926	.3038	.6428
23.8	58.60	.1350	.1350	9.9126	0.835	0.835	.2878	.6263
23.7	58.80	.1097	.1110	9.8252	1.038	1.026	.2681	.6023
24.0	58.15	.1202	.1176	9.7378	0.952	0.973	.2691	.6073
24.0	59.40	.1235	.1226	9.6504	0.955	0.962	.2663	.6068
				M_4T_3-30-1				
24.1	61.00	.0396	.0395	30.0000	0.986	0.988	.9311	.6504
24.0	59.30	.1208	.1192	29.8332	0.315	0.319	.8199	.6052
24.0	60.05	.0893	.0878	29.6664	0.434	0.442	.8546	.6233
23.3	59.65	.1099	.1102	29.4995	0.346	0.345	.8664	.6305
22.5	60.00	.0920	.0922	29.3327	0.411	0.410	.8437	.6227
				M_5T_3-25-1				
20.7	58.20	.0861	.0857	25.0000	0.480	0.482	.7710	.6481
21.2	59.05	.1010	.1005	24.8549	0.422	0.425	.7326	.6318
22.5	58.65	.1213	.1203	24.7098	0.362	0.365	.7337	.6345
23.6	60.00	.0934	.0935	24.5648	0.496	0.496	.7257	.6327
24.1	59.70	.1139	.1138	24.4197	0.412	0.412	.6942	.6183

Table 19. (Continued)

Temp. ^{o}C	ΔH cm	$(dV/d\theta)_1$ cm^3/sec	$(dV/d\ )_2$ cm^3/sec	W_c gms	$10^{-9}\alpha_{x1}$ cm/gm	$10^{-9}\alpha_{x2}$ cm/gm	L inch	ϵ
				M_1T_4-25-1				
22.4	58.95	.0821	.0813	25.0000	0.530	0.536	.7869	.6553
23.0	59.15	.1163	.1148	24.8937	0.383	0.388	.7210	.6253
23.3	59.80	.1147	.1149	24.7874	0.396	0.395	.7311	.6321
24.1	60.35	.1008	.1016	24.6811	0.466	0.462	.7322	.6342
24.5	61.00	.0735	.0735	24.5748	0.654	0.654	.7323	.6358
				M_2T_4-20-1				
20.0	58.55	.1163	.1163	20.0000	0.439	0.439	.6129	.6459
20.9	60.18	.0740	.0726	19.8836	0.729	0.743	.5791	.6274
21.5	60.10	.0908	.0909	19.7672	0.606	0.605	.5742	.6264
23.0	60.84	.0604	.0602	19.6508	0.960	0.963	.5988	.6439
22.9	60.20	.0877	.0876	19.5344	0.657	0.657	.5569	.6194
				M_3T_4-15-1				
19.0	58.30	.1198	.1178	15.0000	0.552	0.561	.4520	.6399
19.3	58.52	.1176	.1176	14.9077	0.572	0.572	.4388	.6313
19.5	59.40	.1106	.1103	14.8154	0.625	0.626	.4412	.6356
20.0	60.82	.0455	.0452	14.7231	1.583	1.594	.4250	.6241
21.0	61.25	.0254	.0251	14.6308	2.948	2.983	.4257	.6271
				M_4T_4-10-1				
20.8	59.45	.0726	.0719	10.0000	1.457	1.471	.3047	.6459
21.4	60.32	.0858	.0861	9.9379	1.276	1.271	.2938	.6330
22.7	57.61	.1178	.1167	9.8758	0.921	0.930	.2878	.6276
23.9	61.42	.0296	.0293	9.8137	4.042	4.083	.2851	.6265
23.0	61.50	.0218	.0214	9.5717	5.417	5.518	.2839	.6273
				M_5T_4-30-1				
22.8	61.02	.0369	.0373	30.0000	1.028	1.017	.9553	.6592
23.5	61.14	.0217	.0211	29.8329	1.798	1.849	.9221	.6489
23.9	60.10	.0861	.0856	29.6658	0.450	0.452	.8778	.6333
25.0	60.60	.0837	.0837	29.4987	0.481	0.481	.8570	.6265
25.6	61.30	.0555	.0552	29.3317	0.748	0.752	.8749	.6362

Table 19. (Continued)

Temp. °C	ΔH cm	$(dV/d\theta)_1$ cm3/sec	$(dV/d\theta)_2$ cm3/sec	W_c gms	$10^{-9}\alpha_{x1}$ cm/gm	$10^{-9}\alpha_{x2}$ cm/gm	L inch	ε
				M_1T_5-30-1				
21.5	61.15	.0272	.0264	30.0000	1.355	1.396	.9471	.6563
23.0	59.65	.0957	.0938	29.8526	0.391	0.399	.9161	.6464
23.5	60.05	.0896	.0880	29.7052	0.427	0.435	.9107	.6461
24.2	59.10	.1203	.1199	29.5578	0.320	0.321	.8910	.6400
25.5	61.52	.0656	.0641	29.4105	0.632	0.646	.8738	.6348
				M_2T_5-25-1				
25.6	59.45	.0909	.0912	25.0000	0.519	0.518	.7734	.6492
25.3	59.50	.0962	.0963	24.7934	0.492	0.491	.7392	.6360
25.5	61.39	.0516	.0518	24.5868	0.958	0.955	.7530	.6457
24.8	59.55	.1198	.1285	24.3803	0.398	0.371	.7457	.6452
24.2	60.90	.0756	.0751	24.1738	0.641	0.645	.7239	.6376
				M_3T_5-20-1				
20.0	57.70	.1239	.1231	20.0000	0.409	0.406	.5957	.6357
20.5	58.45	.1148	.1148	19.8721	0.453	0.453	.5881	.6333
22.0	62.38	.0074	.0074	19.7442	7.811	7.811	.5748	.6273
23.0	61.98	.0158	.0141	19.6164	3.744	4.196	.5960	.6259
22.5	61.50	.0219	.0223	19.4886	2.667	2.619	.5760	.6329
				M_4T_5-15-1				
24.0	61.44	.0093	.0093	15.0000	8.437	8.437	.4548	.6421
24.0	62.16	.0141	.0154	14.9243	5.659	5.181	.4365	.6290
24.8	62.32	.0850	.0796	14.8486	0.963	1.028	.4321	.6271
23.0	62.25	.0130	.0125	14.7729	6.069	6.312	.4268	.6244
22.0	62.11	.0112	.0114	14.6971	6.903	6.782	.4166	.6172
				M_5T_5-10-1				
20.8	61.80	.0085	.0092	10.0000	12.936	11.952	.3099	.6498
21.0	62.12	.0069	.0069	9.9137	16.241	16.241	.2818	.6183
20.8	60.85	.0498	.0481	9.8274	2.212	2.290	.2882	.6300
23.0	61.85	.0185	.0179	9.7412	6.426	6.642	.2780	.6198
23.5	62.11	.0103	.0105	9.6550	11.822	11.597	.2727	.6158